Republic of Iraq

Ministry of Higher Education & Scientific Research

University of Kerbala

College of Engineering

Civil Engineering Department

(Flexural Behavior of Reinforced Sustainable Concrete Beams Strengthened by CFRP and Steel Fibers)

A Thesis Submitted to the Council of the Faculty of the College of the Engineering/University of Kerbala in Partial Fulfillment of the Requirements for the Master Degree in Civil Engineering

Written By:

Ali Nasser Hussein

Supervised By:

Asst. Prof. Dr. Zainab M.R. Abdul Rasoul

Asst. Prof. Dr. Aymen J. Alsaad

October 2022   Rabii-awel 1444

Republic of Iraq

Ministry of Higher Education & Scientific Research

University of Kerbala

College of Engineering

Civil Engineering Department

(Flexural Behavior of Reinforced Sustainable Concrete Beams Strengthened by CFRP and Steel Fibers)

A Thesis Submitted to the Council of the Faculty of the College of the Engineering/University Of Kerbala in Partial Fulfillment of the Requirements for the Master Degree in Civil Engineering

Written By:

Ali Nasser Hussein

Supervised By:

Asst. Prof. Dr. Zainab M.R. Abdul Rasoul

Asst. Prof. Dr. Aymen J. Alsaad

October 2022   Rabii-awel 1444

بسم الله الرحمن الرحيم

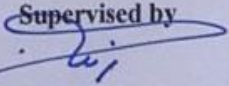يَرْفَعِ اللَّهُ الَّذِينَ آمَنُوا مِنكُمْ وَالَّذِينَ أُوتُوا الْعِلْمَ دَرَجَاتٍ

صدق الله العلي العظيم

(المجادلة: من الآية 11)
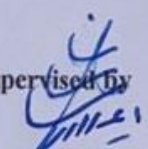
Examination committee certification

We certify that we have read the thesis entitled "**Flexural Behavior of Reinforced Sustainable Concrete Beams Strengthened by CFRP and Steel Fibers** " and as an examining committee, we examined the student " **Ali Nasser Hussein**" in its content and in what is connected with it and that in our opinion it is adequate as a thesis for the degree of Master of Science in Civil Engineering.

Supervised by

Signature:

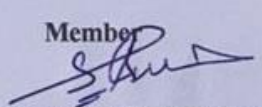Name : Asst. Prof. Dr. Zainab M.R. Abdul Rasoul

Date: / / 2022

Supervised by

Signature:

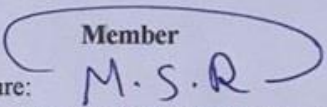Name : Asst. Prof. Dr. Aymen J. Alsaad

Date: / / 2022

Member

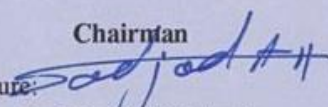Signature:

Name :. Asst.prof.Dr.Haider Ahmed Abid Al-Katib

Date: / / 2022

Member

Signature: M·S·R

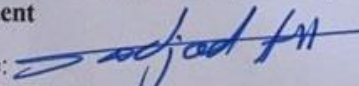Name :. Asst.prof.Dr.Mushtaq Sadiq Radhi

Date:25/12/ 2022

Chairman

Signature:
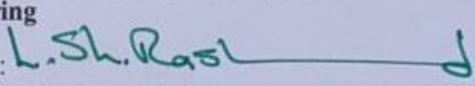
Name :. Prof.Dr.Sadjad Amir Hemzah

Date: / / 2022

Approval of Head of Civil Engineering Department

Signature:

Name : Prof.Dr.Sadjad Amir Hemzah

Date: / / 2022

Approval of Deanery of the College of Engineering

Signature: L.Sh.Ras
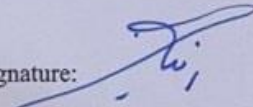
Name : prof.Dr.Laith Shaker Rashid

Date:8 /1 / 2023

Supervisor certificate

We certify that the thesis entitled **"Flexural Behavior of Reinforced Sustainable Concrete Beams Strengthened by CFRP and Steel Fibers"** was prepared by **Ali Nasser Hussein** under our supervision at the Department of Civil Engineering, Faculty of Engineering, University of Kerbala as a partial of fulfilment of the requirements for the Degree of Master of Science in Civil Engineering.

Signature:

Asst. Prof. Dr. Zainab M.R. Abdul Rasoul
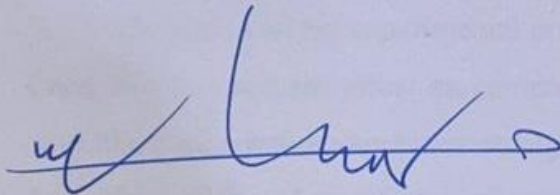
Date: /   / 2022

Signature:

Asst. Prof. Dr. Aymen J. Alsaad

Date: /   / 2022

Linguistic certificate

I certify that the thesis entitled " **Flexural Behavior of Reinforced Sustainable Concrete Beams Strengthened by CFRP and Steel Fibers** " which has been submitted by **Ali Nasser Hussein** has been proofread and its language has been amended to meet the English style.

Signature:

Name: Assist. Professor Dr. Hayder Hussein Alwun Algrotawee

Date: / / 2022

30 10

Abstract

The concrete industry has only been around for the past 120 years, yet it has already left a significant mark on the way the landscape looks. The main objectives of this thesis are to study the behavior of pozolime concrete properties and study the response of reinforced pozzolime concrete beams under two-point loads. The CFRP sheets approach was used for the testing, which focused on determining how the percent of steel fibers, position, and length of CFRP sheets affected the results. The main variables of the experimental work are the location of the CFRP sheet (internal or external), length of CFRP, and volume fraction of steel fiber.

The experimental program consists of testing thirteen reinforced concrete beams designed as simply supported beams constructed using pozzolime concrete. Specimens are divided into three groups plus a reference beam according to the strengthening techniques and the percent of steel fibers used in each group.

The results of the experimental program show that the percent of steel fibers has a significant effect on compressive strength. Adding 0.5 and 1% steel fibers increases compressive strength by 4.1% and 37.6% for age of 28 days. The addition of steel fibers enhanced compressive strength by 4.9% and 12.8% compared to the reference specimen at 28 days. There are two kinds of failure modes that occurred on the CFRP-strengthened beams in this experiment. The first is the intermediate flexure crack-induced debonding failure which occurred in the externally strengthened beams. The second is the intermediate flexure crack-induced debonding along with the internal CFRP sheets that began from the mid-span with a horizontal crack with concrete cover separation and delamination. For Full externally strengthening,

the effect of increase steel fibers percent on ultimate load was 3.3, and 5.7% for specimen with 0.5 % of steel fiber, and specimen with 1 % of steel fiber compare with the reference specimen respectively. For Full internally strengthening the percentage of the increase in ultimate load was 4.4, and 7.7% for specimen with 0.5 % of steel fiber, and specimen with 1 % of steel fiber respectively with respect to the reference specimen, regarding the group of internally full strengthening.

Undertaking

I certify that research work titled "**Flexural Behavior of Reinforced Sustainable Concrete Beams Strengthened by CFRP and Steel Fibers**" is my own work. The work has not been presented elsewhere for assessment. Where material has been used from other sources it has been properly acknowledged / referred.

Signature:

Ali Nasser Hussein

Date: /   / 2022

Acknowledgements

Signature:

Ali Nasser Hussein

Date: /   / 2022

List of contents

List of figures

List of plates

List of tables

Notations

Symbol	Description
a	Total length of column (mm)
Ac	Cross-sectional area of the concrete (mm2)
Ag	Cross-sectional area of a section (mm2)
As	Cross-sectional area of steel reinforcement (mm2)
b	Total width of column (mm)
db	Dimeter of steel reinforcement
Ec	Concrete modulus of elasticity (GPa)
Es	Steel modulus of elasticity (GPa)
fc'	Compressive strength
$f$cu	Concrete compressive strength (MPa)
f_{fe}	The effective FRP strengthening stress
fsp	Splitting tensile strength of concrete(MPa)
fsu	Ultimate strength of steel reinforcement(MPa)
$f$sy	Strength of steel reinforcement (MPa)
fy	Yield strength of steel reinforcement (MPa)
Pcr	Cracked load
t	CFRP sheets thickness
V	Volume of specimen
w	CFRP sheets width
W$_{dry}$	Oven-dry mass
γ_{dry}	Dry density

Abbreviations

Symbol	Description
ABAQUS	Finite Element package
ACI	American Concrete Institute
AFRP	Aramid fiber reinforced polymer
ASTM	American Society for Testing and Materials
BS	British Standard
CC	Control combination
CFRP	Carbon fibre reinforcement polymer
CFRP	Carbon fibre reinforcement polymer
DOF	degrees of freedom
EFNARC	European guidelines for self-compacting concrete
et al.	others
FEA	Finite Element Analysis
FRCC	Fiber-reinforced cementitious composites
FRP	Fibre reinforcement polymer
GFRP	Glass fibre reinforcement polymer
GHG	greenhouse house gas
HVFA	high-volume fly ashes
HVFAC	high-volume fly ash concrete
IQS	Iraqi specification
LWA	lightweight aggregate
LWAC	lightweight aggregate concrete
mm	Millimeter
MPa	Mega Pascal (N/mm2)
NC	Normal concrete
No.	Number
NSM	Near-surface mounted
NSM	Near-Surface Mounted technique
NVC	Normal vibrated concrete
RC	Reinforced concrete
SCC	Self-compacted concrete
SCMs	Supplemental Cementitious Materials

Chapter one
Introduction

1.1 Introduction

Today, concrete is the most widely utilized building material in the world. Components of concrete may be found naturally in any region of the globe. In Iraq, it is produced with local resources and local know-how. For many years, concrete has been utilized in the construction of long-lasting bridges, highways, water supply structures, housing, and commercially buildings to provide a social basis, a healthy economy, and functional facilities **[Berndt, 2009]**.

As resources dwindle and the impact of green house gas emissions (GHG) becomes more apparent, minimizing the environmental impact and energy- and CO2-intensity of concrete used for building is of growing importance. Therefore, it makes sense to incorporate life cycle and sustainable engineering strategies into the concrete mix design.

This needs multiple elements: increasing the longevity of concrete, conserving materials, using waste and additional cementing ingredients, and recycling concrete. As partial substitutes for Portland cement, waste and supplemental cementing materials such as fly ash, blast of furnace slag, silica fume, and metakaolin can be utilized. These materials can increase the durability of concrete, reduce the risk of thermal cracking in mass concrete and have a lower energy and carbon dioxide foot print than cement **[Berndt, 2009].**

In engineering, reinforced concrete buildings are utilized in a number of conditions and purposes. The preservation of a structure's serviceability and strength

over its lifetime might be one of the chief challenges facing structural engineers. Changes in a structure's circumstances might result in the structure's inability to fulfill its service function in connection to the current load and environmental conditions. Existing concrete structures or any of their components may be deemed undesirable for a variety of reasons.

This might appear as poor performance under service loads as excessive deflections, cracking, or diminished strength. In such cases, there are two viable solutions: destroying and rebuilding, or implementing a rehabilitation program to restore the normal structural performance, enhance the structure's strength, and meet stricter serviceability criteria. The decision between these options is influenced by a number of variables, including material and labor costs, structural downtime, and interruption to other operations. **[Klaiber et al., 2003]** found that in the current economic context, the second option is becoming significantly more appealing, particularly if a simple and rapid strengthening approach is available.

Fiber Reinforced Polymer (FRP) components have indeed been proven to be effective for flexural enhancement, shear strengthening, thereby satisfying the need to develop cost-effective and efficient techniques for upgrading, and repairing, or strengthening old reinforced concrete structures. In the construction industry, reinforcing reinforced concrete beams using fiber-reinforced Polymer (FRP) composite is gaining favor. **[Klaiber et al., 2003]** These laminates offer all the benefits of composite materials, including corrosion resistance and a high strength-to-weight ratio. Refer to **Plate1.1.**

Plate 1.1: Overview of the FRP strengthening work **[Klaiber et al., 2003].**

1.2   Sustainable concrete materials

Supplemental Cementitious Materials (SCMs) provide a major amount of the cementitious component or binder in the concrete produced today. The three most common SCMs are ground powdered blast-furnace slag (slag), fly ash, and amorphous silica. Fly ash and amorphous silica are pozzolanic minerals that harden by reacting with the calcium hydroxide produced in the hydration of Portland cement. Slag will interact with water in the presence of alkaline chemicals, such as Portland cement, to generate a solid binder. The use of SCMs further minimizes concrete's environmental effect by lowering the quantity of produced cement

required in a particular concrete mix. As an industrial by-product, SCMs may be acquired at a cheaper price than produced cement, resulting in superior economic outcomes for concrete building **[Cement Concrete & Aggregates Australia, 2010].**

1.3   Pozzolime concrete

Lime might be considered a sustainable binder since it requires less energy to produce, emits less CO2 during manufacture, and absorbs CO2 through carbonation in the setting. Pozzolans, like silica fume, fly ash, and slag, which are often referred to as supplemental cementitious materials, may be found in the majority of byproducts from a variety of industrial operations. Pozzolanic reaction is the chemical interaction between finely ground siliceous in Pozzolans and $Ca(OH)_2$, by product of the synthesis of calcium silicate hydrates CSH in Portland cement, to generate compounds with cementitious characteristics **[Kadum et al., 2017].** See **Plate 1.2.**

| Silica Fume | Blast-furnace slag | Fly Ash |

Plate 1.2: Pozzolanic materials **[Kadum et al., 2017].**

1.4 Fiber reinforced polymer (FRP)

Fiber Reinforced Polymer (FRP) is becoming the material of choice for the strengthening and restoration of old structures. In contrast to traditional building materials, FRP provides an excellent combination of weight, strengths, stiffnesses, durability, and resistivity to corrosion. Due to its low weight and ease of usage, it does not require mechanical lifting or anchoring equipment, resulting in little service interruption throughout the strengthening and maintenance operation. It is particularly useful in restricted spaces. Due to the application's simplicity, cost-effectiveness, and short duration, sustainable savings are possible when all project expenses are included. **Plate 1.3** illustrates the use of CFRP in reinforcing beams **[Khan, 2002].**

Plate 1.3: The application of CFRP in the strengthening of beams **[Khan, 2002].**

FRP materials are much less dense than steel. This can lead to lower transportation costs, a slight increase in the dead load of the reinforced structure, and easier material handling and application on-site. Based on the kind of fibers, resins, and fiber volumes percentages, the coefficient of thermal expansion varies amongst FRP systems. When placed in direct tension, FRP materials exhibit linear elastic stress-strain behavior till rupture. Consequently, failure is abrupt and potentially catastrophic. On the basis of the net-fiber area or the gross-laminate area, the qualities of a FRP system may be determined. The load-carrying capacity is unaffected by the manner in which the attributes are reported. ACI Committee 440-2R (2017) states that FRP systems should not be utilized as compression reinforcement owing to a lack of testing in this application type. FRP laminates subjected to longitudinally compression fail via transverse tensile failure, fiber micro buckling, and shear failure. **[ACI Committee 440-2R, 2017].**

1.5 Steel fiber

Steel fibers improve the shear behavior of concrete as it is randomly distributed at closed spacing, which Increases tensile strength, and Increases shear friction strength. Also, Steel fibers increase durability, improve flexural properties, and reduce the absorption of water **[Oh, B. H., 1992].**

1.6 Aim and objective of the study

The objective of the present thesis is to study, experimentally, the behaviors of reinforced sustainable concrete beams externally and internally strengthened with Carbon Fiber Reinforced Polymer sheet (CFRP). The research presented in this thesis covers the following areas of study.

1- Experimental study and a comparison of the performance of reinforced sustainable concrete beams enhanced with CFRP sheets attached to flexural sides. The main variables of the experimental work are the location of CFRP sheet (internal or external), length of CFRP, and volume fraction of steel fiber.

2- In the present study tested beams are divided into three groups according to the added steel fiber percent (0, 0.5, 1) %, each group has four samples with different lengths and locations of CFRP, as well as reference beam without strengthen and fiber.

1.7   Layout of thesis

The thesis is arranged into five chapters:

Chapter one: Describes numerous fundamental ideas for the sustainable concrete materials, and fiber reinforced polymer (FRP) properties. The objectives, and the field of work are defined.

Chapter two: Includes a summary of past research on the topic of the properties and uses of Pozzolime concrete materials and Fiber reinforced polymer (FRP).

Chapter three: The third chapter explains the experimental work and the specimens' detail, as well as the materials and the preparation of Pozzolime concrete in addition to the proposed strengthening techniques for the beam.

Chapter four: In this chapter, the experimental results, as well as a description, discussion, and evaluation of these data, will be displayed.

Chapter five: Presents the inferences that may be derived from this thesis, along with a recommendation and a proposal for more investigation.

Chapter two
Literature review

2.1   Introduction

Lime-natural Pozzolana is an ancient building material that was utilized in the construction of masonry. The use of lime-natural pozzolana has been discontinued throughout the history of inorganic binders due to its sluggish setting and hardening. After the discovery of Portland cement in the nineteenth century, the use of natural pozzolan-lime binding material decreased considerably due to its rapid setting and great strength in the early eras. The environmental repercussions of the Portland cement production process have increased interest in lime-natural pozzolan cement during the past 50 years **[Moropoulou et al., 2020]**.

Due to the numerous benefits of utilizing FRP as an exterior reinforcement for RC members, substantial study has been conducted on their performance. The majority of research has been on flexural strengthening, in which FRP laminates are bonded to the top or bottom surfaces of beams at regions of maximal moment. In recent years, however, the number of studies in which FRP is bonded to beam webs as shear reinforcement has grown.

The purpose of this chapter is to provide an overview of the existing data about the behavior of sustainable reinforced concrete members with exterior and internal FRP.

2.2   Pozzolime Concrete

Pozzolans are natural or man-made materials that are not cementitious on their own but, because they are made of aluminosilicates, when mixed with lime hydrate start

creating a hydraulic cement. **[Mouli and Khelafi, 2008]** investigate the viability of employing pozzolan derived from natural sources in Algeria as pozzolanic substance. This pozzolan is seldom used in concrete since its features have not been thoroughly examined. To learn more about the effectiveness of pozzolan concrete works, 6 concrete mixes were tested: one with Portland cement (as a control) and five with 10 percent, 20 percent, 30 percent, 40 percent, and 50 percent pozzolan substitution of cement. To make lightweight aggregate concrete, shattered pozzolan was used as the lightweight aggregate (LWA), and natural sand was added to all mixes (LWAC). Workability and density of fresh concrete mixes were evaluated. The compressive strength, splitting tensile strength, and flexural strength of hardened concrete specimens were measured after 3, 7, 28, 90, and 365 days.

[Al-Chaar et al., 2013] examined the use of natural pozzolan just as a partial replacement for cement in concrete materials. Four mixtures including three types of natural pozzolan and Class F fly ash are examined through a series of tests. Each pozzolan's efficiency in regulating alkali-silica reactions has been examined. Between the mechanical characteristics of the suggested mixtures and a Portland cement control mixture, correlations have been discovered. Industry requirements for fly-ash and silica fume mortars are also examined. According to the conclusions of this study, one form of pozzolan can serve for fly ash, but just not silica fume replacement.

[Kadum et al., 2017] analyzed the characteristics of concrete mixtures made mostly of hydrated lime and various Pozzolan kinds. This combination, referred to as Pozzolime, was proposed as a sustainable alternative to Portland cement for use in concrete. The research aims to maximize the proportion of Pozzolan to lime in relation to the strength, durability, and workability of concrete. The factors evaluated include the ratio of water to binder, the ratio of aggregate to binder, and the kind of Pozzolan. These parameters' influence on the characteristics of the combination in its fresh and cured forms are investigated. Some of the tests that were done were the temperature

description, the slump, the fresh and oven-dry densities, the compressive, splitting tensile, and flexural strengths, and the dynamic elastic modulus. In this investigation, Silica fume, fly ash, and types of metakaolin were employed as Pozzolan. The temperature profile during hydration demonstrates that all Pozzolime combinations have much fewer environmental effects (generated heat) than Portland cement. The results also indicate that structural concrete with a compressive strength larger than 28.0 MPa at 28.0 days of age may be produced using a binder containing a weight ratio of 1:1 between silica fume and hydrated lime and an overall binder content of 333.0 kg/m³. **Figure 2.1** shows the effect of water to binder, W/B, ratio on strength development.
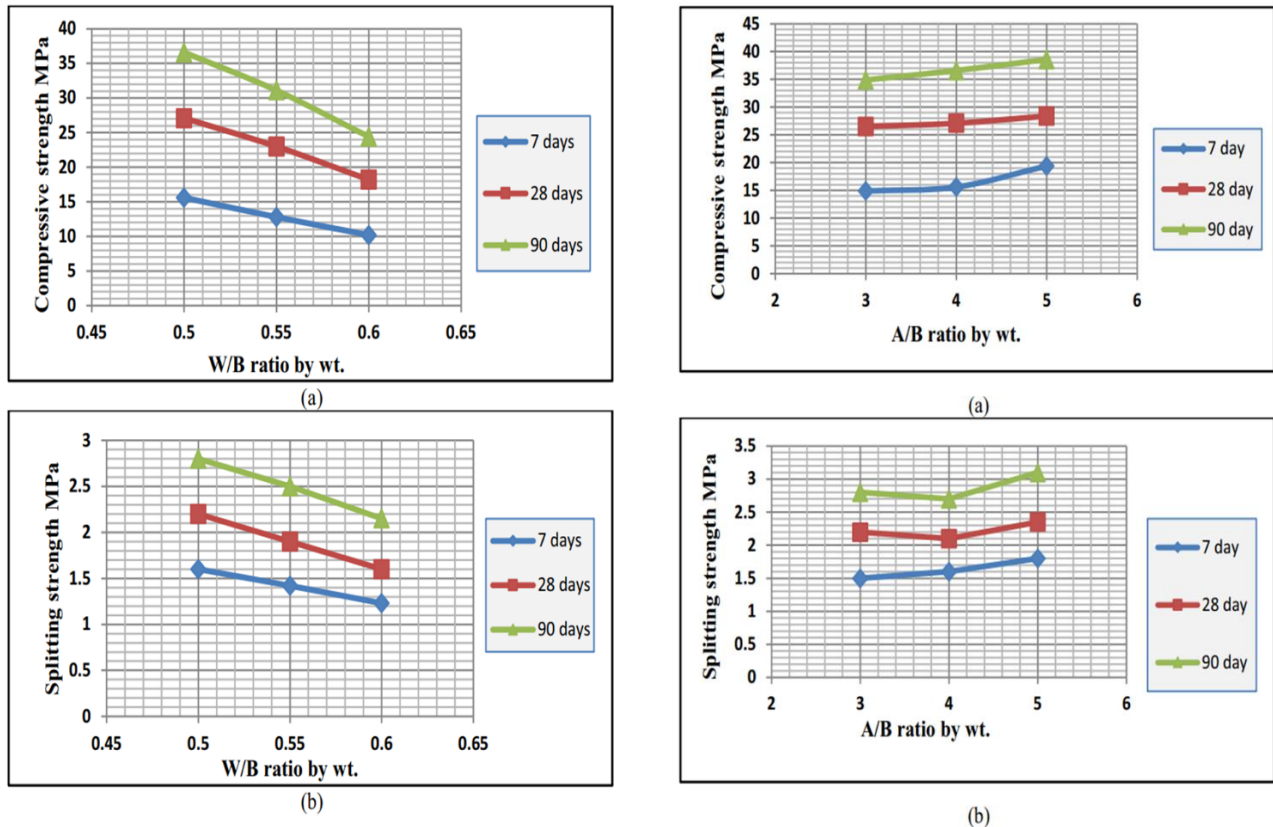
Figure 2.1: Impact of W/B ratios on strength developments of LS_1, LS_2 and LS_3 mixes: - a: compressive strengths, b: splitting tensile strengths. **[Kadum et al., 2017].**

The stress-strain relation for Pozzolime concrete mixes M25 and M40 at different curing periods are presented in **Figure 2.2**. The main observation is that the

E value for Pozzolime develops slower with time than Portland cement concrete and that is mainly due to the slow rate of Pozzolanic reaction. With respect to the linearity limit of the relation, the value of 0.45 σp could be considered as an upper limit whereas after this value the curves shown in figure 1 starts to deviate from linear relationship. Therefore, it could be concluded that Pozzolime has a similar behavior to that of Portland cement concrete under compression stress **[Al-Attar et al., 2020].**
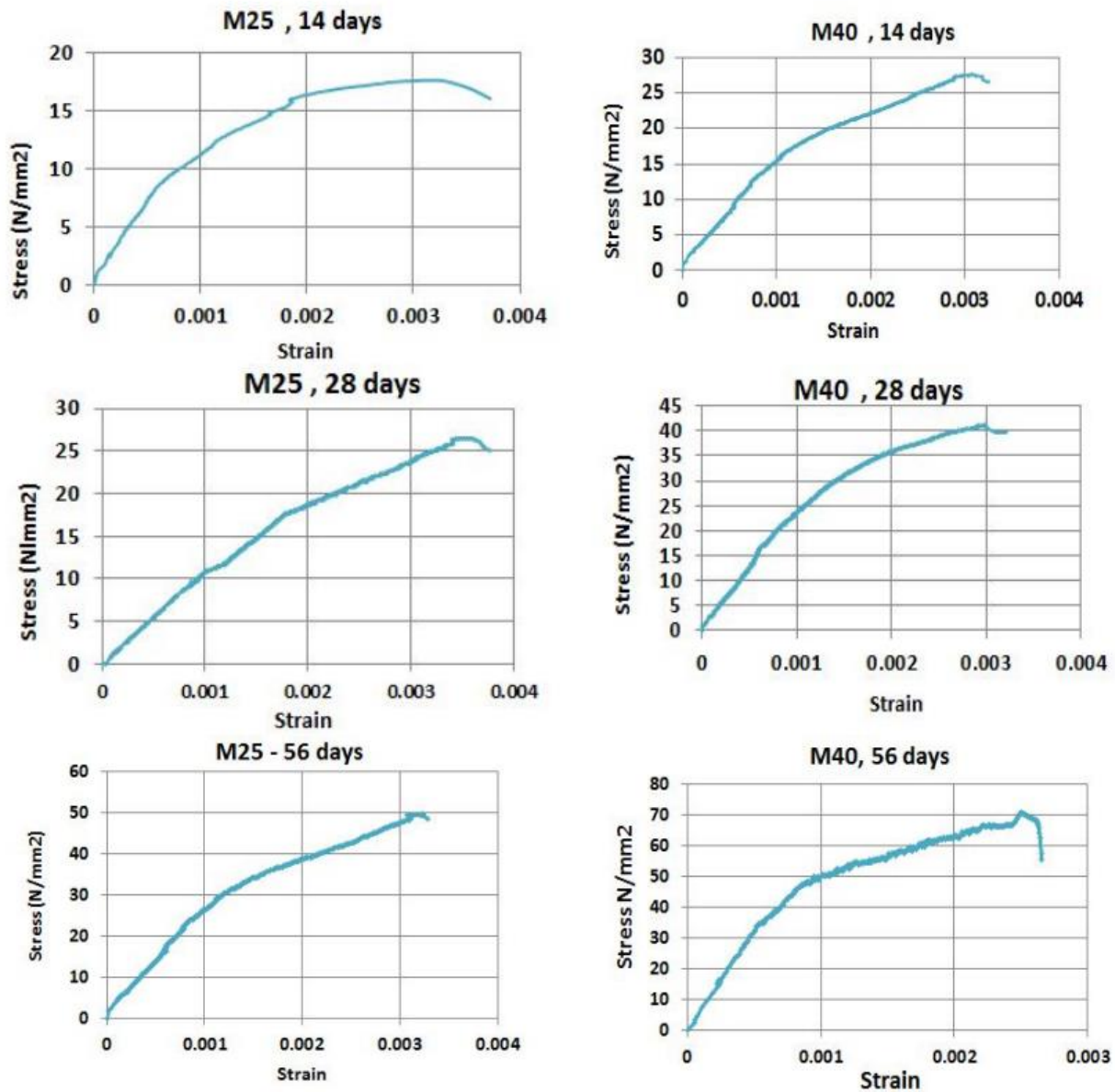
Figure 2.2: Compressional stress-strain relations for Pozzolime concrete mixes at different strength levels and ages **[Al-Attar et al., 2020].**

According to **[Al-Attar et al., 2021]**, high-strength at fractions of the volume of 0.5, 1, 1.5, and 2 percent, steel fibers with hooked ends were used to strengthen pozzolime concrete. The fiber content was tuned based on the workability and tensile strength of the fiber-reinforced mixture. Incorporating 1.5 percent steel fiber raised the compressive strengths at 14 and 90 days by 71.4 percent and 58.3 percent, respectively, as determined by the findings. At 1.5 percent, the 14-day, 28-day, and 90-day flexural strength of pozzolime concrete improved by 170.04 percent, 203.20 percent, and 191,4 percent, respectively, whereas an increase in fiber content decreased the strength. This study's findings revealed that the volume fraction (1.5 percent) may be deemed the optimal concentration.

2.3   Sustainable Concrete

[Berndt, 2009] examined the viability of utilizing more "sustainable" concrete for special foundations and other requirements requiring significant amounts of concrete. In order to lessen the energy; the environment, and CO2 effect of concrete, material replacements were implemented. This was achieved by replacing some of the cement with a lot of blast furnaces slag or fly ash and recycles the concrete aggregate. Five basic types of concrete mixtures were looked at. There was a standard mix with no changes to the materials, a mix with 50% fly ash instead of cement, a mix with 50% blast furnace slag instead of cement, a mix with 70% blast furnace slag instead of cement, and a mix with 25% fly ash and 25% blast furnaces slag instead of cement. It was discovered that 50 percent slag mixtures provided the optimum overall performance. The use of slag in concrete with recycled aggregates was very advantageous and might prevent strength losses. Tests on the durability of recycled concrete aggregate revealed small improvements in the coefficient of permeability and the coefficient of chloride dispersion. Incorporating slag into the mixture increased the chloride diffusion coefficient and maintained acceptable levels for durable concrete.

For the ingredients and mixture proportions employed in this study, concrete containing 50 percent fly ash performed poorly, and it is advised that such mixes be properly investigated prior to use in building projects.

The use of slag in concrete with recycled aggregates was very advantageous and might prevent strength losses. Tests on the durability of recycled concrete aggregate revealed small improvements in the coefficient of permeability and the coefficient of chloride dispersion. Incorporating slag into the mixture increased the chloride diffusion coefficient and maintained acceptable levels for durable concrete. For the ingredients and mixture proportions employed in this study, concrete containing 50 percent fly ash performed poorly, and it is advised that such mixes be properly investigated prior to use in building projects **[Berndt, (2009)].**The compressive strength of concrete within natural aggregate is shown against time in **Figure 2.3**.

.
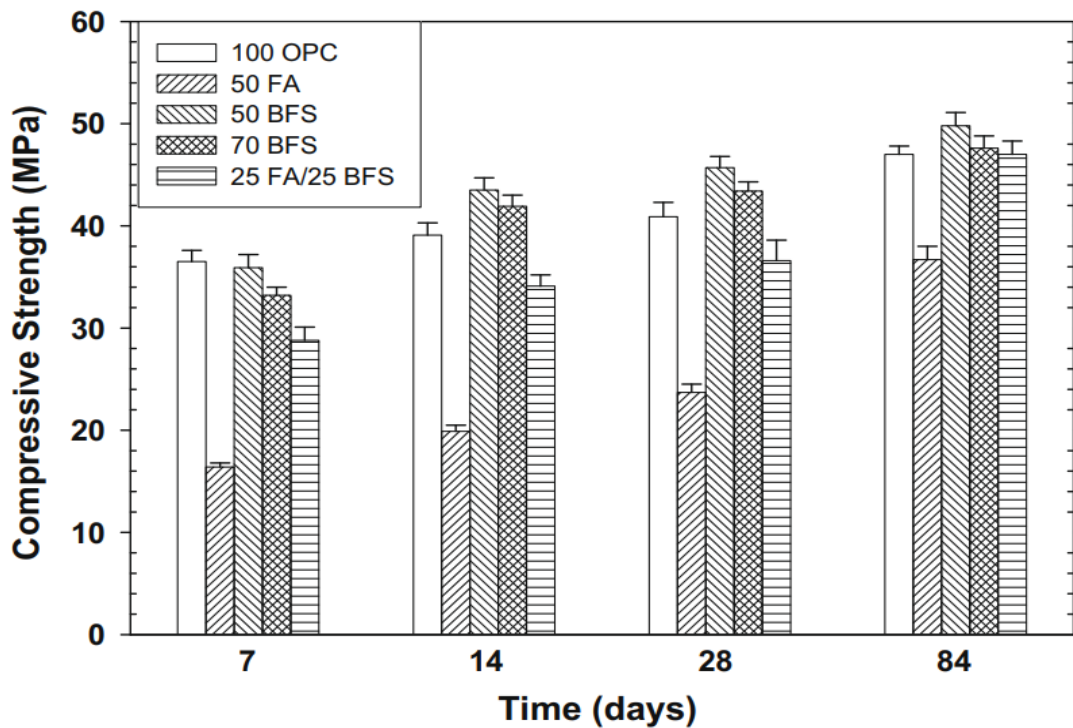
Figure 2.3: Concrete with natural aggregate's compressive strength vs time. **[Berndt, (2009)].**

2.4 Sustainable concrete in reinforced beams

[Yoo et al., 2015] presented the findings of flexural tests done on reinforced concrete beam samples with varied fly ash substitute ratios of 0.0%, 35.0%, and 50.0%, many ratios of tension steel, and compressive strengths of concrete. In addition, an analytical model was established based on the experimental data to anticipate the performance of reinforced concrete beams. The compare with the experimental data demonstrates that the analytical findings properly anticipate the behavior of the beams for all of the fly ash replacement ratios investigated.

As established by the material test, eighteen test elements were produced with fly ash replacement ratios of 0%, 35%, and 50% and concrete compressive strengths of 20, 40, and 60 MPa. **Figure 2.4** illustrates the characteristics of the test individuals. The ultimate load-to-yield load ratios of the test elements ranging from 1.10 to 1.46, and the fracture load was closely proportionate to the compressive strength of concrete. In addition, the elements with a high tensile steel ratios have inherently greater load resistance compared to the members with a low tensile steel ratio.

The ductility index defined as the ratio of the ultimate deflection to the yield deflection appeared to be larger than 4.0 for the L-series members, which indicated that these members could prevent brittle failure. Besides, the H-series members exhibited ductility index relatively smaller than the L-series members. The ductility index was seen to decrease with higher compressive strength regardless of the content in fly ash. The deflection, strain, crack load, yield load and ultimate load observed in the members were seen to be practically indifferent to the content in fly ash since the structural behavior of the test members with fly ash replacement ratio of 35% and 50% was quasi-similar to that of the members without fly ash.
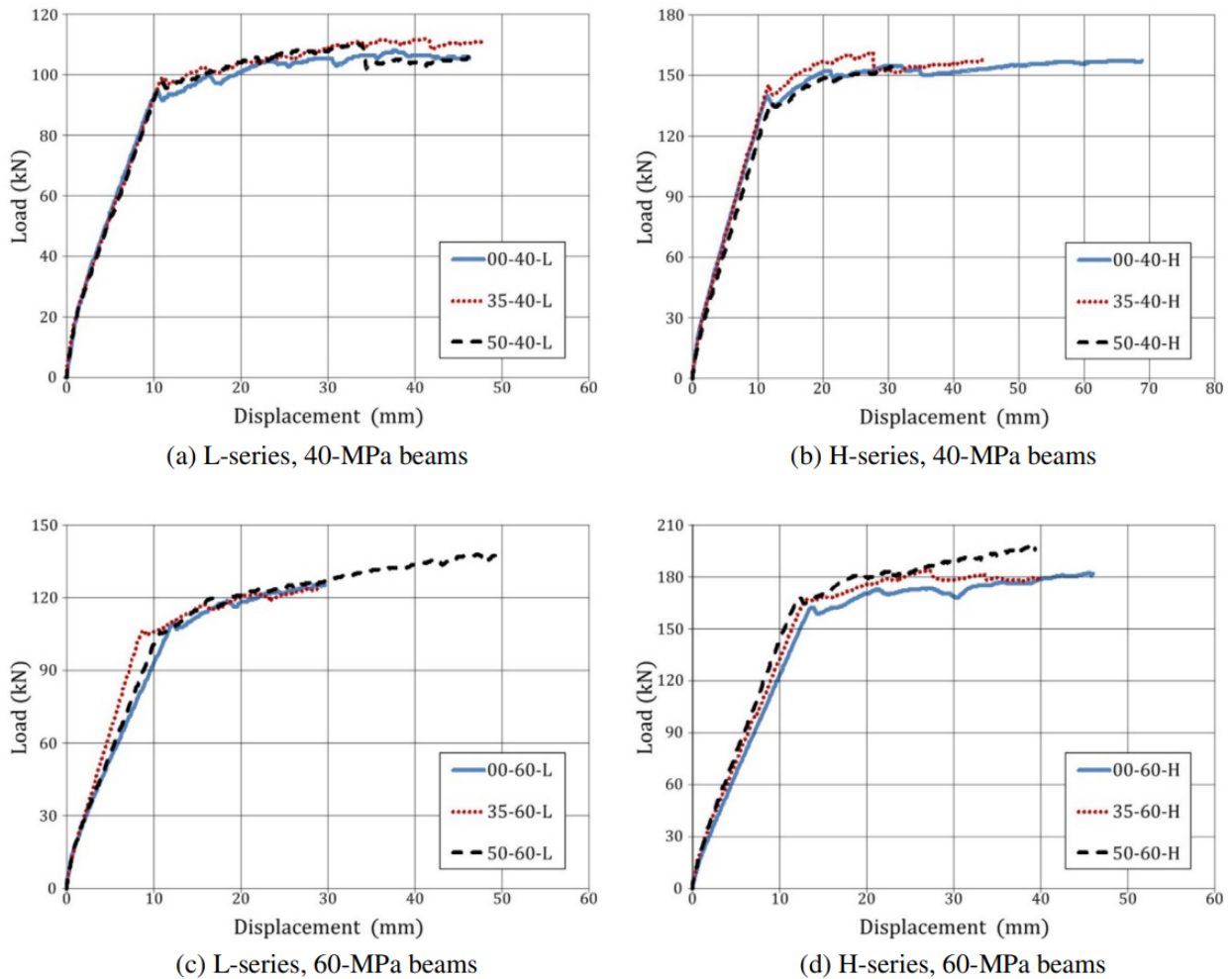
Figure 2.4: Comparison of load–displacement curves of test members **[Yoo et al., 2015].**

The effect of fly ash on the flexural behavior of reinforced concrete beams was explored by **[Sunayana and Barai, 2018].** The particle packed technique of composites was used in an approach to the flexure inquiry. This technique by the principle takes into account the additional mortar that adheres to the outer face of recycled coarse aggregates when predicting optimum packing density, hence reducing the demand for fresh mortar. For the examination of moment bearing capacity, deflection, and failure patterns, parameters like materials (aggregate kind and fly ash), mixed design technique, and percentage of reinforcement are analyzed. On the basis

of experimental data, a numerical evaluation of the constitutive relation for cracked and natural aggregate concrete demonstrates a tension stiffening effect. recycled coarse aggregates beams with fly ash and natural aggregate concrete beams have the same moment carrying capability at the ultimate limit condition, the results show. Fly ash in recycled coarse aggregates have been shown to increase the maximum midspan deflection, however this difference is negligible under service load. Cracked concrete's expected stress-strain relationship supports recycled coarse aggregates higher midspan deflection because of the lessened tension-stiffening effect. Code requirements for natural aggregate concrete beams with fly ash beams are being reexamined for their current application. Results reveal that 100 percent reused coarse aggregates and up to 30 percent fly ash may be utilized in a reinforced concrete beam without impairing its flexure behavior.

The influence of locally available pozzolan on the resistance to corrosion of steel in reinforced concrete beams was examined by **[Nguyen et al., 2020]**, who split eight RC beams with sizes of 10 cm by 15 cm in cross-section; and 100 cm in length into 2 sets. For every set, ordinary Portland cement was partially substituted with locally generated fly ash in quantities of 0 percent (control samples), 10 percent, 20 percent, and 40 percent by weight, respectively. After curing, reinforcing steel bars were weighed and exposed to expedited corrosion using an anodically impressed voltages of 10.0 V DC (Set 1) and 20.0 V DC (Set 2) for 378 hours. The results reveal that fly ash generated from Vietnam considerably increases the corrosion resistive of reinforcing steel, with a greater fly ash replacement producing strong resistance to corrosion. With partial cement replacement by fly ash, the flexural strength of pre-corroded reinforced concrete beams is enhanced by up to 16 percent for Set 1 and 120 percent for Set 2.

Using load-deflection diagrams from the tests of reinforced concrete (RC) beams and slabs, **[Hashmi et al., 2020]** evaluated the flexural behavior of high-

volume fly ashes (HVFA) concrete components. A total of 32 slabs and beams, eight out of each mixed group, were cast using fly ash replace percentages ranging from 0.0% to 60.0% for two plain concrete categories. The RC beams were exposed to a 4-points bending test until failure, whereas the central load was given to slab samples. After 28 days of cure, structural modules are tested. Determining the center deflections, cracking patterning, yielding, and final state properties of RC beams and RC slabs. In furthermore, the finite element simulation of RC beams and RC slabs with static stress was done using the ABAQUS 2017 program, and the results have been compared to the experimental data. The yielding and final condition of RC concrete with HVFA goes the same manner as RC concrete without HVFA. The measured load-deflection performance and cracking patterning of plain and fly ash concrete reinforced concrete (RC) beams and slabs are in reasonable agreement with the numerical model. The cracking patterns of RC beams and slabs made with or without fly ash are equivalent. However, the cracks are bigger in HVFA concrete structural components, such as RC slabs and beams.

2.5   Strengthening technique for beams

The goal of the repair work and strengthening procedures is to enhance the behavior of the concrete elements, re-establish and strengthen the strength and stiffness of the concrete, enhance the look of the concrete surface, make the concrete more watertight, stop corrosive materials from getting to the reinforcing, and rise the concrete members' total durability.

2.5.1 FRP strengthening

The correct repair of deteriorating concrete structures is predicated on a thorough study of the causes and effects of the degradation, as well as the techniques, processes, and materials employed for repair or strengthening. The costs and simplicity of

application, in addition the effectiveness of the repair process, play a significant role in the selection of materials and processes. Several methods can be utilized to retrofit a reinforced or broken structure to an acceptable level of function at an affordable cost. Repairing or strengthening concrete beams by trying to apply repairing methods to the tension side of the beam (like using reinforcement concrete layers, plates of steel, and FRP (Fiber-reinforced polymer) wrapping laminates, that also are among the most commonly used repairing or strengthening methods for beams). The primary purpose of the underneath layer is to boost the concrete beam's load capacity. Depending on the type of wrapping layer employed, stiffness and strength are enhanced. As with any other strengthening or mending procedure, the design of the underlying layer must account for the additional stresses that may impact the beam as well as the connection between the repairing material and the concrete face. The new concrete should have the same compressive strength as the previous structure **[Bashandy, 2013].**

This strategy is applicable in several ways. Typically, the lower face of the concrete beam is covered with a mending layer that is adhered to the beam's tension face. Ferrocement is a good material for structural rehabilitation and reinforcement. It enhances fracture resistance in conjunction with high toughness, the capacity to be cast into any form, quick production without the use of heavy gear, a minimal increase in weight, and inexpensive construction costs. Steel plate repair and reinforcement is regarded as one of the most effective rehabilitation techniques. Plate end anchorages exert a higher influence on shorter beams having a high-shear forces to bending moments ratios than on longer beams. Typically, anchors consist of anchor bolts or bonded cover plates. The method of reinforcing reinforced concrete members by continuously connecting a FRP strip not only has the benefit of being quick, but it also incorporates the essential anchoring mechanism. The use of several little fasteners as opposed to a single large fastening bolts with a larger diameter distributes the load more equally over the strip **[Bashandy, 2013].**

Four different repair operations were investigated: epoxy injections, ferrocement, steel plate bonding, and a mixture of epoxy system installed and ferrocement. The results revealed that beams rebuilt by ferrocement layer, steel plate bonding, and a mixture of epoxy system installed and ferrocement had greater flexural strength than their original counterparts. The flexural strength and cracking behavior of the epoxy injection-repaired beams were identical to those of the original beams. A larger number of fractures and finer cracks were seen in rehabilitated beams compared to unrehabilitated beams, indicating that the ferrocement layer or epoxy injection in conjunction with a ferrocement layer provided enhanced cracking behavior. The lower ductility of beams enhanced with plate bonding can result in rapid failure, which can be mitigated in part by modifying the design of the steel plate to provide a more ductile failure **[Bashandy, 2013].**

2.5.2 Steel fiber strengthening

[Abdul-Rahman et al., 2018] invistigated the effect of the addition of fly ash particles with different weight ratios of 15%, 20%, and 25% as well as the addition steel fibers with different volume fractions of 0.25%, 0.75%, and 1.25% on the mechanical properties of concrete (compressive strength and modulus of rupture) was studied. To carry out this research, ten concrete mixes were prepared, one of which is the reference normal concrete (without any additives), the others contain steel fibers and fly ash as additives with the mentioned volumetric and weight proportions. For each type of concrete mix, three standard 150×300 mm cylinders and three standard prisms $100 \times 100 \times 500$ mm were casted, water to cementing material ratio was fixed for all concrete mixes (W/cm = 0.435) and the superplasticizer was used with ratio of 0.98%-1.22% by weight of the cementitious material in mixtures that contain steel fibers and fly ash particles as a partial replacement of cement weight. The results showed that the addition of fly ash particles had little effect on the mechanical properties of normal

concrete, while the steel fibers had the greatest effect. The highest increase in compressive strength and flexural strength compared with reference concrete was 61.60% and 78.84%, respectively in the volume fractions 1.25% of steel fiber.

Utilizing deformed fibers, such as hooked, corrugated, and twisted fibers, can further boost the mechanical strength of composite materials. Reportedly, deformed steel fibers give three to seven times the fiber-matrix binding strength of straight fibers. Several factors, including fiber shape, fiber length, and curing conditions, influence the degree to which mechanical properties are enhanced. The following conclusions can be derived from the study's findings: The addition of SF significantly reduced the flowability of ultra-high-performance concrete, the flowability steadily reduced as the volume of fibre raised, the incorporation of distorted fibres could also decrease flowability, compressive and modulus of rupture increased with fibre volume and age, and the compressive strength (CS) and modulus of ruptures of fibreless ultra-high-performance concrete samples were 111 MPa and 23 MPa after 90-d, respectively. With the addition of 2.5 % straight SFs, the equivalent values increased to 165 MPa and 42 MPa, respectively **[Mohammed et al., 2020].**

[Ali et al., 2022] investigated the impact of steel fibers on the engineering characteristics of concretes were explored experimentally in this work. Steel fibers of 0.5, 0.7, and 0.9 percent by volume fraction were applied to concretes mixture with water/cements (W/C) proportions of 0.43 to accomplish this. There have been a total of 24 cubic specimens produced for compressive strengths testing, 24 cylindrical specimens for splitting tension strengths testing, and 12 cubic specimens for toughened unit weight testing. The experimental findings reveal that applying 0.5 percent to 0.9 percent of fibers made of steel to concrete boosts both compressive and tension strengths concurrently when compared to ordinary concretes; however, there is no discernible gain in hardened unit weight with increased fiber amounts.

2.5.3 Hybrid strengthening

In order to improve its flexural ductility, and at the same time retain the high strength feature of the FRP bars, **[Lau and Pam, 2010]** proposed that steel longitudinal reinforcement should be added to form a hybrid FRPRC beam. Twelve specimens consisting of plain concrete beams, steel-reinforced concrete (SRC) beams, pure FRPRC beams and hybrid FRPRC beams were fabricated and tested. The test results show the hybrid FRPRC beams behave in a more ductile manner when compared with the pure FRPRC beams. Also, it is observed that a higher degree of over reinforcement in the beam specimen resulted in a more ductile FRPRC beams. Hence, the addition of steel reinforcement can improve the flexural ductility of FRPRC members, and over-reinforcement is a preferred approach in the design of FRPRC members.

2.6   Reinforced concrete beams with FRP

Steel plate bonding technology inspired the concept of bonding fiber-reinforced polymer (FRP) or composite plates to strengthen concrete constructions. This kind of material is an excellent counterpoint to steel since it prevents plate corrosion at the interface. Small fibers joined together with a resin matrix make up the constituent ingredients in commercially available (FRP) systems. The resins are utilized to saturate the reinforcing fibers, fix them in place, and provide a load path for effective load transfer between the fibers. Polyesters, vinyl esters, and epoxies are the most frequent resins utilized. The physical characteristics of the fiber composite are determined not only by the characteristics of the components but also by their relative proportions and fiber orientation. There are three types of Fiber Reinforced Polymer: Glass Fiber Reinforced Polymer (GFRP), Carbon Fiber Reinforced Polymer (CFRP), and Aramid Fiber Reinforced Polymer (AFRP). This Figure presents the linear elastic behavior of FRP, which has a higher tensile strength in the limit of (2400 - 3400) MPa. The shear

forces formed among the fibers are restricted to the properties of the matrix. In addition, the matrix limits the applying forces vertical to the fibers **[Valerio, 2009].**

Due to the significant advantages of carbon fiber reinforced plastic (CFRP) over usual construction materials such as steel and concrete, these materials have grown in popularity as reasonable options for retrofitting and reinforcing concrete buildings. Typically, these composites are utilized as "externally bonded" systems to increase the axial sectional, flexural, torsion, and shear capacities of the structural elements of the reinforced concrete, to improve the structural members' stability and serviceability, and to provide additional confinement. The concrete surface is then coated with CFRP materials. This approach of external reinforcement is uncomplicated and easy to implement. For new structures, there are three types of CFRP reinforcements: (1) internal reinforcement using CFRP bars, (2) permanent CFRP formwork for RC members, and (3) CFRP tendons for prestressed concrete components, **[Sharifianjazi et al., 2022].**

2.6.1 Experimental studies on reinforced concrete beams with FRP

Since **[Meier, 1987],** the Swiss Laboratories for Materials Testing and Research have been performing studies incorporating bonded CFRP to reinforced concrete beams. This program comprises the substitution of steel plates with FRP laminates for the repair and strengthening of reinforced concrete beams. Prior research centered on the strength and rigidity of beams constructed with unidirectional carbon fiber composite plates.

[Duthinh and Starnes, 2001] examined the tensile strengths and ductility of a prismatic concrete beams enhanced with carbon-fiber-reinforced polymers and reinforced with steel. Under four-point bending, seven concrete beams were strengthened inside with varied quantities of steel and external carbon fiber reinforced polymer (FRP) laminates added just after concrete had cracked due to service loads.

Strains observed along the beam depth made it possible to calculate the beam's curvature in the zone of constant moment. According to the findings, FRP is highly efficient for flexural strengthening. As the quantity of steel increases, the carbon FRP laminates provide less additional strength. Despite their brittle failure mechanism, beams reinforced with the both steel and carbon have a considerable deformation capacity compared to those reinforced with steel alone. Clamping or wrapping the laminate's edges increases the strength of adhesively bonded FRP anchoring. Anchorage, permissible stress, ductility, and reinforcement quantity design formulae were addressed. The curvature at ultimate load of beams reinforced with steel and carbon FRP varies between 1.43 and 1.86 times that of a beam with a steel reinforcement ratio of 75 % of the balanced ratio (maximum allowed by ACI). Thus, beams reinforced with steel and carbon FRP have adequate deformation capacity in spite of their brittle failure modes (concrete crushing, laminate debonding or delamination).

By mechanically attaching fiber-reinforced polymer strips, **[Lamanna et al., 2004]** examined the flexural strengthening of reinforced concrete beams. The existing process for gluing fiber-reinforced polymer (FRP) strengthening strips to concrete buildings needs substantial time and semiskilled labor. Attaching FRP strips to concrete using a commercially available powder-actuated fastening system is an alternate option. Fifteen reinforced concrete beams were subjected to a battery of flexural tests. Each beam has dimensions of (304 x 304 x 3657) mm. Two unreinforced beams, twelve beams reinforced with mechanically affixed FRP strips, and one beam reinforced with a bonded FRP strip were evaluated, as well as the impacts of three different strip moduli, different fastener lengths and designs, and pre-drilling are all investigated. Three of the beams reinforced with mechanically attached fiber reinforced plastic strips demonstrated equivalent strength to the beam reinforced with bonded fiber reinforced plastic strips. The three identical beams reinforced with

mechanically attached FRP strips were likewise more ductile than that of the beam reinforced with bonded FRP strips, indicating that mechanically linked FRP strips were superior.

Whereas early laboratory and field research on the use of NSM FRP to reinforce concrete buildings was undertaken with circular FRP bars, more current research has utilized rectangular or square NSM FRB strips or bars. This novel strategy was developed to obtain higher stresses in FRP prior to debonding failure. Due to the three-dimensional distribution of bond stresses created in the concrete surrounding the NSM strips as contrasted to the NSM bars **[Al-Mahmoud et al., 2009]**, NSM FRP strips often have a greater average bond strength than round bars, assuming all other conditions are equivalent. The NSM technique using CFRP rods is very effective in strengthening reinforced concrete beams in shear. When using only one surface pre-conditioned CFRP rod, the increase in shear strength compared to beams reinforced with stirrups only was about 43.6% when using an epoxy resin as filling material and about 34.6% when using a mortar. But, as already reported by other authors, shear capacity of the beams raises a lot by increasing the number of NSM CFRP rods in the shear zone. Results show that epoxy resin still performs better than the mortar but the gain is only moderate. Interface between mortar and surface pre-conditioned CFRP rod performs very well as the failure occurred at the interface between the mortar and the substrate concrete. Increasing the surface roughness of the groove in the substrate concrete could be considered in order to improve the strengthening performance.

In generally, the surface features of NSM reinforcement induce frictional forces and mechanical interlocking that influence bonding behavior. **[Lee et al., 2012]** conducted a bond test based on the strain resulting from sand coated, ribbed, roughened, spirally coated with sand, and smooth surface treatments. For each type of surface treatment, there are at least nine unique failure modes, including a mix of cracking, splitting, and FRP fracture.

Experimentally and analytically, **[Lin and Zhang, 2013]** examined the flexural and bond--slip properties of fiber reinforced polymer (FRP) reinforced concrete beams. Reinforced concrete beams enhanced with carbon fiber, glass fiber, and basalt fiber rebars are tested to examine their flexural and bond-slip characteristics. Finite element models with and without the bond–slip phenomenon have recently been constructed by researchers, the flexural and bond-slip behaviors of the test beams are examined computationally. The results of numerical modeling and experimental study are very consistent. To examine the effect of various rebar surfaces and kinds on the structural behavior of FRP-reinforced concrete beams, a parametric study is performed. **Figure 2.5** exhibit the longitudinal and cross sections of the test beams, respectively. The results suggest that the wrapped rebar surfaces of the BFRP reinforced concrete beams have high adhesion with the concrete. They have significantly better load bearing capacities prior to load–slip curve decay than CFRP- and GFRP-reinforced concrete beams, whose load–slip curves decay abruptly at considerably lower load values. **Table 2.1** illustrates the properties of beams. **Figure 2.6** shows the load–deflection relationships at mid-span of CFRP, GFRP and BFRP reinforced concrete beams.

Table 2.1: Properties of beams, **[Lin and Zhang, 2013].**

Beam	f_c (MPa)	E_c (GPa)	Age (days)
BC1	48.24	32.54	126
BG1	51.75	33.49	110
BG2	44.51	28.71	55
BB1	53.84	32.54	107
BB2	50.98	32.72	130
BB3	45.10	29.57	57
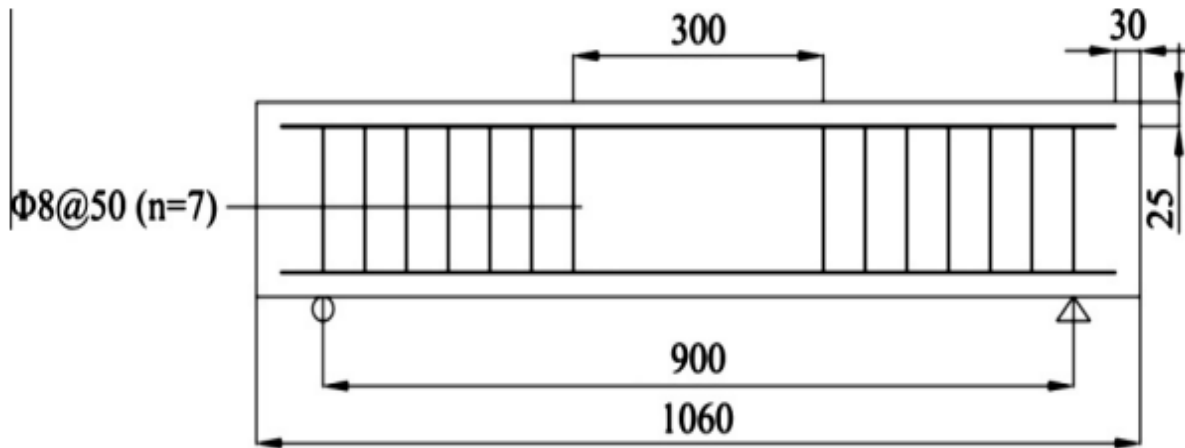
Figure 2.5: Profile section of the test beams (units: mm), **[Lin and Zhang, 2013].**
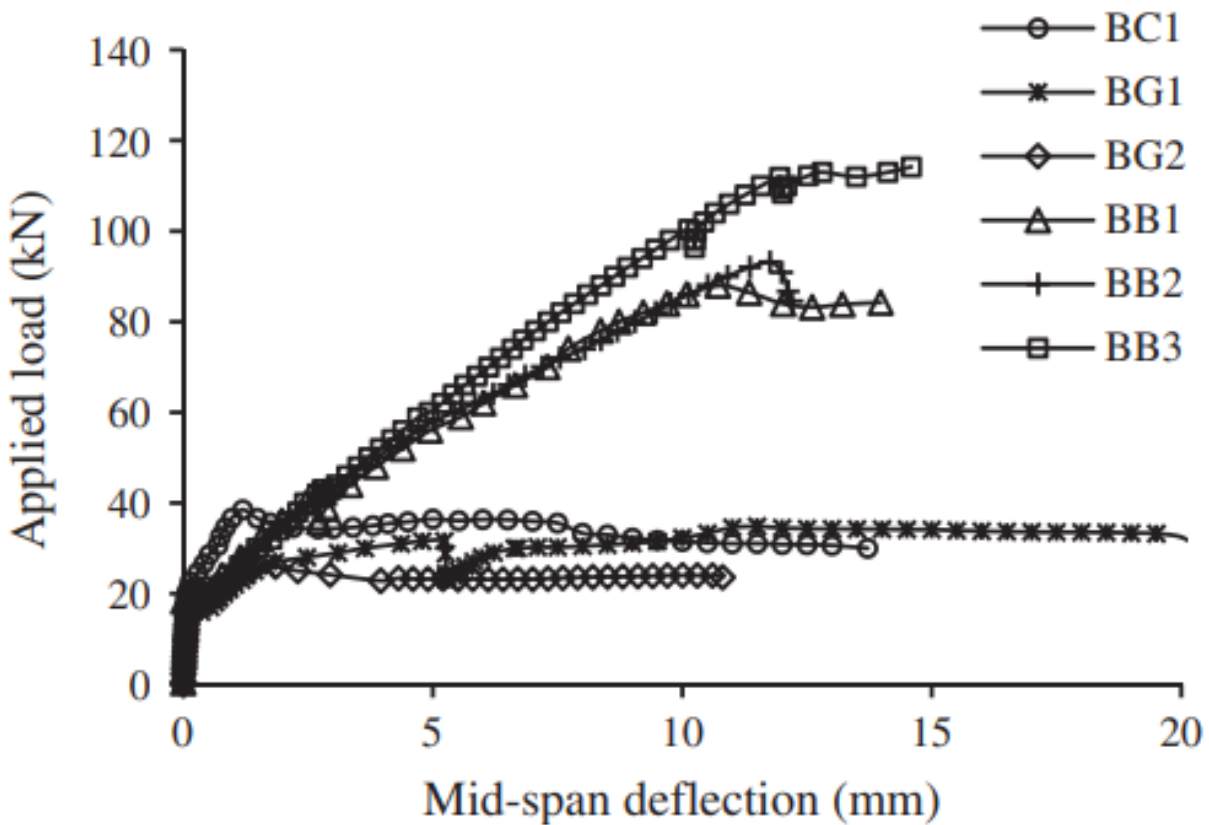
Figure 2.6: Load–deflection relationships at mid-span of CFRP, GFRP and BFRP reinforced concrete beams, **[Lin and Zhang, 2013].**

[Karayannis et al., 2018] studied the behavior of seven slender concrete beams reinforced with carbon-FRP bars under increasing static loading is experimentally

investigated. Load capacities, deflections, pre-cracking and after-cracking stiffness, sudden local drops of strength, failure modes, and cracking propagation have been presented and commented. Special attention has been given in the bond conditions of the anchorage lengths of the tensile carbon-FRP bars. The application of local confinement conditions along the anchorage lengths of the carbon-FRP bars in some specimens seems to influence their cracking behavior. Nevertheless, more research is required in this direction. Comparisons of experimental results for carbon-FRP beams with beams reinforced with glass-FRP bars extracted from recent literature are also presented and commented. Comparisons of the experimental results with the predictions according to ACI440.1R-15 and to CSA S806-12 are also included herein. **Table 2.2** illustrates the characteristics of the tested beams and experimental results. **Figures 2.7** and **2.8** show the geometry, reinforcement, and cross-section details of beam specimens and application of local confinement along the anchorage length of the C-FRP bars respectively, while **Figure 2.9** show the Comparison of the load to midspan deflection curves of the tested beams.
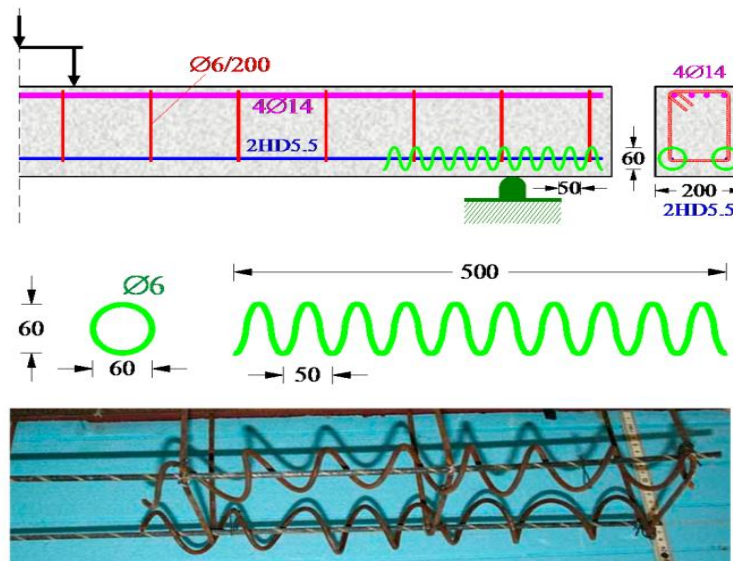
Figure 2.7: Application of local confinement **[Karayannis et al., 2018].**

Table 2.2: Characteristics of the tested beams and experimental results.

[Karayannis et al., 2018]

Group	Beam Name	Type and Diameter	Tensional Bars			Experimental Results			
			ρ [1] (%)	ρf [2] (MPa)	ω [3]	P_{exp} (kN)	$V_{exp} = M_{exp}$ (kN) or (kNm)	δ_{peak} (mm)	Observed Failure [4]
"S"	S10	2Ø10	0.39	2.16	0.07	*30.6 ** 35.0	*15.3 ** 17.5	*6.0 ** 62.8	Y
	S12	2Ø12	0.57	3.11	0.11	*45.2 ** 53.6	*22.6 ** 26.8	*11.1 ** 63.8	Y
"BF5"	BF5-0	2HD5.5	0.12	2.14	0.07	51.6	25.8	49.5	F-R
	BF5-1	2HD5.5	0.12	2.14	0.07	53.6	26.8	65.5	F-R
	BF5-2	2HD5.5	0.12	2.14	0.07	52.4	26.2	64.6	F-R
"BF10"	BF10-0	2HD10	0.39	7.07	0.24	82.8	41.4	38.4	S-T
	BF10-1	2HD10	0.39	7.07	0.24	84.4	42.2	51.1	S-T

[1] Geometrical reinforcement ratio: ρ_s for the steel bars and ρ_f for the C-FRP bars. [2] Geometrical reinforcement ratio × tensile strength: $\rho_s f_y$ for the steel bars and $\rho_f f_{fu}$ for the C-FRP bars. [3] Mechanical reinforcement ratio: $\omega_s = \rho_s f_y / f_c$ for the steel bars and $\omega_f = \rho_f f_{fu} / f_c$ for the C-FRP bars. [4] Failure mode notation: Y: Typical flexural failure after steel Yielding with adequate ductility; F-R: Flexural failure due to the rupture of the carbon fibers of the C-FRP bars; S-T: Shear failure due to the diagonal Tension cracking. * Test results at steel yielding.
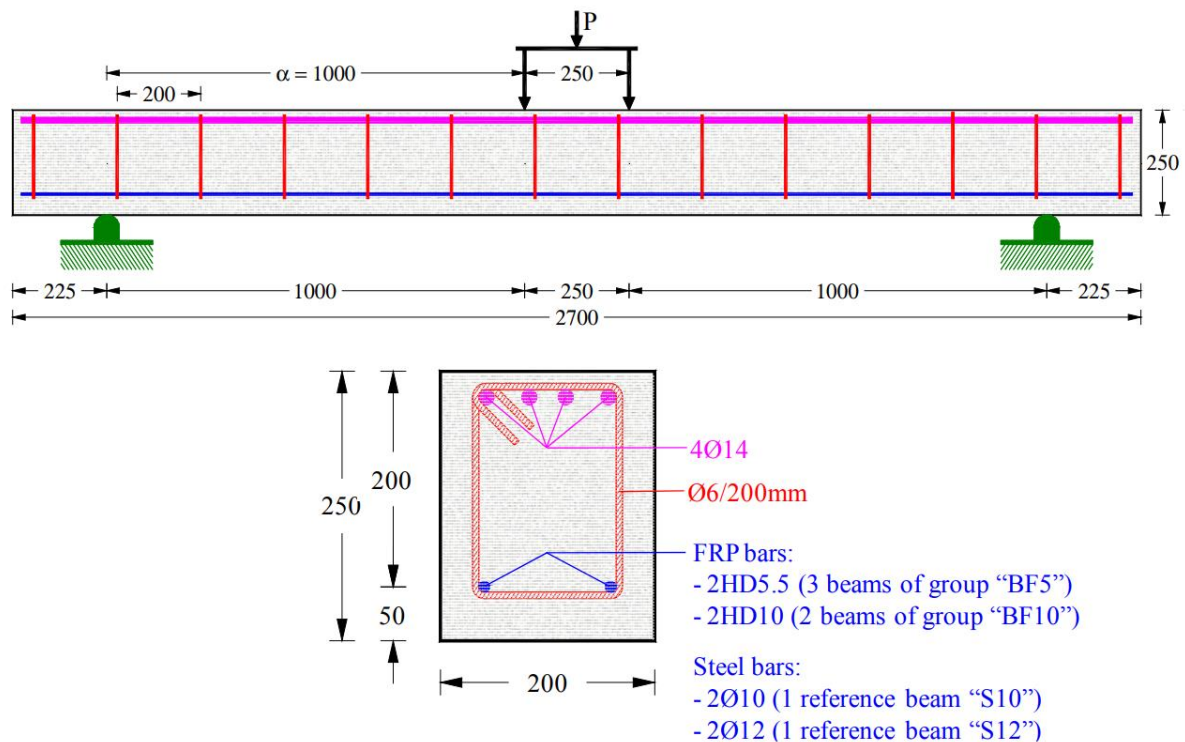
Figure 2.8: Geometry, reinforcement, and cross-section details of beam specimens (dimensions in mm). **[Karayannis et al., 2018]**
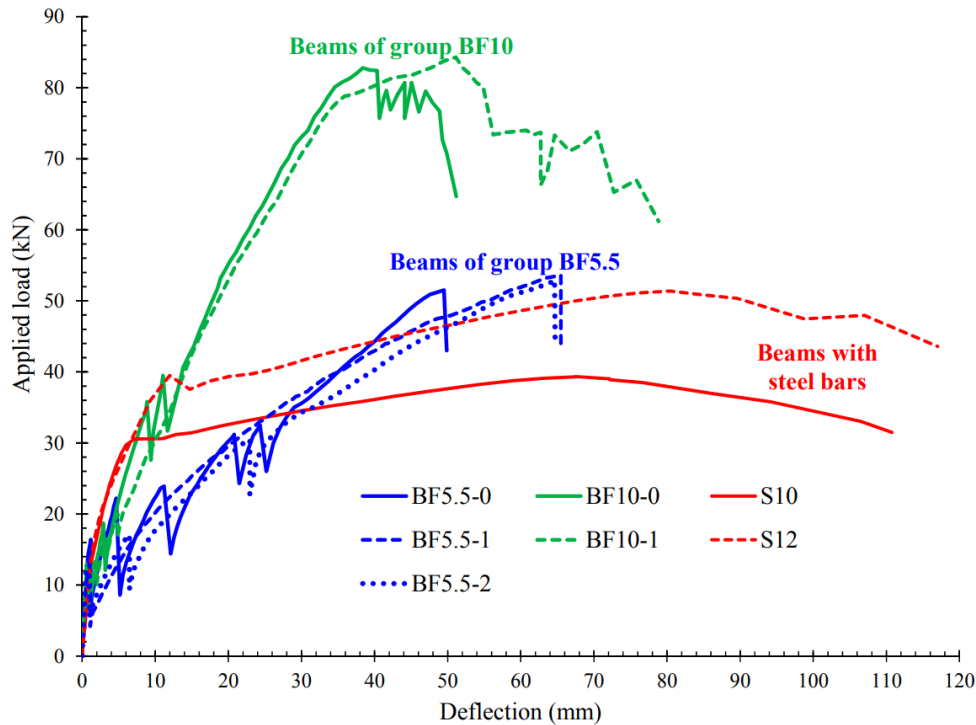
Figure 2.9: Comparison of the load to midspan deflection curves of the tested beams**. [Karayannis et al., 2018].**

[Sun et al., 2019] examined the flexural behavior of reinforced concrete beams utilizing hybrid steel/FRP bundles. Five concrete beams were used in the experiment, each one having a unique combination of bundled reinforcements of a different kind. After the steel bar broke, all of the beams displayed concrete crushed failure modes, with the plastic expansion of the steel bar being limited by the FRP bar. The binding behavior between the main reinforcement and the surrounding concrete declined as the concentration of the main reinforcement increased. As a result, the post-cracking stiffness and crack amount of the related concrete beam fell, whereas the crack width broadened. The initial and post-yield stiffness of the concrete beam with three-bar bundles was roughly fifty percent of that of the beam with two-bar bundles. Compare this to the beam with two-bar bundles. The displacement ductility of every single concrete sample was greater than 6.0 millimeters. The ultimate displacements of the beams with three-bar bundles and six-bar bundles were roughly 1.60 and 1.90 times

that of the beam with a single bar of reinforcement, respectively. This was because of the variations in bond behavior between the three-bar and six-bar bundles. Every single one of the test specimens was built in the form of a simply supported rectangular beam with a cross-section of 220.0 millimeters by 300 millimeters. The beam had a total length of 2200.0 millimeters, **Figure 2.10**, with a pure bending length of 600 millimeters and a concrete cap of 20 millimeters. The mean compressive strength of the three 150 mm 150.0 mm 150 mm concrete cubes was around 43 MPa. The results indicate that when the number of bundled bars in a concrete beam grows, the number of cracks drops and the crack width correspondingly increases dramatically. The concrete beams with longitudinally bundled reinforcement showed cracks that were practically spread symmetrically, and the fracture width expanded at a quicker rate when the steel bars yielded. **Figure 2.11** shows the several strengthening techniques of this study. **Figures 2.12** and **2.13** illustrate the load-deflection curves of beams.
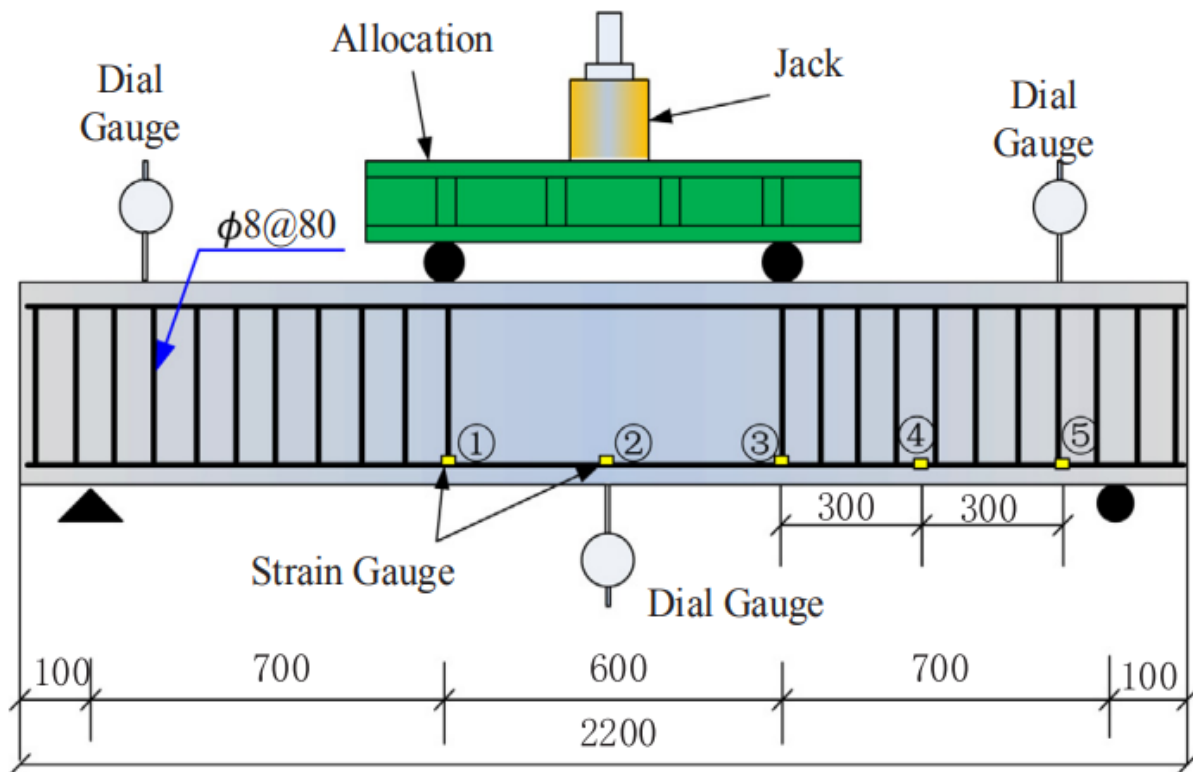
Figure 2.10: Test specimen's design and loading (in millimeters), **[Sun et al., 2019].**
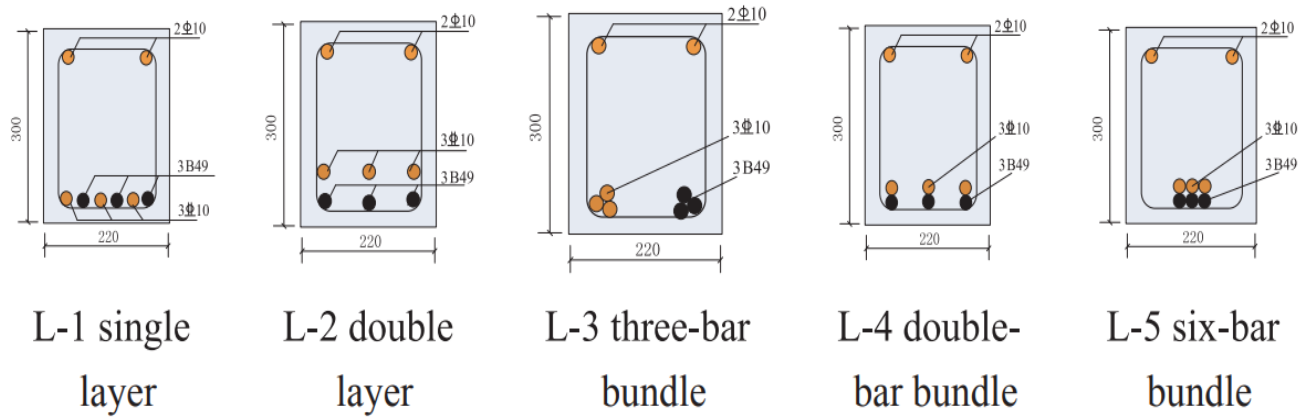
Figure 2.11: Several strengthening techniques for concrete beams (in millimeters), **[Sun et al., 2019].**
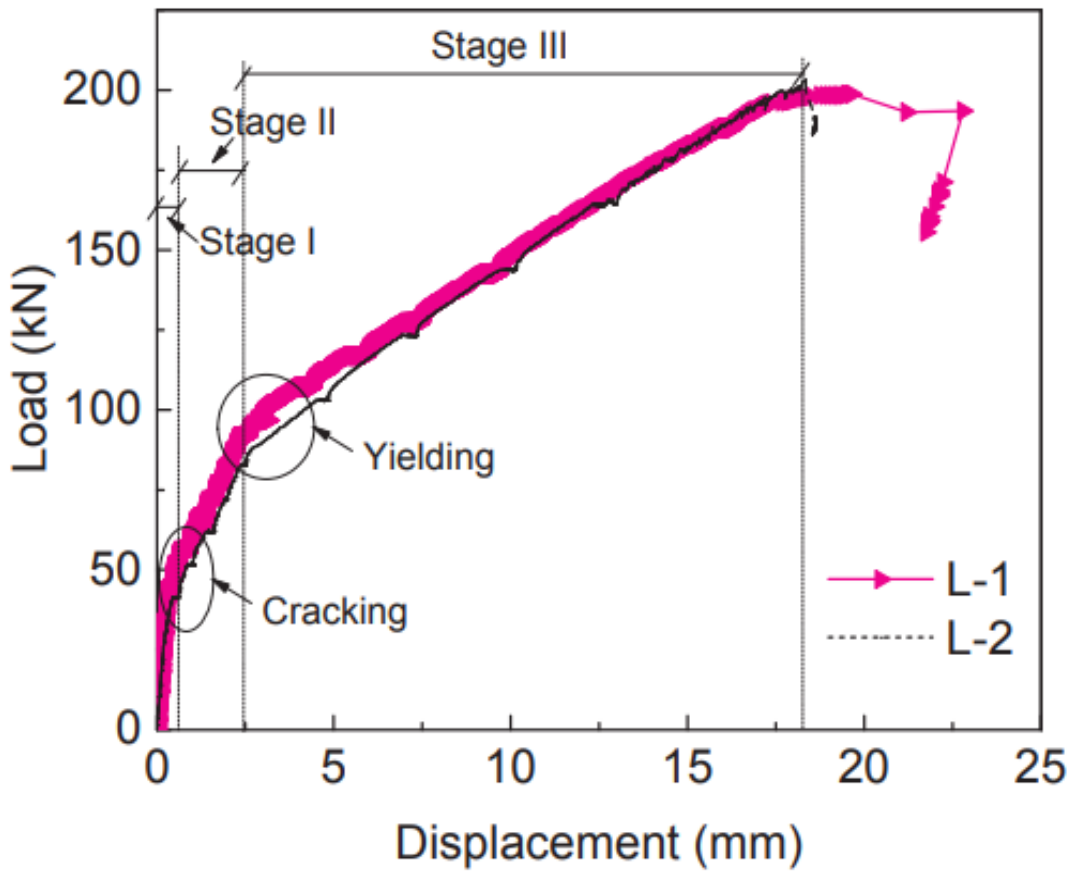
Figure 2.12: Load-deflection curves of L-1 and L-2, **[Sun et al., 2019].**
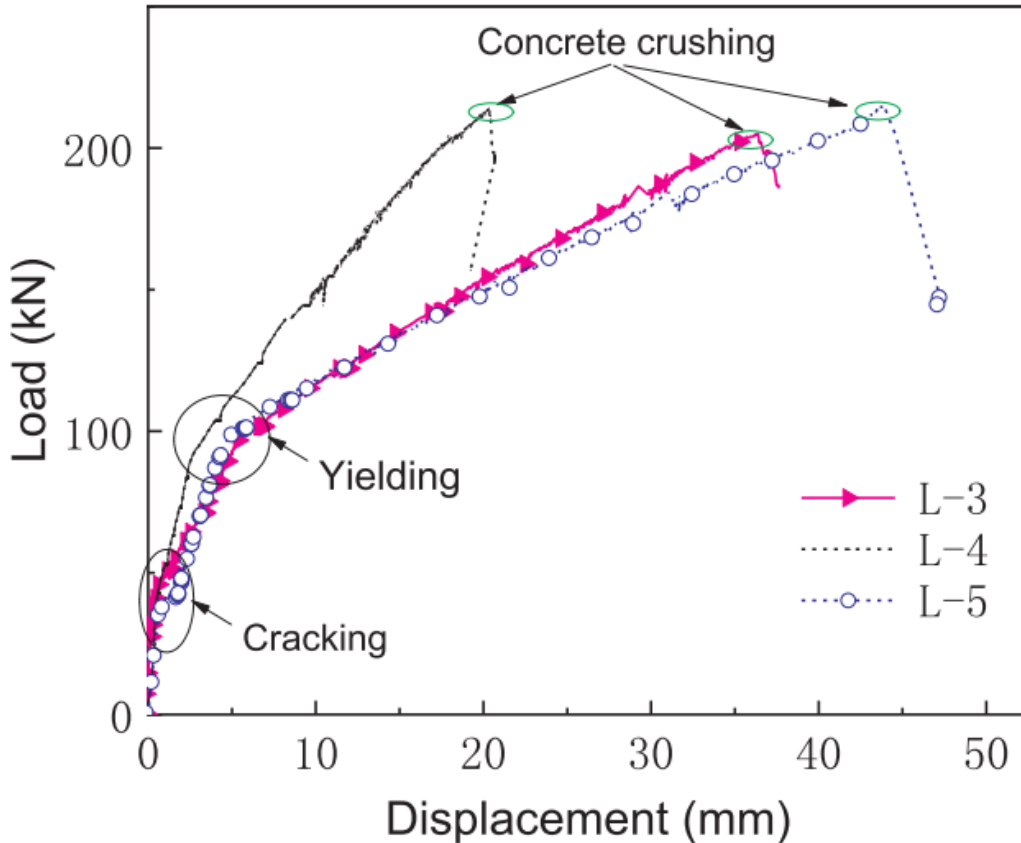
Figure 2.13: Load-deflection curves of L-3, L-4 and L-5, **[Sun et al., 2019].**

An investigation into the flexural behavior of internally reinforced (GFRP) RC beams that were supplemented with Carbon Fiber Reinforced Polymer (CFRP) strips utilizing the Near-Surface Mounted (NSM) technique was made available as part of a research plan, **[Barris et al., 2020]**. Cracked section analysis is used to determine their theoretical load-carrying capability. In addition, analytical study was undertaken to determine the impact that a variety of factors have on the flexural capacity of NSM CFRP reinforced concrete beams that have either steel or GFRP bars installed inside as reinforcement. In most cases, a greater flexural capacity may be achieved by increasing the reinforcement ratio as well as the internal or NSM mechanical qualities. Nevertheless, a modification in the parameters might affect the rise ratios differently and lead to distinct failure scenarios. **Figure 2.14** depict the configuration and test equipment for reinforcements. The results indicate that the experimental failure load

is predicted pretty well by analytical assumptions, with a mean ratio of 0.95 between the experimental and theoretical loads. The variation of this ratio might be attributable to the smaller-than-0.003 ultimate concrete strain observed in some beams (considered in the theoretical calculations).
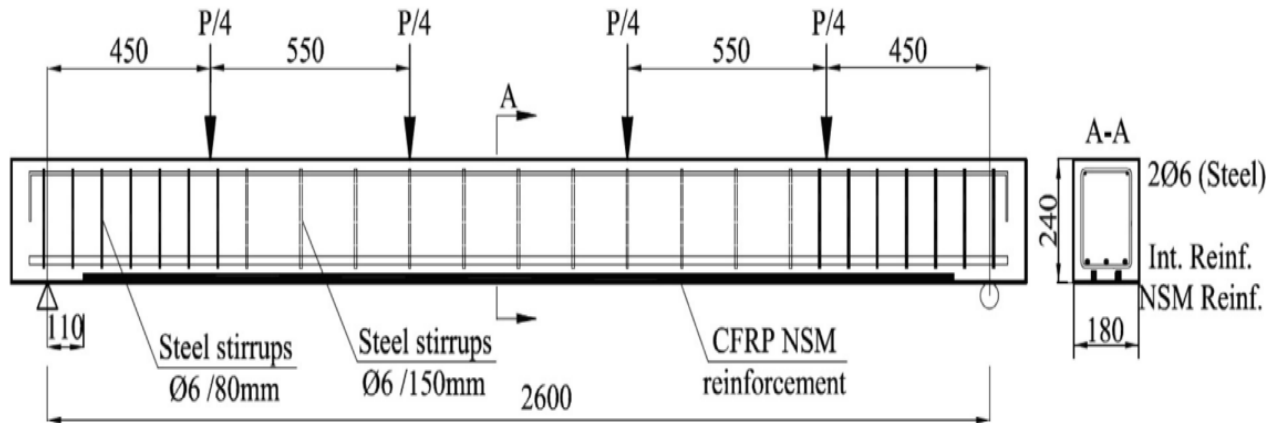
Figure 2.14: Reinforcement arrangement and test setup, **[Barris et al., 2020].**

[**Yang, et al., 2021**] carried out an experiment to investigate the viability of strengthening beams with corroded reinforcement by applying directly FRP laminates that were externally linked to one another and were coupled with U-jackets. This was done without first repairing the damaged concrete cover. The four-point bending tests were performed on ten different beams. As standards, we utilized two beams that were both undamaged and unreinforced. The remaining eight were subjected to preloading in order to bring about flexural fractures, which were then followed by fast corrosion. On the beam soffits of the six damaged beams, two of them did not have any reinforcement, three of them had laminates made of glass-fiber reinforced plastic (GFRP), and the remaining three had plates made of carbon-fiber-reinforced plastic (CFRP). CFRP U-jackets were installed on each of the six reinforced beams that ran the length of the bridge. A 3D-scanning technique was used to do an analysis of the local corrosion levels. As a result of pitting corrosion, the load-bearing and

deformation capabilities of the beams were significantly reduced. In spite of the fact that the mean corrosion levels were 20 percent, local corrosion levels were as high as 57 percent, and corrosion-induced cracks were as wide as 1.9 millimeters, the FRP strengthening technique was successful in increasing the load-carrying capacity and stiffness of the samples (it was applied directly to the beams without repairing the deteriorated concrete cover). Due to the effectiveness of the U-jackets in preventing the delamination of the concrete cover, the GFRP laminates were broken, and the usage rate for the CFRP plates was increased to as high as 64 percent. Despite this, there was no observable enhancement in the material's power to resist deformation; this calls for more research.

The last experimental study investigated the feasibility of using externally bonded FRP laminates combined with U-jackets for flexural strengthening of deteriorated concrete beams with highly corroded steel reinforcement. The FRP-strengthening system was applied to the beams without repairing the deteriorated concrete cover. The efficiency of the FRP-strengthening method was evaluated based on the flexural behavior of the specimens subjected to four-point bending tests to failure. Based on the experimental results, the following conclusions were drawn:

1-The combined use of externally bonded FRP on beam soffits and CFRP U-jackets along the span was efficient in upgrading the load-carrying capacity of deteriorated concrete beams, even though maximum local corrosion levels of the reinforcement were up to 57%. For example, after strengthening, the ultimate load capacity of the deteriorated specimen DC2 increased to 212 kN, which was 417% and 165% higher, respectively, than that of deteriorated non-strengthened specimens and the reference beams.

2-The FRP-strengthening method was effective, even though it was applied directly to the beams without repairing the deteriorated concrete cover. Given that the maximum width of corrosion-induced cracks was up to 1.9 mm on the deteriorated concrete

cover, the applied U-jackets effectively suppressed the delamination of the concrete cover and led to the rupture of GFRP laminates and a utilization ratio of CFRP plates up to 64%. Compared to the utilization of 20–30% in most applications of externally bonded CFRP, the current strengthening efficiency was satisfactory.

2.7   Summary

Depending on the previous studies, can be conclude that all studies deal with the effect of individual mixes or multiple mixes of Pozzolanic materials with lime on behavior (physical, dynamic, volume change length, absorption and durability) properties of Lime Pozzolana mixture. It is observed that there is a delaying in setting time for lime Pozzolana mixture and the addition of superplasticizer accelerated the setting process. The decrease of the binder/aggregate ratio will lead to decrease in mechanical strength of lime Pozzolana mixes especially flexural strength. It could be also noticed that the compressive strength increases with decreasing of curing temperature.

The literature reviews clearly demonstrated that the FRPs can be used for the restoration and strengthening of reinforced concrete beams falling in shear as well as in flexure. The degree of percentage increase in flexural capacity of strengthened beams with FRP composite materials depends on the concrete compressive strength, steel reinforcement tensile strength, and tensile strength of the FRP. Using FRP decreases the propagation cracks width and prevent it from expansion.

NSM technique has been used for structures required strengthening or retrofitting in order to increase their live load bearing capacity. Carbon fibers are used for their high performance and are characterized by high strength. The benefit of using carbon fiber rods is to increase the structural strength, light weight about 1/5 weight of steel, and repair the damaged structures through the structural strengthening method.

Very limited literature is currently available on strengthening sustainable concrete beam. Also, no research is available to study the effect of applied NSM FRP rods in pozzolime concrete.

Chapter three

The experimental work

3.1   Introduction

In this section of the thesis, the experimental work is described and depicted. Specifications for material qualities, mix proportions, mixing process, casting, curing processes, beam specimens, and techniques of CFRP reinforcement and testing are provided.

3.2   Experimental program

Pozzolime is a patent-protected sustainable binder developed by **[Kadum et al., 2017].** This binder consists of hydrated lime, silica fume, and fly ash but no Portland cement; the compositions were chosen for two Pozzolime mixes based on prior research **[Kadum et al., 2017].** When Ca $(OH)_2$ is combined with pozzolan in water, a solution with a pH of around 12.5 is produced rapidly. In a solution with a high pH value and OH-, the pozzolan is melted and depolymerized into ions such as (Ca+2, K+, and Na+). Through the interaction of the depolymerized or dissolved aluminate species with mono-silicate, the following hydration products are formed:

$$Ca(OH)_2 \ + Pozzolan + Water \rightarrow Hydration \ products \ (gel) \qquad (3.1)$$

The experimental program comprised of testing 13 reinforced concrete beams designed as simply supported beam constructed using pozzolime concrete, in which one beam is considered as a reference beam that tested up to a failure to compare

results. All beams have similar dimensions and reinforcement. They have an overall length of 1400 mm, an effective span of 1300mm, a width of 120 mm, and a height of 200 mm. All specimens were tested under two-point loads. The beams are designed according to ACI (318-19**) [ACI 318, 2019]**, (For more details, see Appendix A). The primary reinforcement consisted of 2Ø8 mm as top reinforcement and 2Ø10 mm as bottom reinforcement rebar, one at each corner, while the stirrups started at a distance 20 mm from both ends and spaced at 60 mm, as shown in Figure (3.1). Specimens are divided into three groups plus a reference beam according to the strengthening techniques and the percent of added steel fibers used in each group, as given in Table (3.1). Plate 3.1 shows the internal all-strength (the length of the CFRP sheet is 1300 mm) and part-strength (the length of CFRP is the middle 850mm distance) layout. While Plate 3.2 shows the external all-strength and part-strength.
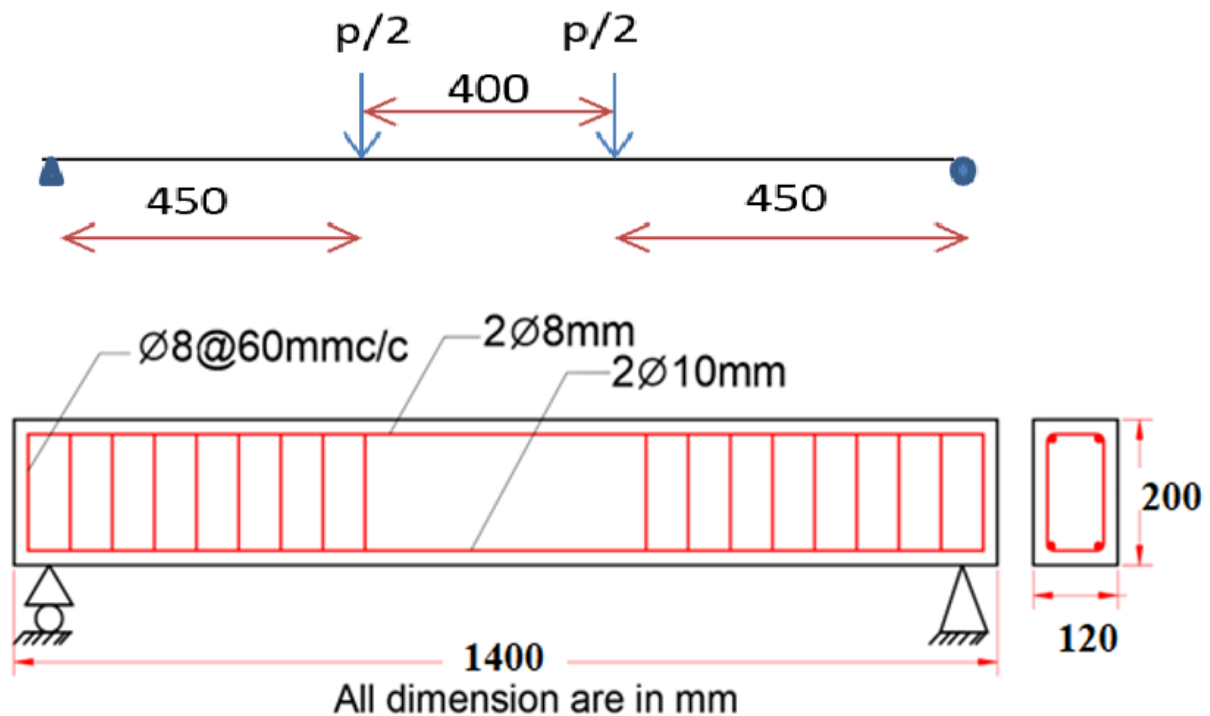
Figure 3.1: Schematic layout of beams and the details of steel reinforcement.

Table 3-1: Details of tested beams.

Group	Beam-ID	Added CFRP sheet type	Steel fibers%	Added CFRP sheet length
reference	B0	-	0	-
1	B0EA	external	0	All-strength
	B0EP	external	0	Part-strength
	B0IA	internal	0	All-strength
	B0IP	internal	0	Part-strength
2	B0.5EA	external	0.5	All-strength
	B0.5EP	external	0.5	Part-strength
	B0.5IA	internal	0.5	All-strength
	B0.5IP	internal	0.5	Part-strength
3	B1EA	external	1	All-strength
	B1EP	external	1	Part-strength
	B1IA	internal	1	All-strength
	B1IP	internal	1	Part-strength

Table 3.1 shows the details of the tested beams, where the letter B represents beam, the subsequent digit number 0, 0.5, or 1 implies the percentage of the added steel fibers. The next subsequent symbols show the added CFRP sheet type E or I (external or internal), while the last symbols show the added CFRP sheet length A or P (All-strength (100%) or Part-strength (65%)).
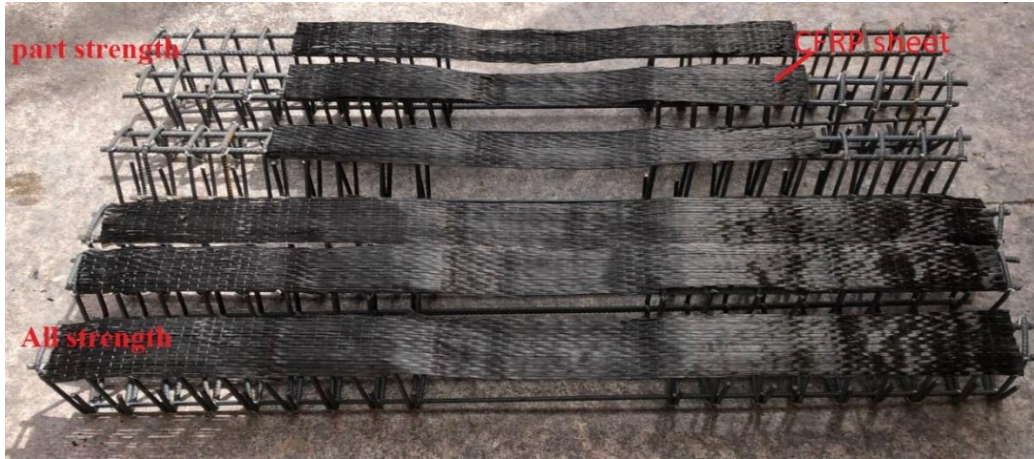
Plate 3.1: Internal all-strength and part-strength CFRP sheet.

Plate 3.2: External all-strength and part-strength CFRP sheet.

3.3   Materials

3.3.1 Hydrated lime

Hydrated lime is mostly made of calcium hydroxide Ca $(OH)_2$. Hydrated lime is employed in Pozzolime concrete compositions. The hydrated lime used has been manufactured by the Karbala cement and lime factory and meets Iraqi standard **[IQS No. 807 /2004].** The chemical analysis and physical tests are shown in Table 3-2.

Table 3-2: Chemical analysis and physical tests of hydrated lime*

	Components	Test results %	Limits IQS NO. 807
Chemical analysis	CaO + MgO	73.1	Minimum 65%
	SiO_2	2.28	
	Al_2O_3	1.08	
	Fe_2O_3	0.23	
	MgO	0.46	5% Max.
	$Fe_2O_3 + Al_2O_3 + SiO_2$	3.60	5% Max.
	SO_3	0.2	
	Loss on ignition	22.8	
	$Ca(OH)_2$	92.49	85% Min
	Available CaO % activity	70.12	
Physical test	CO_2 %	2.27	5% Max.
	Residue on 90µm	2.2	10 % Max.
	Slaking time Min.	24	5-30 Min
	Fineness m^2/kg	361	
	The tests were carrying in Karbala plant for cement and lime		

3.3.2 Cement

Sulfate-resisting Portland cement was employed in this study because it is widely accessible in commercial markets, and all underground construction must utilize sulfate-resistant cement. It is Iraqi cement and commercially known as Al-Jisier. It was employed in producing previous concrete mixes. The physical and chemical properties conform to limits of Iraqi standard **[IQS No.5/2019],** as shown in Table 3-3; and Table 3-4 below.

Table 3-3: Chemical composition and main compounds of Sulfate-resisting Portland cement [*]

Oxides composition	Content %	Limits of Iraqi standard No.5/2019
CaO	62.15	---
SiO_2	19.88	---
Al_2O_3	3.5	---
Fe_2O_3	4.7	---
MgO	3.23	<5.00
SO_3	1.84	<2.50
Na_2O	0.26	
K_2O	0.51	
L.O.I.	1.25	<4.00
Insoluble residue	0.80	<1.5
Lime Saturation Factor	0.928	0.66-1.02
Main compounds (Bogue's equations)		
C_3S	54.51	---
C_2S	18.77	---
C_3A	1.51	<3.50
C_4AF	14.14	---
* Chemical analyses were carried out in the Karbala Construction Laboratory.		

Table 3-4: Physical properties of cement[*]

Physical Properties		Test results	Limits of Iraqi standard No.5/2019
surface area (Blaine) m^2/kg		282	≥250
Setting time (Vicat),	Initial setting, hrs: min.	3:51	≥ 45 min.
	Final setting, hrs: min	6:20	≤ 10 hrs.
Compressive strength, MPa	2 days	23.7	≥20.00
	28 days	43	≥42.5
Soundness (Autoclave) %		0.13	≤0.8
* Physical analyses were carried out in the Karbala Construction Laboratory.			

3.3.3 Fine aggregate

Al-Ukhaidir, natural sand made use of as a fine aggregate conforming's to zone II of the. Table 3-5 displays fine aggregate grading. The findings indicate that fine aggregate meets the required grading of the Iraqi standard **[IQS No. 45-1984].** Also, Table 3-6 shows some properties of fine aggregate that used**.**

Table 3-5: Fine aggregate grading.*

Sieve size (mm)	Cumulative passing %	Iraqi standard No.45/1984 zone (2)
10	100	100
4.75	91	90 -100
2.36	86	75 -100
1.18	72	55 – 90
0.6	51	35 -59
0.3	26	8 -30
0.15	9	0 -10
Fineness modulus	2.68	
* Grading of fine aggregate was performed by, Kaarbala construction laboratory.		

Table 3-6: Some properties of fine aggregate *

Physical properties	Test results	Iraqi specification No. 45/1984
Specific gravity SSD	2.66	-
Bulk Density (kg/m^3)	1750	
Sulfate content %	0.16	≤ 0.5 %
Absorption %	0.63	-
* Properties of fine aggregate were performed by Karbala construction laboratory.		

3.3.4 Coarse aggregate

River gravel that was crushed and sized locally was used as coarse aggregate with a maximum size of 14.0 mm from Al-Nebaei region was used in all mixes. Table 3-7 lists the gradings of coarse aggregate, which matches to the Iraqi standard **[IQS No.45-1984].** Table 3-8 displays some properties of coarse aggregate.

Table 3-7: Coarse aggregate grading.*

Sieve size (mm)	Cumulative passing %	IQS.No.45/1984 grad 5-14 mm
37.5	100	----
25	100	----
20	100	100
14	100	90 - 100
10	77	50 - 85
5	8.6	0 - 10
2.36	2.1	---
* Grading of coarse aggregate was performed by Karbala construction laboratory.		

Table 3-8: Some properties of coarse aggregate *

Physical properties	Test results	Iraqi specification No. 45/1984
Specific gravity	2.73	-
Bulk Density (kg/m^3)	1625	-
Sulfate content %	0.072	≤ 0.1 %
Passing from sieve 75 μm %	0.53	≤ 3 %
Absorption %	0.65	-

* Properties of coarse aggregate were performed by Karbala construction laboratory.

3.3.5 Silica fume

Micro silica, also referred as silica fume, is a product of producing silicon composites in electrical arch kilns. It has been found to be effective as a supplementary cementitious ingredient in achieving desirable results in concretes. The CONMIX construction chemical company's Mega-Add MS (D) type Densified Micro- silica fume was employed. The chemical characteristics of the used silica fume is shown in Table 3-9 and are conforming to the **[ASTM C1240].**

Table 3-9: Chemical analysis of Silica fume*

NO.	*Components*	*Silica fume %*	*ASTM C1240 limitations*
1	CaO	1.22	
	SiO_2	91.05	≥ 85
	Al_2O_3	0.018	
	Fe_2O_3	0.012	
	MgO	0.01	
	SO_3	0.225	
	Na_2O	0.205	
	K_2O	0.155	
	Loss on ignition	2.975	≤ 6
	Moisture content	0.68	≤ 3
2	Activity Index with Portland cement at 7 days	132.4	≥ 105
	Percent retained on 45µm (No. 325) sieve, max, %	7	≤ 10
	Surface area (Blaine) m^2/kg	20000	≥ 15000

3.3.6 High-range water reducing admixture

As shown in Table 3-10, a third generation of superplasticizer identified as this admixture was given the marketable label of Glenium 51. The admixture satisfies the prerequisites for type F as outlined in **[ASTM C 494].**

Table 3-10: Technical description of Glenium 51 for Pozzolime concrete [*]

Chemical Base	Polycarboxylic ether based
Appearance / colors	Amber homogenous liquid
Density	1.082 - 1.142 kg/liter, at 20°C
Chlorine Content%	< 0.1
Alkaline Content%	< 3
Recommended dosage	(0.5 - 1.5) of Binder weight %

*Giving by data sheet of manufacturer.

3.3.7 Water

Mixing and curing were both done using water from the tap (Pozzolime concrete). According to **[Siegel et al. 2013],** the molten salts have a concentration of less than one thousand parts per million. The distant water was used throughout the mixing and curing processes of the concrete.

3.3.8 Steel fibers

Micro Steel fiber was RC 59/13 BN type low carbon and it's both ends were straight. The steel fibers have a length of 13 mm, diameter of 0. 22mm, aspect ratio of 59, tensile strength of 2850 MPa, and density of 7.85 g/cm3. See Plate 3-3.

Plate 3.3: Steel fibers.

3.3.9 Steel reinforcing bars

As reinforcing bars, two sizes of deformed bars with nominal diameters of 10, and 8 mm were employed. All of these bars' tensile tests produced the characteristics shown in Table 3.11, with all values presented are the average of three samples for each rebar diameter. A photograph of testing machine is shown in Plate 3-4. The testing was done in accordance with the American Standard Specification for Deformed Steel Bars **[ASTM A496, 2007].** All tests were done at the University of Karbala /civil engineering laboratories.

Table 3.11: Tensile properties of the used steel reinforcing bars.

Nominal Diameter (mm)	Equivalent diameter (mm)	Surface texture	Area (mm²)	Average of Yield Tensile Stress, fy (MPa)	Average of Ultimate Tensile Strength, fu (MPa)	Elongation at Ultimate Stress (%)
8	8	deformed	50.3	374.2	550.2	14
10	10	deformed	78.5	536.7	686.7	14

Plate 3-4: Steel bar tensile test.

3.3.10 CFRP sheets

Carbon fiber sheets were used in this present study for strengthening (see Plate 3-5). Table 3-12 present mechanical properties of Carbon fiber sheets as given by the manufacturer.

Table 3-12: Mechanical properties of carbon fiber sheets.

Product name	SikaWrap®-300 C
Tensile strength (MPa)	4000
E- modulus (GPa)	230000
Strain at break (min.) %	1.7
Width (mm)	100
Thickness (mm)	0.167
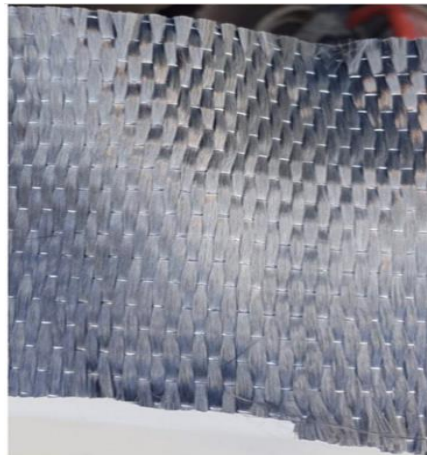
Plate 3-5: Carbon fiber sheets

3.3.11 Epoxy

Epoxy (Sikadur®-330) was used in this study as bonding material between concrete and Carbon fiber sheets. This adhesive material consists of two parts; part A (white) color and part B (black) color as shown in Plate 3-6. These two parts were mixed with 4A:1B ratio. The mechanical and physical properties of bonding resin are presented in Table 3-13.

Plate 3-6: Epoxy material.

Table 3-13: Mechanical properties of epoxy resin (manufactured).

Product name	Sikadur®-330
Tensile strength (MPa)	(33.8 MPa) (7 days)
E-Modulus (MPa)	(3,489 MPa) (7 days)
Flexural strength (MPa)	(60.6 MPa) (7 days)
Compressive Strength	(77.2 MPa) (7 days) (23ºC)
Mixing ratio	1B:4A
Elongation at Break	1.2 % (7 days)

3.4 Concrete Mixes

Pozzolime is the name of a trademarked sustainable binder that was called in Iraq by **[Kadum et al., 2017],** this binder consists of hydrated lime, silica fume, fly ash, and some other ingredients, but it does not comprise Portland cement. According to the findings presented in the last reference, the mix proportions for two different pozzolime mixes, referred to as Mix1 and Mix2, were chosen. These results may be found in Table 3-14. Mix 2 was prepared by adding just trace quantities of cement in an effort to speed up the setting time.

Table 3-14: Pozzolime concrete mix proportions and properties.

Mixing	Materials								
	Hydrate lime kg/m³	Cement kg/m³	Silica fume kg/m³	Fine Agg. kg/m³	Coarse Agg. kg/m³	W/B ratio by wt.	HRWR by wt. of cement, %	Slump mm	Compressive strength, fcu 28 days (MPa)
Mix1	225	-	225	625	945	0.45	2.9	100	24.3
Mix 2	310	25*	110	600	940	0.5	2.5	115	23.8
* For accelerating setting time.									

Firstly, six cubes were tested for compressive strength (fcu) for each mix (Mix 1 and Mix 2), where the results show that the value of fcu for Mix 2 was 15.4 and 18.3 MPa for age 7 and 14days respectively, while the value of fcu for Mix 1 was 16.6 and 18.6 MPa for age 7 and 14 days respectively. So, the Mix 1 was chosen for the rest of the experimental work.

3.5 Mixing of Concrete

The procedure of mixing concrete is vital if the necessary workability and consistency of the concrete mix are to be achieved. The technique for mixing was carried out using a sloping mixer with a capacity of about 0.03 m3 in accordance with **[ASTM C192-06].** Before it can be used, the mixer has to be thoroughly cleaned and dried out completely. The Pozzolime cement was first added to the mixer, followed by the addition of the coarse aggregate and a small quantity of mixing water (the admixture was completely mixed with the water at this point), and finally, the addition of the fine aggregate, the dry mix of hydrated lime and silica fume, and the remaining mixing water. At that time, all of the components were carefully blended until they obtained a combination that was homogeneous throughout its whole.

3.6   Casting and curing of control specimens

Following are the kinds and dimensions of the molds utilized for this study:

- Cylindrical steel molds, with a diameter of 100 mm and a length of 200 mm for modulus of elasticity, density and splitting tensile strength of concrete; and
- Steel cubes molds with dimension of 100 mm for compressive strength of concrete.

To prevent concrete from adhering to molds following hardening, the internal faces of each mold were completely lubricated and maintained clean. The concrete was poured in two layers before being compacted using a tamping rod or vibration machine to eliminate as much air as possible. The specimens' top faces were then troweled, and they were covered with plastic sheets for 24 hours to prevent the loss of mixing water and moisture from the top surface and plastic shrinkage cracking. The samples were then demolded and completely submerged in tap water until test time. The curing schedule for pervious concrete was 7 days followed by 28 days of water curing. Mention that the opening of molds is delayed because the final setting time is slow, which requires 2-3 days to open the molds, unlike Portland cement concrete.

3.7 Testing of fresh Concrete

3.7.1 Slump test

In conformance with **[ASTM C 143],** the slump test was done. Its main purpose is to show how workable a certain batch of concrete is. Within a batch of nearly identical concrete, the slump estimation shouldn't change by more than about 25 mm.

3.8 Testing of hardened Concrete

3.8.1 Dry Density

Cylinder mold were employed to calculate the dry density according to **[ASTM C138]** of concrete. The samples were tested at age of 28 days of tap water curing. The density of hardened concrete was determined according to the following processes:

3.8.2 Compressive Strength

As illustrated on Plate 3-7, the compressive strength was measured using a standard hydraulic digit. "ELE machine of 2000.0 kN capacity" at a rate of loading about 0.30 MPa per second. This was done in accordance with **[BS EN – 12390]**. At each test, the average value of three cubes with 100 mm dimension was taken. For Pozzolime concrete, tests were done when it was 7 days old and 28 days old.

Plate 3-7: Compressive test machine.

3.8.3 Splitting tensile strength (fsp)

The splitting tensile strength was measured according to [**ASTM C 496/C496M-(2017)**]. A testing machine hydraulic digital "ELE machine of 2000 kN capacity" was used to load 100x200mm cylinders constantly up to failure at a loading rate of 2.2 kN/sec. The mean splitting tensile strength was calculated using the average splitting tensile strength of two cylinders. See Plate 3-8.

Plate 3-8: Splitting tensile strength test.

The splitting tensile strength is calculated by the following formula:

$$f_{ct} = \frac{2P}{\pi \, DL} \tag{3.2}$$

where:

f_{ct} = splitting tensile strength of concrete (MPa)

P = failure load (N)

D = diameter of cylinder (mm)

L = length or height of cylinder (mm)

3.8.4 Modulus of elasticity (Ec)

The concrete modulus of elasticity (Ec) was carried using 3 concrete cylinders of 100x 200 mm in accordance with **[ASTM C-469-(2002)].** The modulus of elasticity is calculated from a stress-strain curve using a compress meter gauge with a length of 20 cm and an accuracy of 0.001mm. The load was applied at a steady rate of up to 40% of the maximum load. See plate 3-9.

Plate 3-9: Modulus of elasticity test

3.9 Molds and reinforcement of beams

To cast the examined beams, wooden molds were devised and built. The molds are built of 22 mm thick plywood. As illustrated in Plate 3-10, longitudinal and transverse steel bars have been placed and linked using steel wire.
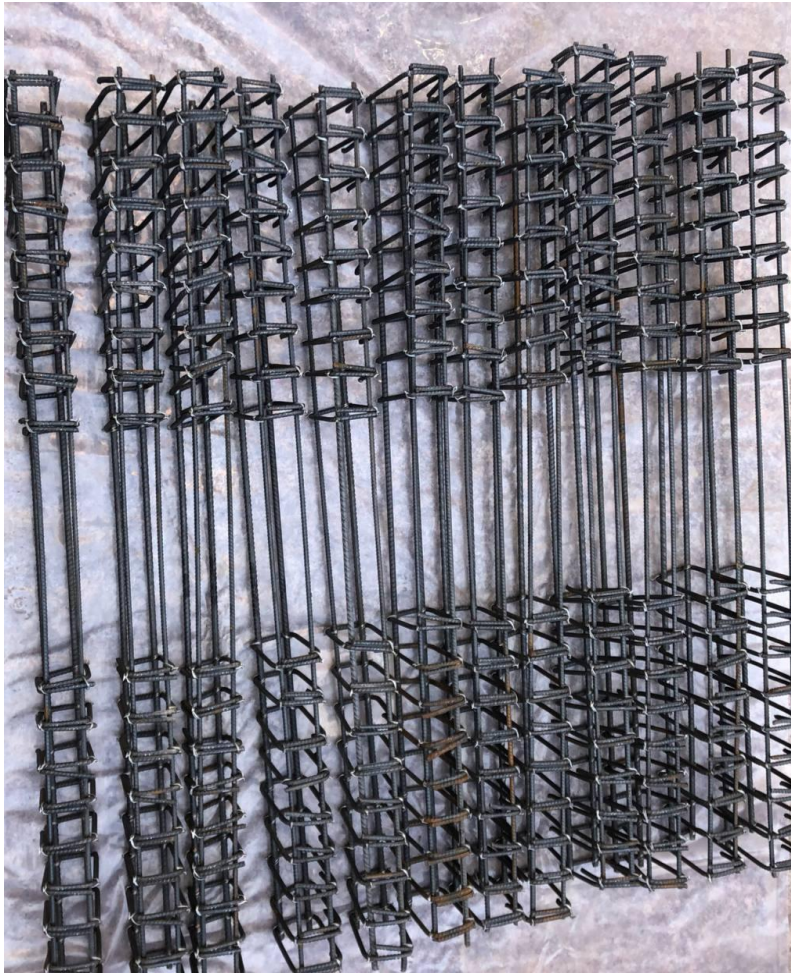
Plate 3-10: Steel reinforcement details.

After that the mixing process was done, each beam was made by pouring it in two layers. Fresh concrete was put in the mold, and a laboratory rod vibrator was used to pack down the layer for a long enough time. The second layer also kept vibrating. The concrete surface was made even and smooth with a steel trowel. Polyethylene (Nylon sheet) was used to cover the molds so that water loss and shrinkage wouldn't cause cracks.

All concrete beam specimens' molds along with the control specimens were removed (2-3) day after casting. To make sure a good curing treatment, wet canvas was used and soaked in water over and over again for 28 days. Plate 3-11 shows the cast of the concrete for each beam.

Plate 3-11: Beam specimens cast.

3.10 Testing of control specimens

Control specimens (cubes and cylinders) were divided into 3 groups according to percent of added steel fibers as shown in table 3-15.

Table 3-15: Number and classification of Control specimens.

Control specimens' type	Percent of steel fibers (%)	No. of Control specimens	Test type
Cube	0	3 6	Density Compressive strength (7,14 and 28 days)
Cylinder	0	2 2	splitting tensile strength, 28 days, modulus of elasticity, 28 days
Cube	0.5	3 6	Density Compressive strength (7,14 and 28 days)
Cylinder	0.5	2 2	splitting tensile strength, 28 days, modulus of elasticity, 28 days
Cube	1	3 6	Density Compressive strength (7,14 and 28 days)
Cylinder	1	2 2	splitting tensile strength, 28 days, modulus of elasticity, 28 days

3.11 Beams test

Deflection measurements at every load step were taken in this investigation to predict the behavior of sustainable reinforced concrete beams under two points monotonic loading.

3.11.1 Deflection measurements

One type of deflection measurement was used, this type was linear displacement sensor (LVDT-KTR-50mm) used to find the deflections at mid span and under the point load.

3.11.2 Strain indicator

A multi-channel data logger is used to measure strain as shown in Plate 3-12, this device consists of 11 channels for strain gauges and 4 channels for LVDT-KTR-50 mm, which means 15 channels, were provided. The operating software of the strain indicator permit to record the channel's reading every five seconds; this facility assists to obtain a suitable estimation for the behavior of the concrete surface under consideration.
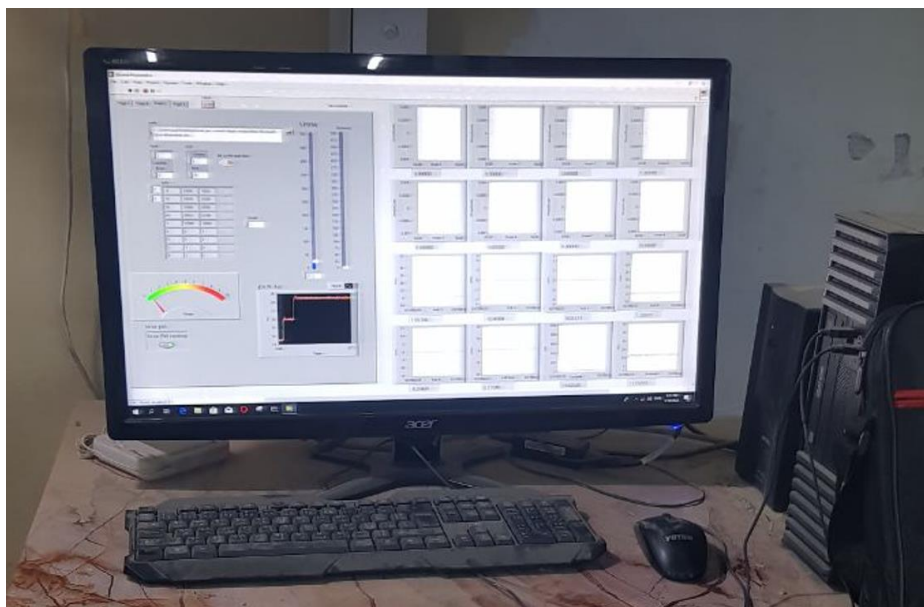
Plate 3-12: Strain indicator device and software interface window.

3.11.3 Microscopic observation

One of the serviceability requirements for structural concrete members is crack width. Due to concrete's limited tensile strength, it is predicted that reinforced concrete components may break under service stresses. Controlling cracking is essential for maintaining an acceptable appearance and guaranteeing the longevity of concrete structures. Utilized as a high-definition microscope with lenses that amplifies and clarifies the micro-cracks up to 10 times; this high-definition microscope is supplied by an adjustable source of light and high-capacity batteries. Plate 3-13 depicts the crack meter tiny device.

Plate 3-13: Crack meter microscopic devise.

3.12 Loading test setup

The test setup was installed at the Structural Laboratory in Department of Civil Engineering / College of Engineering / University of Kerbala, the test was carried out with a frame in load-control mode, measuring 5.5 m in width and 3.00 m in height. A steel frame of I-section was fixed at the load frame by welding and bolts to support and carry the crane which is used for lifting and positioning the tested beams. Plate 3-14 illustrates a schematic depiction of the specimen's test setup. The positioning was then maintained by applying a modest pre-load. Up to a load intensity of 30 kN, the load was applied in 4.0 kN increments, and for greater loads, the load was applied in 2 kN increments. The time period of each loading increment consisted of 10 min/stage. A load cell was used to record the applied load, and LVDT-KTR-50mm were used to record the vertical deflections beneath load, and at mid-span.

Plate 3-14: Test setup.

Chapter four

Experimental results and discussion

4.1 General

Pozzolime reinforced concrete beams with and without strengthened by CFRP sheets (externally and internally) tested under monotonic loads are investigated and discussed in this chapter. Various factors, such as the percent of added steel fibers, length, and position of CFRP sheets, will be compared in order to better understand the impact of the various variables. For thirteen beam specimens, the experimental results have been presented. Observation of load against deflection under monotonic load tests, crack pattern, and failure mechanism are all important considerations for each specimen. Crack propagation was documented using images following the monotonic load test, and the cracks were labeled as the loading progressed. Also, many control specimens tested and divided into three main groups according to percent of steel fibers to investigate the effect of steel fibers on the density, compressive strength, splitting tensile strength, and modulus of elasticity of pozzolime concrete.

4.2 Effect of steel fibers on concrete properties

4.2.1 Density

Laboratory test results for concrete mix1 density are shown in table 4.1 and Figure 4.1. Table 4.1 indicated that the percent of steel fibers has a small impact on the fresh density, the increase of the percent of steel fibers increased the fresh density

by about (0.2, and 0.4%) for the added steel fiber percent of 0.5 and 1% with respect to the reference specimen. Also, the percent of steel fibers has a small impact on the dry density, the increase of the percent of steel fibers increased the dry density by about (0.9, and 1.6%) for the added steel fiber percent of 0.5 and 1% with respect to the reference specimen.. Figure 4.1 shows comparison of three densities of concrete at different percent of steel fibers. Figure 4.2 shows the effect of steel fibers percent on density

Table 4.1: Results of Laboratory tests of density for concrete mix 1.

Concrete property	Percent of steel fibers (%)	Density (Kg/m^3)	Increase ratio (%)
Fresh Density	0	2283	Ref.
Fresh Density	0.5	2288	0.2
Fresh Density	1	2292	0.4
Dry Density	0	2250	Ref.
Dry Density	0.5	2270	0.9
Dry Density	1	2285	1.6
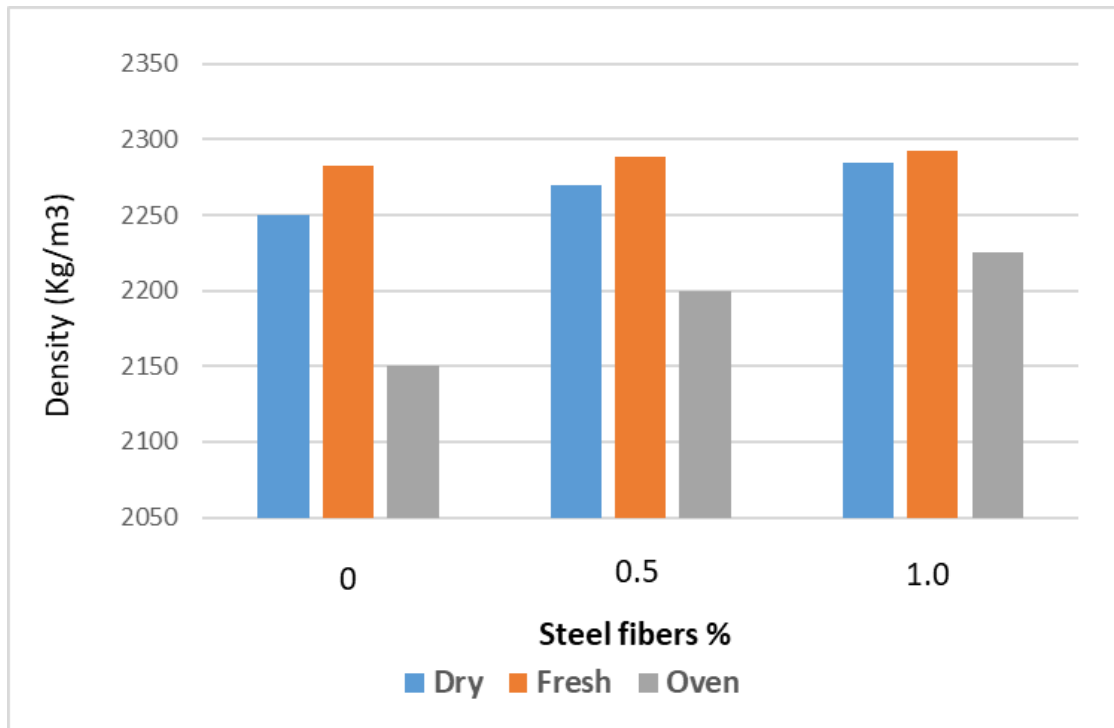
Figure 4.1: The comparison of three densities of concrete at different percent of steel fibers.
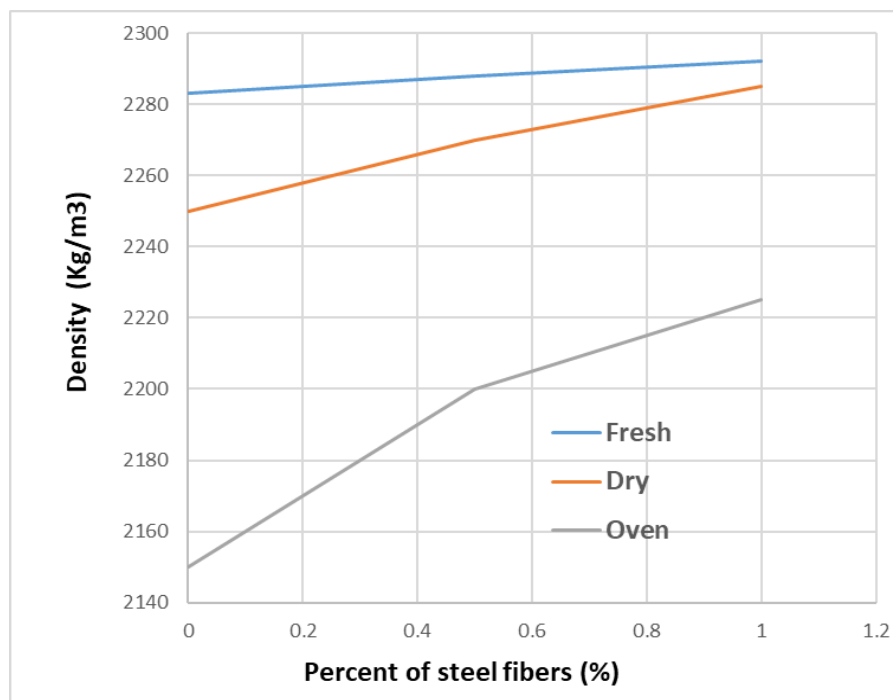
Figure 4.2: Effect of steel fibers percent on density.

4.2.2 Compressive strength

Table 4.2 indicated that the percent of steel fibers has a significant impact on the compressive strength (f_{cu}), the increase of the percent of steel fibers increased the compressive strength by about (2.4, and 16.3%) for the added steel fiber percent of 0.5 and 1% with respect to the reference specimen for age 7 days, while the increase of the percent of steel fibers increased the compressive strength by about (4.1, and 37.6%) for the added steel fiber percent of 0.5 and 1% with respect to the reference specimen for age 14 days. the increase of the percent of steel fibers increased the compressive strength by about (4.9, and 12.8%) for the added steel fiber percent of 0.5 and 1% with respect to the reference specimen for age 28 days. Figure 4.3 shows the effect of steel fibers percent on concrete compressive strength at various ages. Figure 4.4 shows the effect of steel fibers percent on compressive Strength.

Table 4.2: Compressive strength results of control specimens.

Concrete property	Percent of steel fibers (%)	Results (MPa)	Increase ratio (%)
Compressive Strength (f_{cu}), for (7) days	0	16.6	Ref.
	0.5	17	2.4
	1	19.3	16.3
Compressive Strength (f_{cu}), for (14) days	0	18.6	Ref.
	0.5	22.7	4.1
	1	25.6	37.6
Compressive Strength (f_{cu}), for (28) days	0	24.3	Ref.
	0.5	25.5	4.9
	1	27.4	12.8
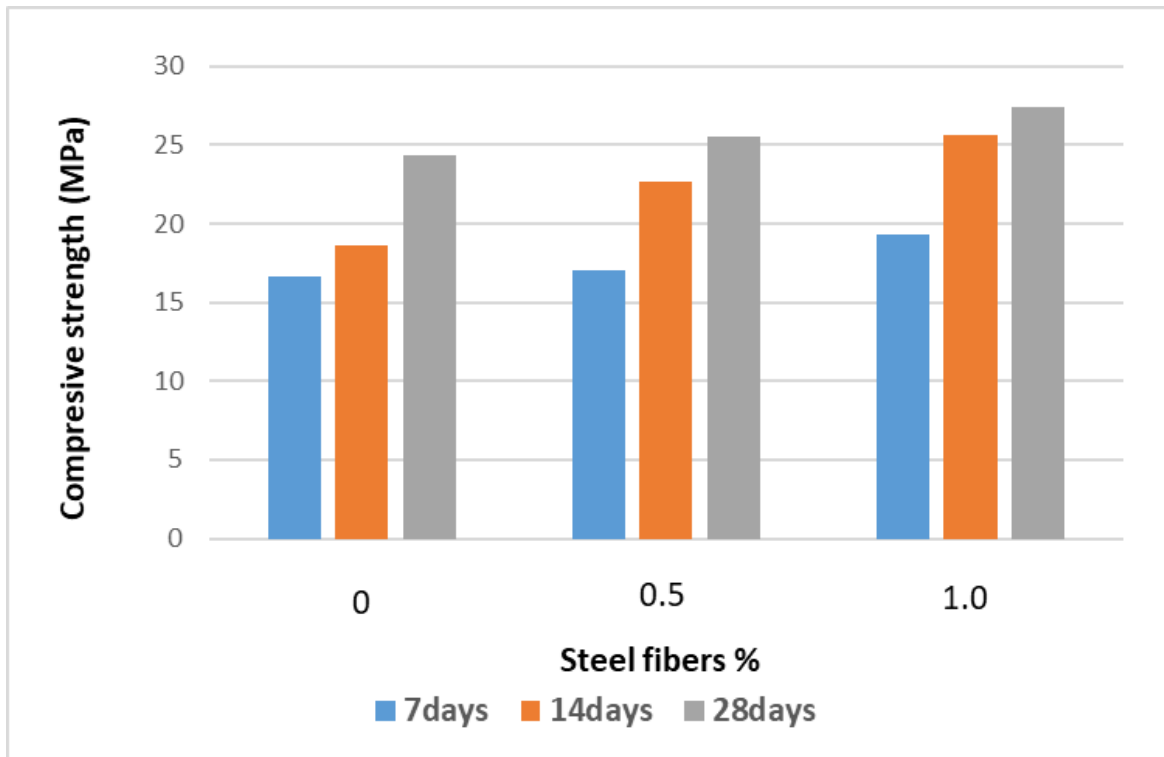
Figure 4.3: The effect of steel fibers percent on concrete compressive strength at various ages.
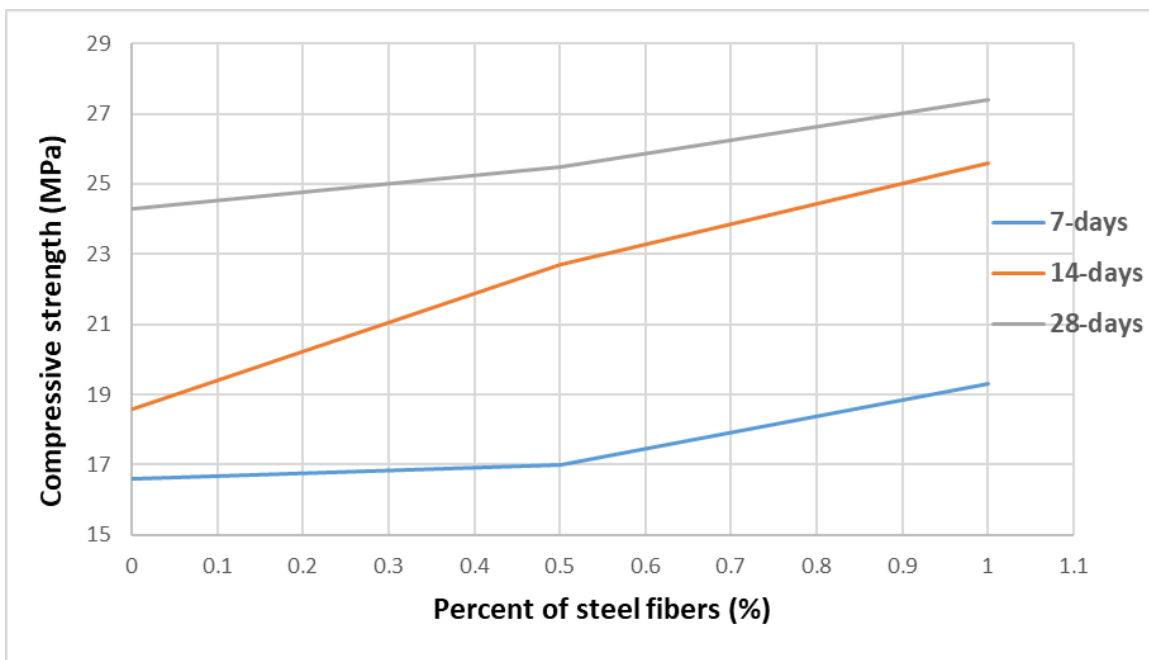
Figure 4.4: Effect of steel fibers percent on compressive strength (f_{cu}).

4.2.3 Splitting tensile strength

Table 4.3 indicated that the percent of steel fibers has a significant impact on the splitting tensile strength (fsp) for 28 days, the increase of the percent of steel fibers increased the splitting tensile strength by about (11.8, and 23.2%) for the added steel fiber percent of 0.5 and 1% with respect to the reference specimen. Figure 4.5 shows the effect of steel fibers percent on splitting tensile strength for 28 days.

Table 4.3: Splitting tensile strength and Modulus of elasticity of control specimens.

Concrete property	Percent of steel fibers (%)	Results (MPa)	Increase ratio (%)
Splitting tensile strength (fsp), for (28) days	0	2.11	Ref.
Splitting tensile strength (fsp), for (28) days	0.5	2.36	11.8
Splitting tensile strength (fsp), for (28) days	1	2.6	23.2
Modulus of elasticity (Ec), for (28) days	0	23800	Ref.
Modulus of elasticity (Ec), for (28) days	0.5	24200	1.7
Modulus of elasticity (Ec), for (28) days	1	25000	5
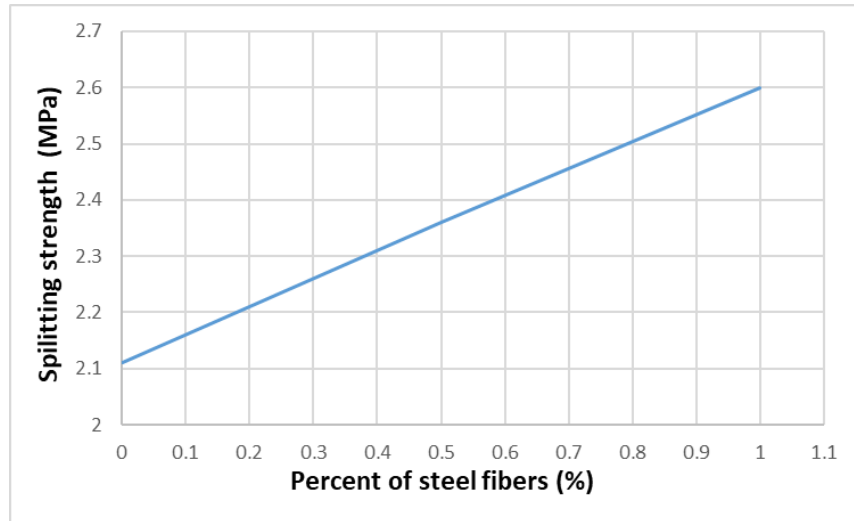
Figure 4.5: Effect of steel fibers percent on splitting tensile strength (fsp).

4.2.4 Modulus of elasticity

Table 4.3 indicated that the percent of steel fibers has an impact on the modulus of elasticity (Ec) for 28 days, the increase of the percent of steel fibers increased the modulus of elasticity by about (1.7, and 5%) for the added steel fiber percent of 0.5 and 1% with respect to the reference specimen. Figure 4.6 shows the effect of steel fibers percent on modulus of elasticity for 28 days.
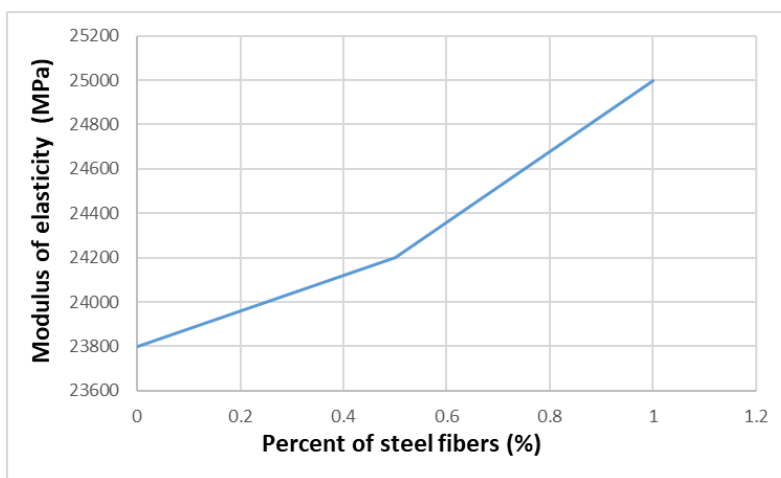
Figure 4.6: Effect of steel fibers percent on modulus of elasticity (Ec),

4.3 Crack Behavior, and Failure Modes

Crack formation was monitored throughout testing to assess the behavior of the strengthened specimens in comparison with the behavior of unstrengthen control beams, also, comparing specimens' behavior according to the percentage of steel fibers, length and position of CFRP.

However, this study focused on the debonding behavior, the formation of cracks that led to debonding of the CFRP sheets especially for internal sheets are also discussed. The first cracking load, cracking patterns, and width of cracks at ultimate loads of all specimens are presented in the following subsections.

4.3.1 First Crack Load and Crack Pattern

The experimental results concerning the cracking loads and the failure loads are listed in Table 4.4. It is noticed that the first flexural crack was occurred at the applied load (13 to 26 kN) for all specimens, with a different first crack load (**Pcr**) / ultimate load (**P u**) percent about (21.2 to 33.9 %) as shown in Table 4.4. Which concluded that increase the added external CFRP sheets length has a significant effect on the **Pcr** / **P u** percent, while increase the added internal CFRP sheets length has a small effect on the **Pcr** / **P u** percent, also, increase the added steel fibers percent has a significant effect on the **Pcr** / **P u** percent. It was in the beam's middle third that the first flexural fracture emerged (max. moment) when tensile stresses in concrete bottom fiber exceeded the concrete modulus of rupture. Then cracks developed slowly towards beam edges parallel to the support's direction. At some points, more flexural cracking appeared and spread along both sides of an original fracture, which was oriented toward the supports. When the beam failed, the cracks spread to the beam's sides and eventually reached the beam's compression cord. In

the center third of the beam, the fractures were found, but no cracks were found near the supports except near the applide loads. It was also observed that no effective shear cracks were generated. The crack pattern for specimens is shown in Plates (4-1) to (4-13). Increase the added steel fibers percent has a small effect on the cracks pattern. It is evident from these plates that flexural cracks are approximately parallel and that there are no cracks were observed near to support regions, also it is clear that cracks pattern for the beam approximately have similar behavior except for beams with internal CFRP strengthening.

For beams with internal CFRP strengthening, the existing internal CFRP sheets between tensile reinforcement and cover of concrete acted as a separated layer which led to a horizontal crack starting at about 55-65% of the ultimate load for each beam then separation of the bottom cover followed by debonding of CFRP sheets.

Table 4-4 Crack and Ultimate Loads of all beams.

Specimens	Cracking Load (P cr) (kN)	% Increase in Cracking Load with Respect to Ref	Ultimate Load (P u) (kN)	(Pu -Pu ref.) / Pu ref.) (%)	Pcr / P u (%)
B0	13	Ref.	55.11	Ref.	23.6
B0EA	22	69	76.17	38.2	28.9
B0EP	20	54	67.06	21.7	29.8
B0IA	14	7.7	63.31	14.88	22.1
B0IP	14	7.7	65.96	19.7	21.2
B0.5EA	24	85	78.66	42.7	30.5
B0.5EP	22	69	69.11	25.4	31.8
B0.5IA	16	23	66.11	19.96	24.2
B0.5IP	16	23	67.89	23.2	23.6
B1EA	26	100	80.53	46.1	32.3
B1EP	24	85	70.83	28.5	33.9
B1IA	18	39	68.23	23.8	26.4
B1IP	18	39	69.9	26.8	25.8

Plate 4.1: Cracks Pattern of Specimen B0.

Plate 4.2: Cracks Pattern of Specimen B0EA.

Plate 4.3: Cracks Pattern of Specimen B0EP.

Plate 4.4: Cracks Pattern of Specimen B0IA.

Plate 4.5: Cracks Pattern of Specimen B0IP.

Plate 4.6: Cracks Pattern of Specimen B0.5EA.

Plate 4.7: Cracks Pattern of Specimen B0.5EP.

Plate 4.8: Cracks Pattern of Specimen B0.5IA.

Plate 4.9: Cracks Pattern of Specimen B0.5IP.

Plate 4.10: Cracks Pattern of Specimen B1EA.

Plate 4.11: Cracks Pattern of Specimen B1EP.

Plate 4.12: Cracks Pattern of Specimen B1IA.

Plate 4.13: Cracks Pattern of Specimen B1IP.

4.3.2 Failure Modes

The control beam specimen, B0 behaved in expected fashion under flexural loading. The failure due to yielding of tension steel reinforcement, see Plate 4.1. The control beam specimens were used as a baseline to compare the remaining strengthening beam specimen.

Two kinds of failure modes occurred on the CFRP-strengthened beams in this experiment. The first is the intermediate flexure crack-induced debonding failure which occurred in the externally strengthened beams, see Plates 4.2. 4.3, 4.6, 4.7, 4.10, and 4.11.

The second is the intermediate flexure crack-induced debonding along the internal CFRP sheets that began from the mid-span with a horizontal crack and concrete cover separation and delamination, see Plates 4.4. 4.5, 4.8, 4.9, 4.12, and 4.13.

4.3.3 Width of Crack

Table 4-5 shows the crack width at ultimate load of monotonic load test for all tested beams. It's clear that adding steel fibers has a significant effect on stiffness of beams which leads to decrease the ultimate crack width, also, the increase of adding externally CFRP sheets area decrease the ultimate crack width, while adding internally CFRP sheets has a small effect on the ultimate crack width.

Table 4-5: Cracking width at ultimate load of monotonic load test.

| Specimens	Ultimate crack width, (mm)	decreasing in Ultimate crack width, (%)
B0	3	Ref.
B0EA	2.1	30
B0EP	2.2	27
B0IA	2.8	7
B0IP	2.8	7
B0.5EA	1.9	37
B0.5EP	2	33
B0.5IA	2.5	17
B0.5IP	2.5	17
B1EA	1.4	53
B1EP	1.5	50
B1IA	2.2	27
B1IP	2.2	27

4.4 Load-Deflection Curves

Deformability can refer to the strain in a body, the curvature in a section, the rotation in a member, and the deflection in a member. During the beam test, the vertical deflection that occurred at the mid-span as well as at the point load was measured and recorded at each load increment. Deflections of beams under service loads as well as ultimate loads were addressed.

Because the load behavior after the peak could not be managed in any of the tested beams, the data displayed in Figure 4-7 concluded at the failure load and its corresponding deflection value. This decision was made because the peak load could not be regulated. The selected serviceability limit was the experimental ultimate load divided by 1.7, as advised by several investigators **(Mansur and Tan, 1992),** because there was no undesirable cracking or deformation at this point.

In general, when a beam is loaded incrementally, at the first stage the deflection will increase at a constant rate (elastic region). After this stage (generation and development of cracks), the deflection will increase at a faster rate and continue to increase until yielding of tension steel reinforcement.

After this point, the slope of the curve will decrease, and the test will stop when the deflection increases without any increase in the applied load. The load-deflection behavior for all tested beams is shown in Figure 4-7. This behavior is shown for the two points (mid span and load point).
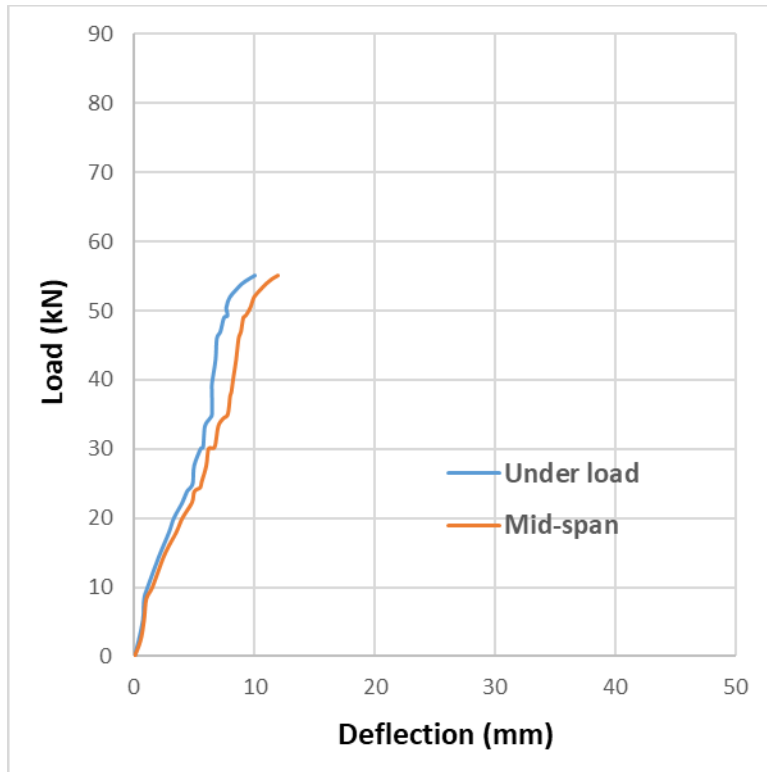
a-B0
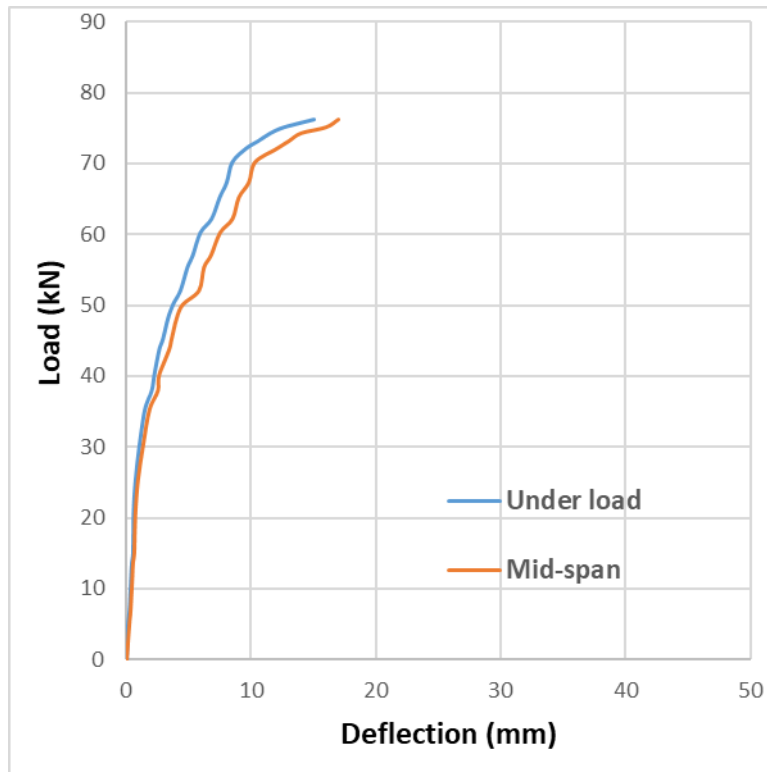
b-B0EA

Figure 4-7: Load-deflection behavior for the two points (mid span and load point).

c-B0EP

d-B0IA

Figure 4-7: (**Continued**) Load-deflection behavior for the two points (mid span and load point).

e-B0IP

d-B0.5EA

Figure 4-7: (Continued) Load-deflection behavior for the two points (mid span and load point).
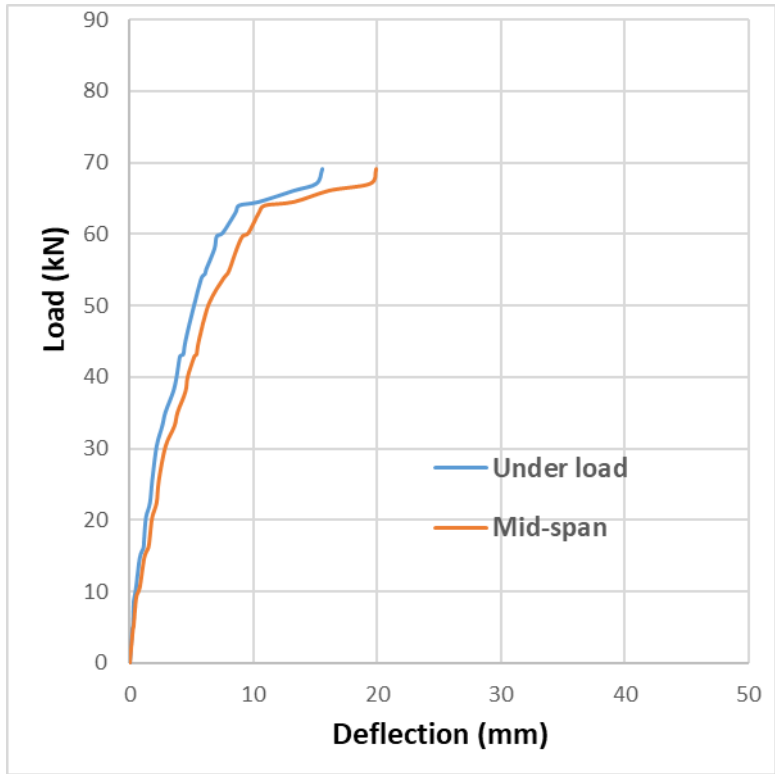
f-B0.5EP
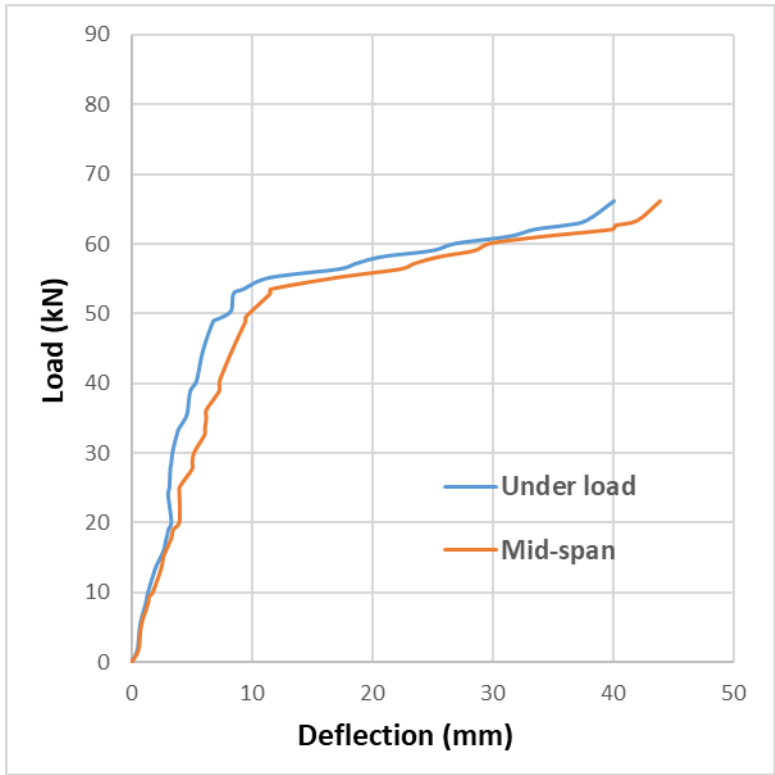
g-B0.5IA

Figure 4-7: (Continued) Load-deflection behavior for the two points (mid span and load point).
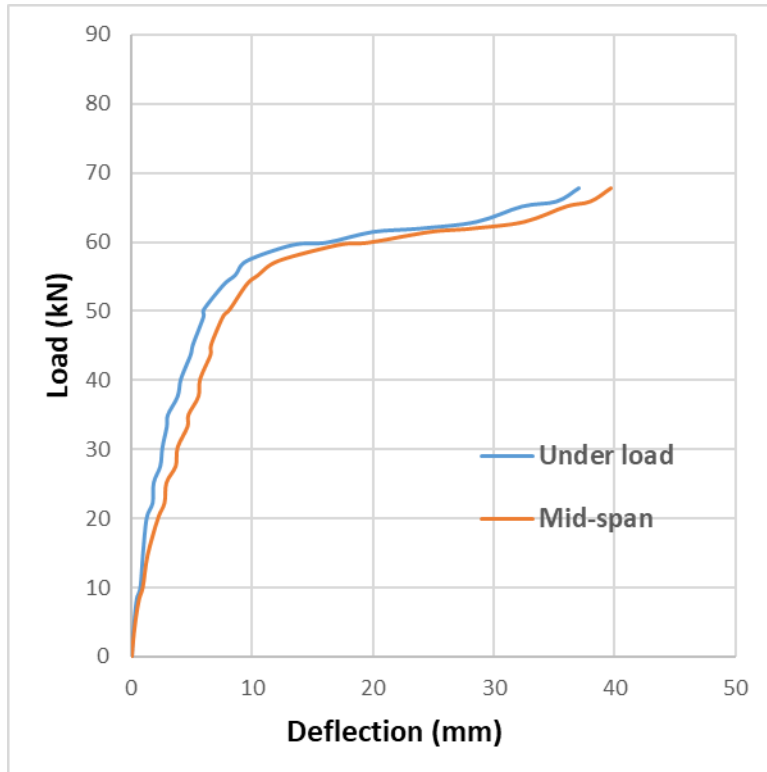
h-B0.5IP
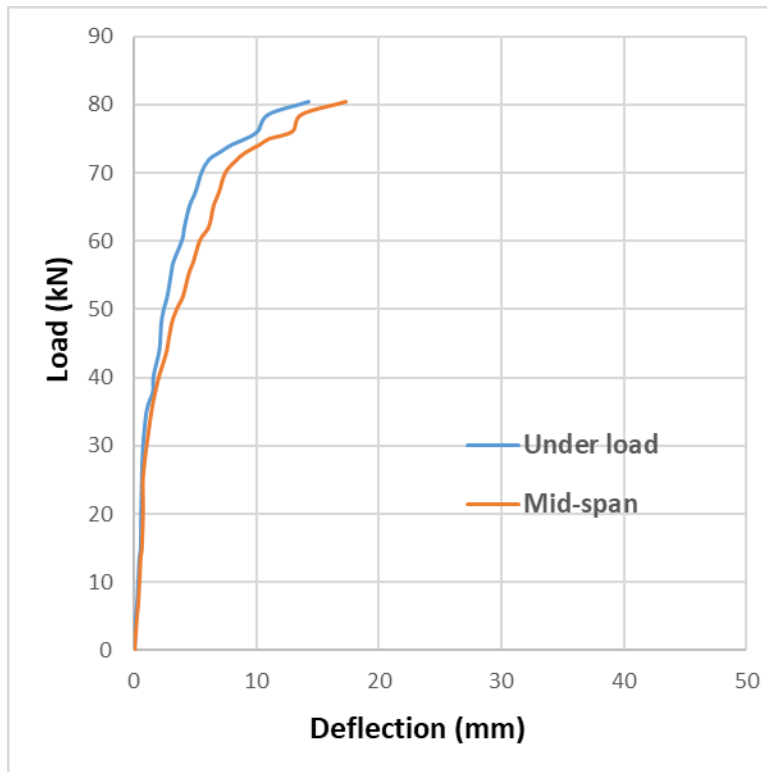
i-B1EA

Figure 4-7: (Continued), Load-deflection behavior for the two points (mid span and load point).
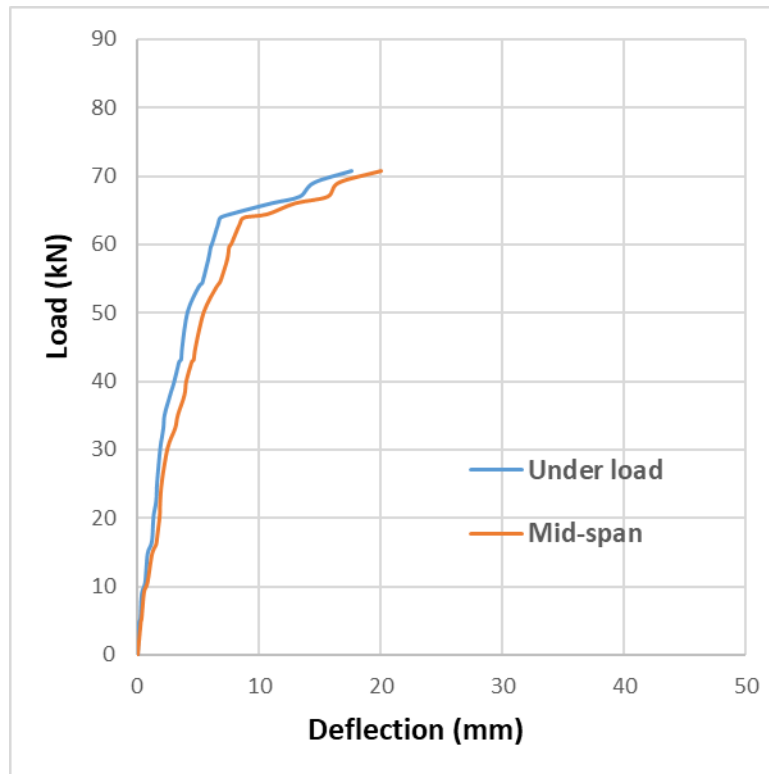
j-B1EP
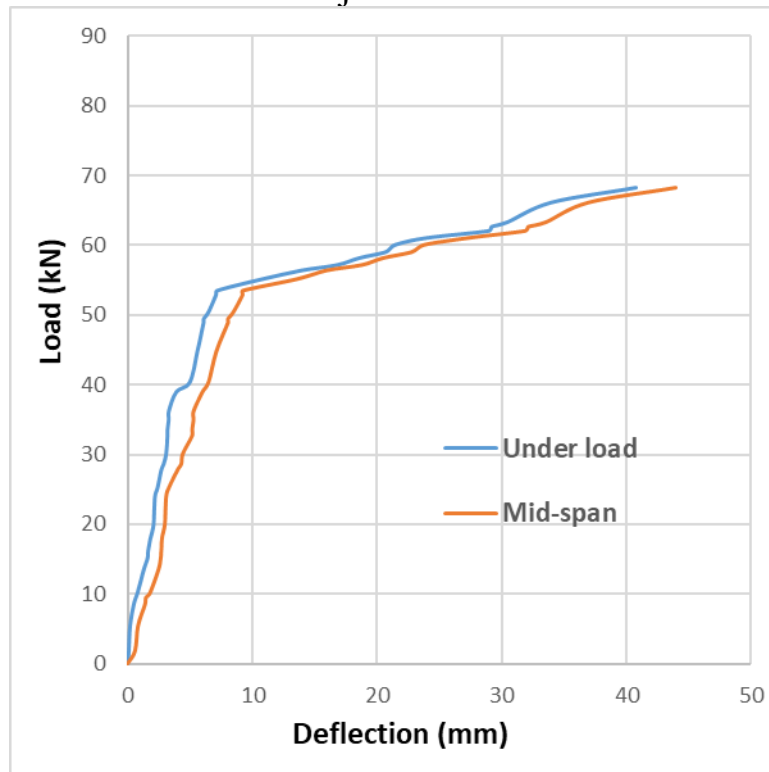
k-B1IA

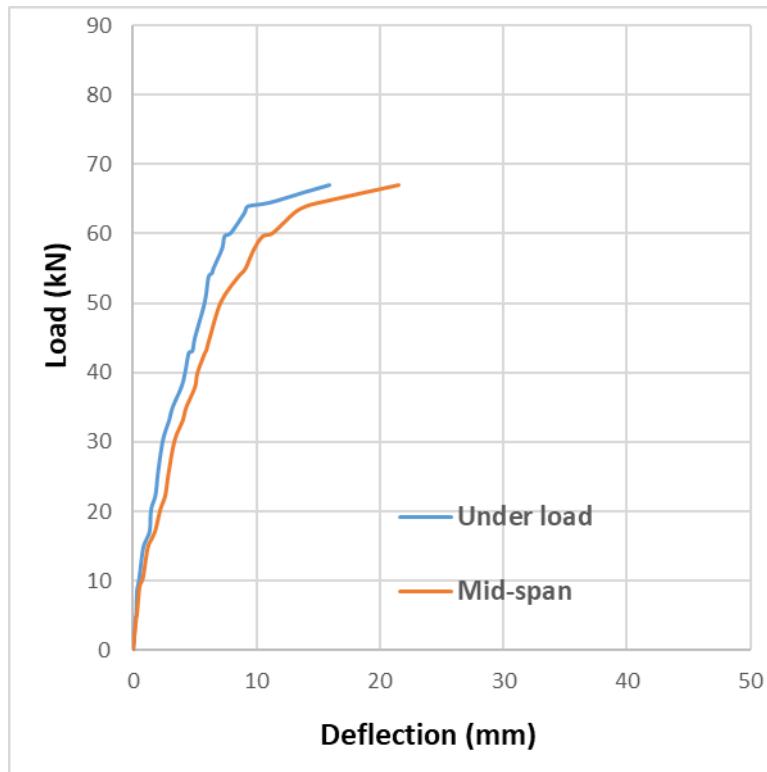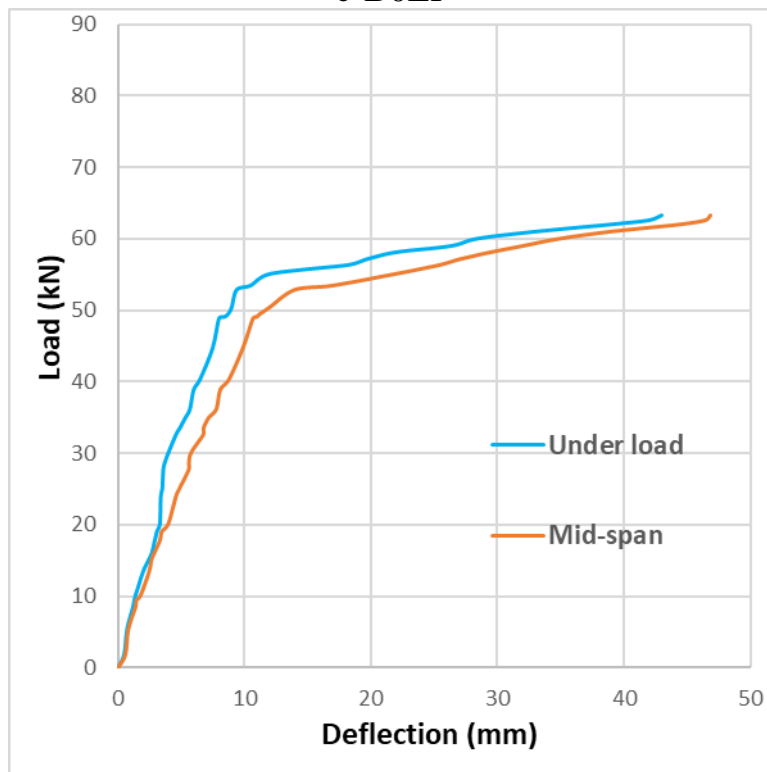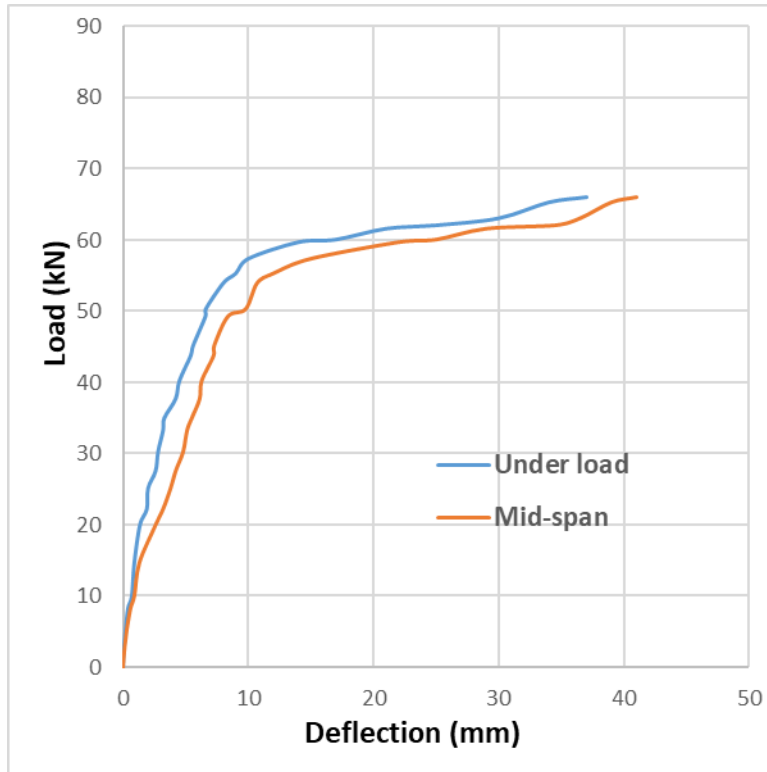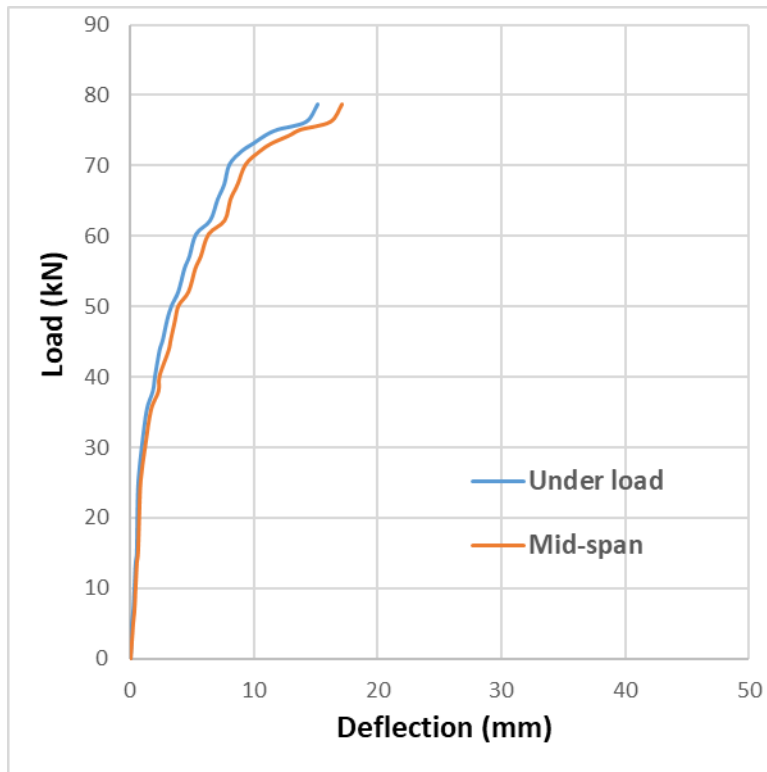**Figure 4-7:** (**Continued**), Load-deflection behavior for the two points (mid span and load point).

1-B1IP
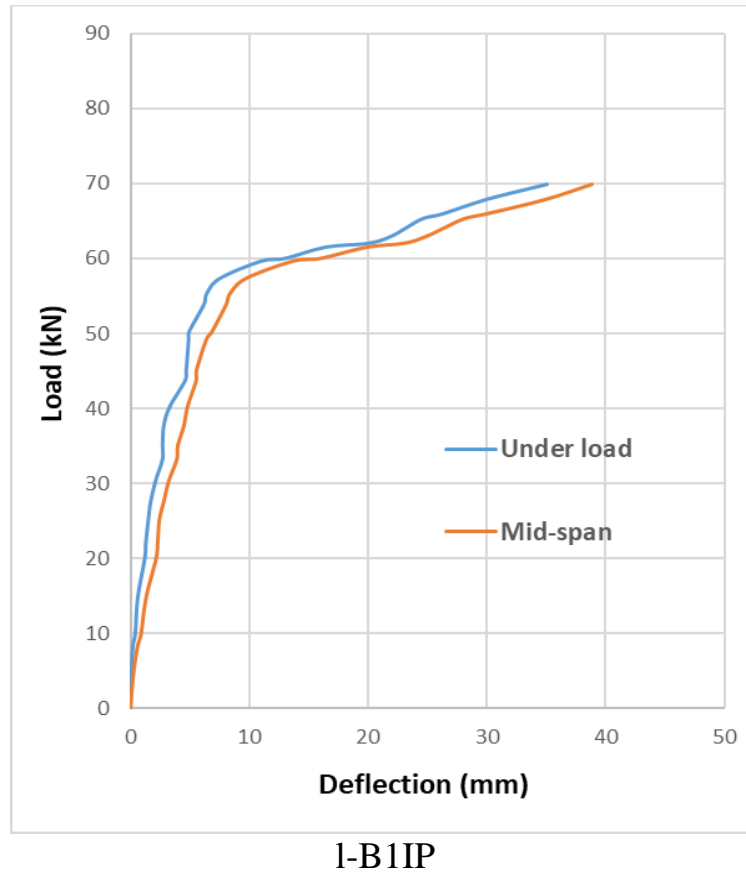
Figure 4-7: (Continued), Load-deflection behavior for the two points (mid span and load point).

4.5 Ductility Ratios

The ductility factor is the ability of structural member to sustain large deformation or in other word, it is the percentage of mid-span deflection at failure loads to the mid-span deflection at the initial yielding of tension main reinforcement bars. Table 4-6 illustrates the influence of adding CFRP sheets length on the ductility factor for specimens. It is observed that increase the adding external CFRP sheets length decrease the ductility factor, as shown in Table 4-6. Also, the percent of added steel fibers has a small enhancement on the ductility factor. The results of research **[Oh, B. H., 1992]** indicate that the ductility and the ultimate resistance are remarkably enhanced due to the addition of steel fibers.

Figure 4-8 shows a comparison in ductility factor for tested beams. Externally strengthening gives ductility factor less than internally.

Table 4-6: Ductility factor for specimens

Specimens	Yield Deflection (mm)	Ultimate Deflection (mm)	Ductility Factor
B0	6.9	12	1.74
B0EA	8.1	17	2.10
B0EP	10	21.5	2.15
B0IA	15	46.9	3.13
B0IP	14	41	2.93
B0.5EA	7.7	17.1	2.22
B0.5EP	8.9	19.95	2.24
B0.5IA	13.5	43.9	3.25
B0.5IP	12.8	39.7	3.10
B1EA	8.1	17.3	2.14
B1EP	9	19.99	2.22
B1IA	13.1	44	3.36
B1IP	12	38.9	3.24
Ductility Factor = Ultimate Deflection / Yield Deflection			
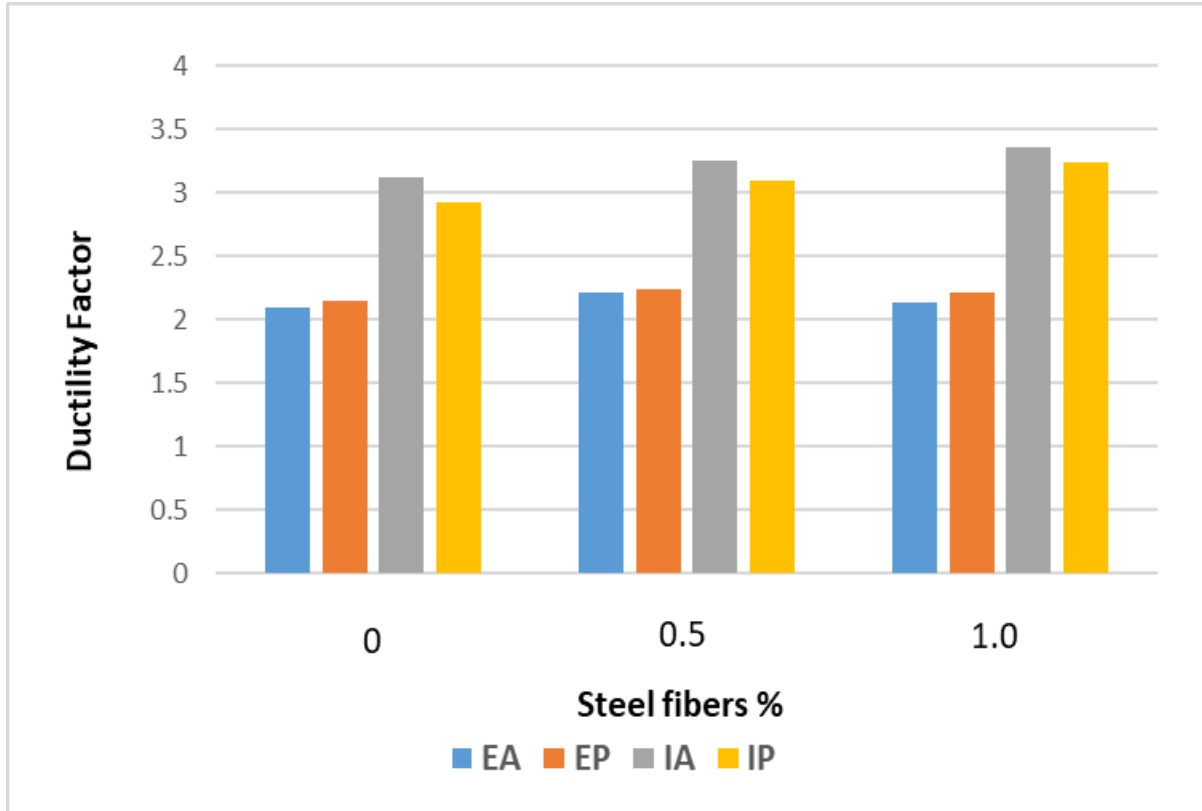
Figure 4-8: A comparison in ductility factor for tested beams.

4.6 Ultimate Load

All the un-strengthened and strengthened RC beam specimens were tested up to failure. The recorded ultimate loads for these beam specimens are presented in Table 4-7.

The experimental test results indicated that the percent of increase in ultimate load was 46.1, and 14.9 % for specimens B1EA, and B0IA, respectively with respect to the reference specimen B0.

Table 4-7: Ultimate loads of all tested beams.

Specimens	Ultimate Load (P_u) (kN)	% Increase in Ultimate Load with Respect to Ref. B0	% Increase in Ultimate Load with Respect to Ref. = (beam with 0% of steel fibers in each group)	Failure Mode
B0	55.11	Ref.	-	F1*
B0EA	76.17	38.2	Ref.	F2**
B0.5EA	78.66	42.7	3.3	F2**
B1EA	80.53	46.1	5.7	F2**
B0EP	67.06	21.7	Ref.	F2**
B0.5EP	69.11	25.4	3	F2**
B1EP	70.83	28.5	5.6	F2**
B0IA	63.31	14.9	Ref.	F3***
B0.5IA	66.11	20	4.4	F3***
B1IA	68.23	23.8	7.7	F3***
B0IP	65.96	19.7	Ref.	F3***
B0.5IP	67.89	23.2	2.9	F3***
B1IP	69.9	26.8	6	F3***

F1*: yielding of tension steel reinforcement.
F2**: intermediate flexure crack-induced debonding failure.
F3***: intermediate flexure crack-induced debonding along the internal CFRP sheets that began from the mid-span with a horizontal crack and concrete cover separation and delamination.

Regarding the effect of added steel fibers percent on the ultimate load, the experimental test results indicated that the percentage of the increase in ultimate load was 3.3, and 5.7% for specimens B0.5EA, B1EA respectively with respect to the reference specimen B0EA, regarding the group of externally full strengthening. Also, the percentage of the increase in ultimate load was 3, and 5.6% for specimens B0.5EP, B1EP respectively with respect to the reference specimen B0EP, regarding

the group of externally partial strengthening, while the percentage of the increase in ultimate load was 4.4, and 7.7% for specimens B0.5IA, B1IA respectively with respect to the reference specimen B0IA, regarding the group of internally full strengthening, and the percentage of the increase in ultimate load was 2.9, and 6% for specimens B0.5IP, B1IP respectively with respect to the reference specimen B0IP, regarding the group of internally partial strengthening. Figure 4-9 shows a comparison in ultimate load for tested beams.

The control beam specimen, B0 had the minimum load carrying capacity and behaved in the expected fashion under flexural loading. The failure was (traditional and predictable) due to the yielding of tension steel reinforcement followed by crushing of concrete in the compression zone at midspan.
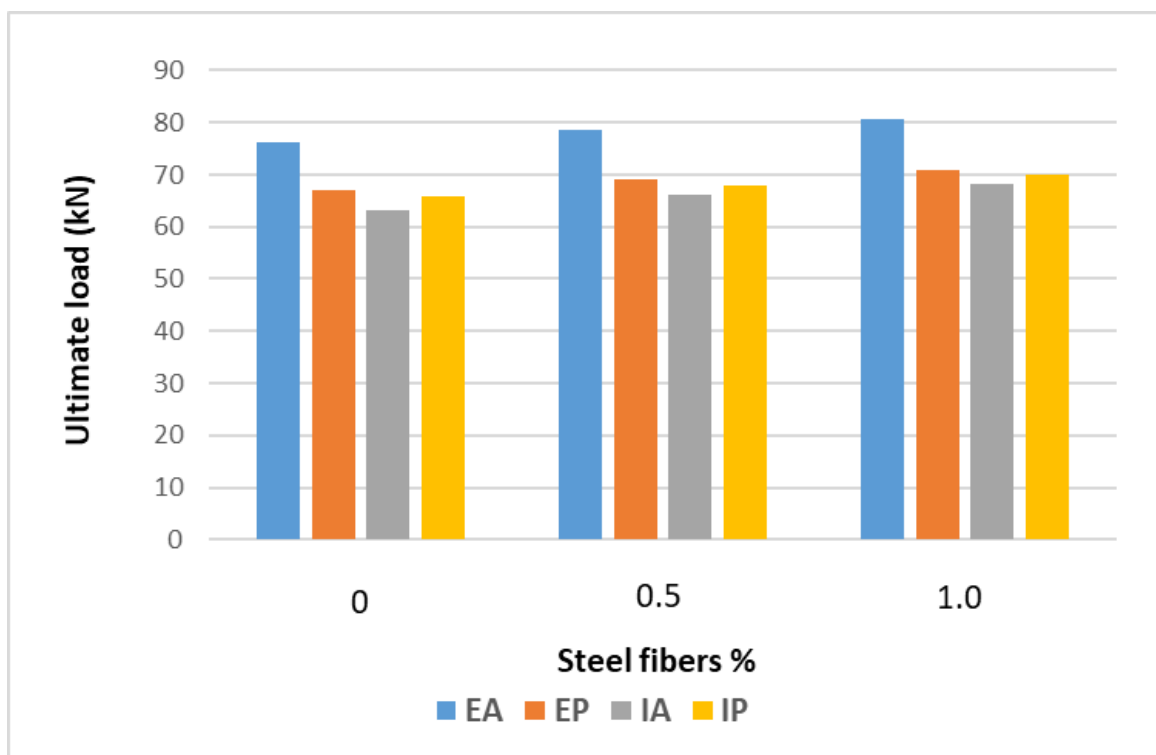
Figure 4-9: A comparison in ultimate load for tested beams.

4.7 Flexural Toughness

The ability to resist crack formation is one definition of flexural toughness. Another way to think about it is that flexural toughness is a measure of the energy absorption capacity. The performance of regions under the load-deflection curve is what is being measured here. Table 4-8 and Figure 4-10 show the toughness values of all tested beams. Figure 4-10 show that the toughness of internal strengthened beams has the large values, while the reference un-strengthened one has the small value.

Table 4-8: Toughness of tested beams.

Group	Beam-ID	Added fiber type	% Of steel fibers	Added fiber length	Area under curve (kN.m)
reference	B0	-	0	-	358
1	B0EA	external	0	All-strength	989
	B0EP	external	0	Part-strength	1100
	B0IA	internal	0	All-strength	2357
	B0IP	internal	0	Part-strength	2180
2	B0.5EA	external	0.5	All-strength	1033
	B0.5EP	external	0.5	Part-strength	1039
	B0.5IA	internal	0.5	All-strength	2252
	B0.5IP	internal	0.5	Part-strength	2167
3	B1EA	external	1	All-strength	1107
	B1EP	external	1	Part-strength	1099
	B1IA	internal	1	All-strength	2382
	B1IP	internal	1	Part-strength	2209
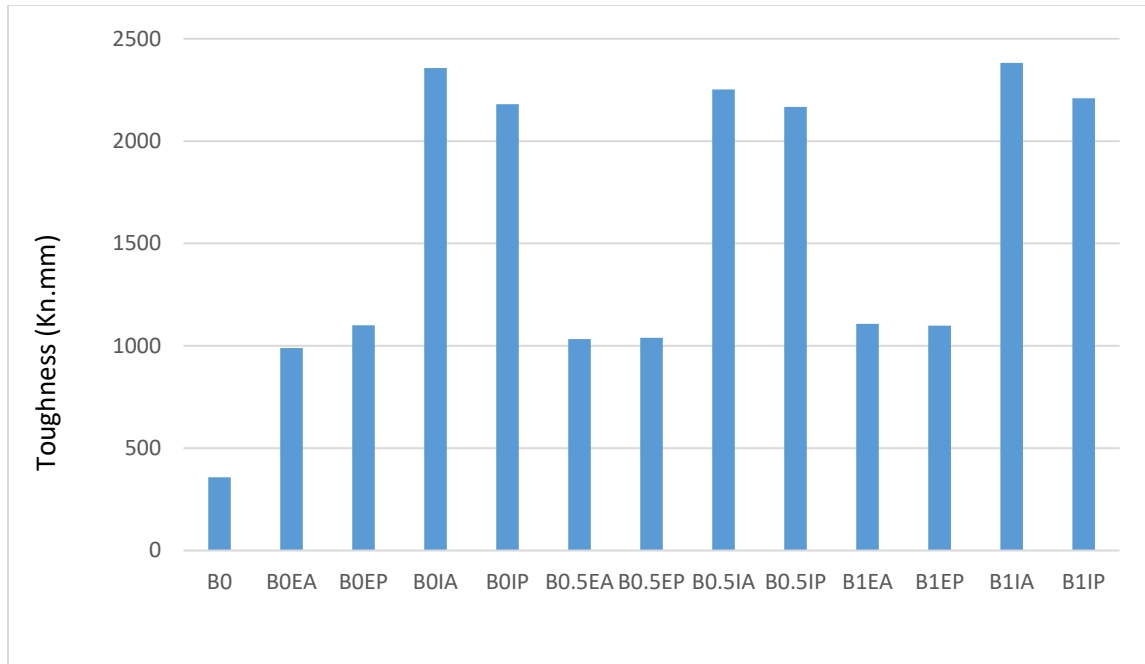
Figure 4-10: A comparison in toughness of tested beams.

4.8 Stiffness

A body's stiffness K is measurement of how resistant an elastic body to deforming. It has beam decided to use "effective secant stiffness," which is based on strength at the service load = Pu /1.7 **(Mansur and Tan, 1992).**

Table 4.9 shows the stiffness of tested beams and Figure 4.11 shows a comparison in stiffness values of tested beams. It is observed that increasing the adding externall CFRP sheets length increases the stiffness, as shown in figure 4.11. Also, increasing the percent of added steel fibers increases the stiffness, and the external CFRP sheets was better than the internal CFRP sheets.

Table 4.9: Stiffness of tested beams.

Beam ID	Service load (kN)	Deflection at service load (mm)	Stiffness, k (kN/mm)	Percent of increasing in k (%)
B0	32.41765	7.5	4.32	Ref.
B0EA	44.80588	4.1	10.93	153.0093
B0EP	39.44706	5.2	7.6	75.92593
B0IA	37.24118	7.2	5.2	20.37037
B0IP	38.8	7.6	5.11	18.28704
B0.5EA	46.27059	4	11.6	168.5185
B0.5EP	40.65294	5	8.1	87.5
B0.5IA	38.88824	6.7	5.8	34.25926
B0.5IP	39.93529	7	5.7	31.94444
B1EA	47.37059	3.9	12.1	180.0926
B1EP	41.66471	4.8	8.7	101.3889
B1IA	40.13529	6.6	6.1	41.2037
B1IP	41.11765	6.8	6	38.88889
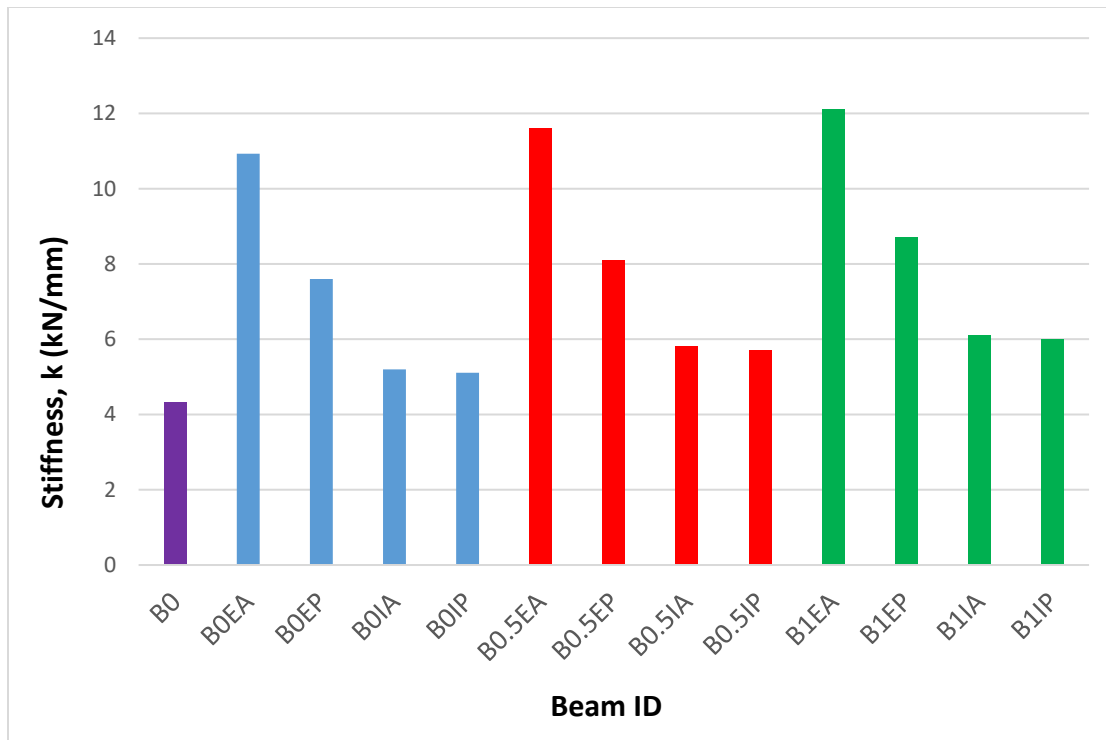
Figure 4-11: A comparison in stiffness values of tested beams.

4.9 Parametric Study

4.9.1 Effect of steel fiber

Figures 4-12 and 4-13 show the effect of steel fiber percent on load-deflection behavior for the mid span point for all beams. The results for 3 specimens with different steel fibers percent are compared together in each Figure. From load-deflection curves, it is cleared that the beams have the same stiffness in the elastic region while after yielding of tension reinforcement the increase of added steel fibers percent is directly proportional with beam stiffness or in other words, the deflection decrease at the same load level. The results of many researches indicate that the ductility and the ultimate resistance are remarkably enhanced due to the addition of steel fibers.
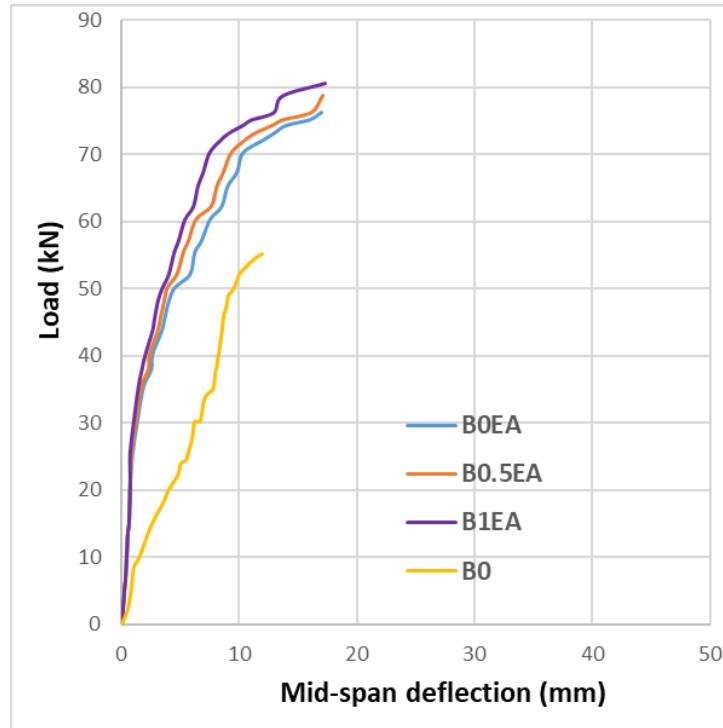
a-Beams with external all strengthening
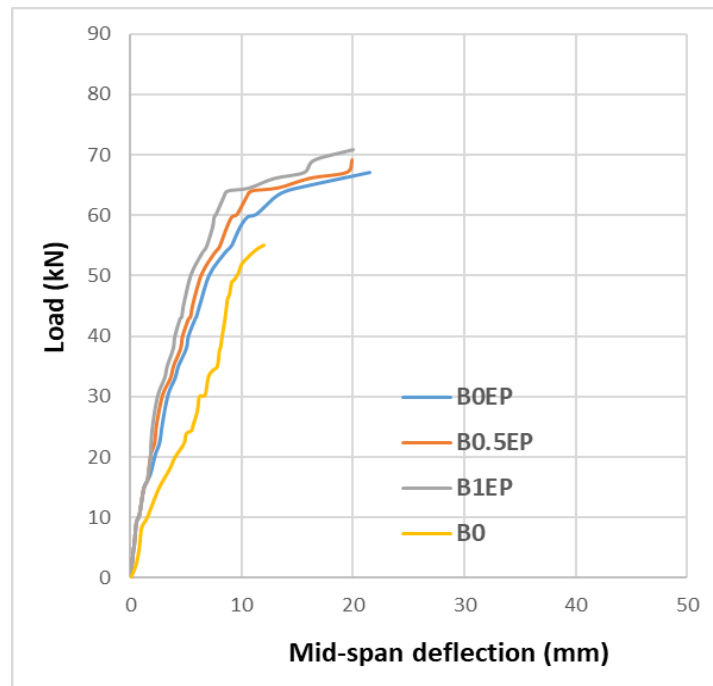
b-Beams with external partial strengthening

Figure 4-12: Effect of steel fiber percent on load-deflection behavior of externally CFRP.
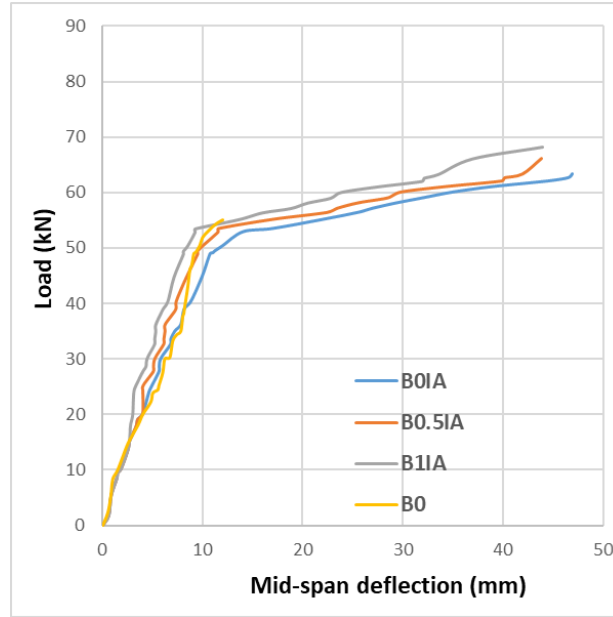
a-Beams with internal all strengthening
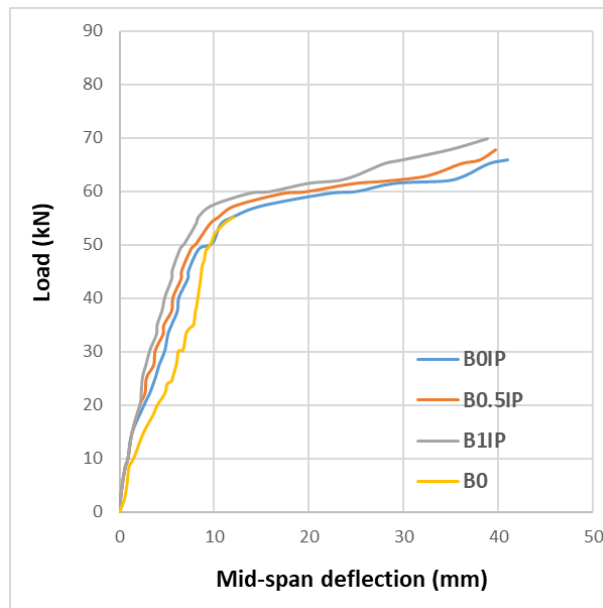
b-Beams with internal partial strengthening

Figure 4-13: Effect of steel fiber percent on load-deflection behavior of internally CFRP.

4.9.2 Effect of position and length of CFRP sheets

Figures 4-14 to 4-16 show the effect of added CFRP sheets (position and length) on load-deflection behavior for the mid span point for all beams. In each Figure the

results for 4 beams with similar steel fibers percent are compared together with different length of CFRP and different position (external or internal). From load-deflection curves, it is cleared that the beams have the same stiffness in the elastic region while after yielding of tension reinforcement the increase of added CFRP sheets length is directly proportional with beam stiffness or in other words, the deflection decrease at the same load level for externally CFRP sheets. The experimental results of many researches have demonstrated that the flexural strengthening capacity of the RC beams using externally bonded of CFRP sheets on bottom faces can significantly enhance the flexural capacity of the beams strengthened. Also, it's clear that the externally CFRP sheets strengthening is better than the internally strengthening. The existing internal CFRP sheets between tensile reinforcement and cover of concrete acted as a separated layer which led to a horizontal crack starting at near surface load for each beam then separation of the bottom cover followed by debonding of CFRP sheets.
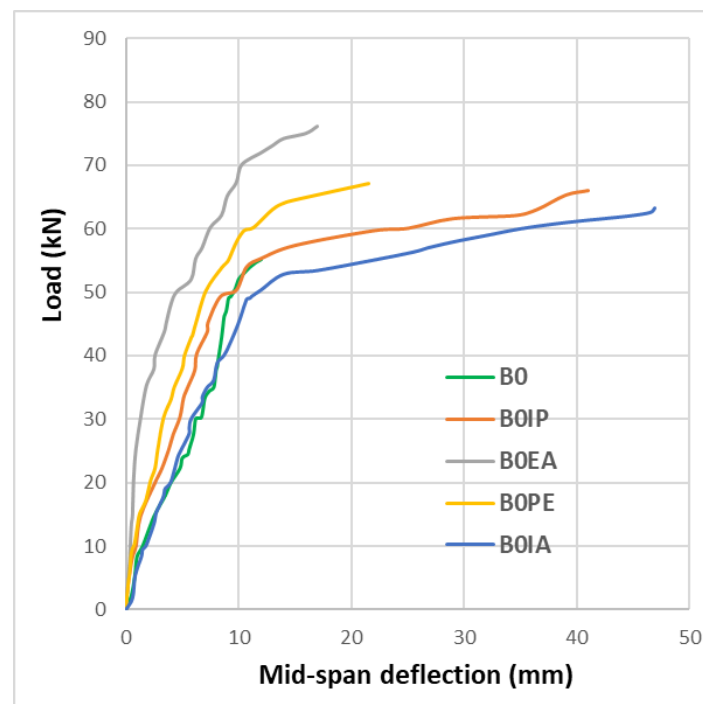
Figure 4-14: Effect of CFRP sheets (Steel fibers =0%) on load-deflection behavior.
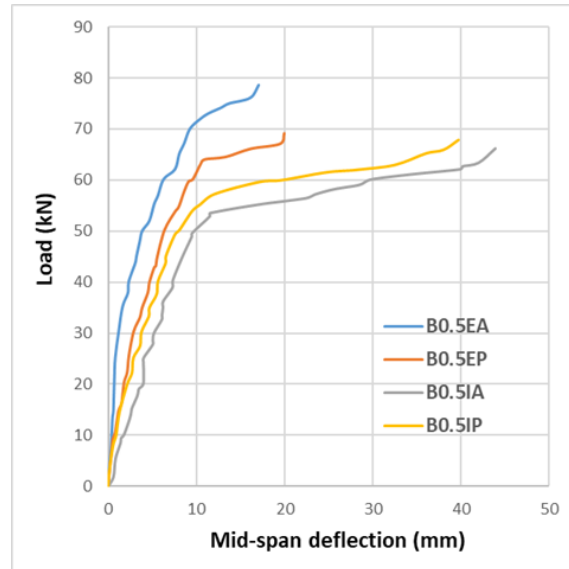
Figure 4-15: Effect of CFRP sheets (Steel fibers =0.5%) on load-deflection behavior.
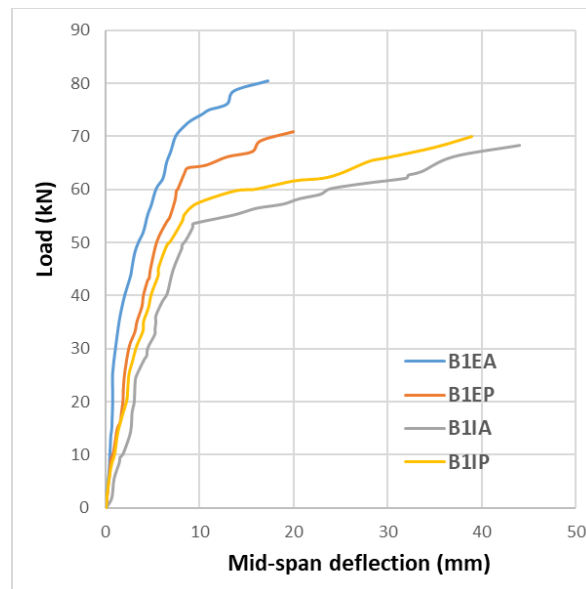
Figure 4-16: Effect of CFRP sheets (Steel fibers =1%) on load-deflection behavior.

Table 4-10 shows the deflections at mid-span of specimens at service and ultimate loads, where the service load was taken as ultimate load divided by 1.7 as mentioned before. The effect of added CFRP sheets length on the central deflection at service load is significant, where the central deflection for each beam with full length is less than the beam with partial length with similar other parameters. Unlike externally, the internally strengthening in B0IA gives negative results. This may be

due to the internal CFRP sheets acting as a separation layer inside the concrete or the segregation of concrete. Also, Table 4-10 shows the deflections at mid-span for all specimens at the 55.11kN where the precents of decrease in deflection were 48, 25, 8,57,33,9,14, 63, 43, 13, and 48% for specimens B0EA, B0EP, B0IP, B0.5EA, B0.5EP, B0.5IA, B0.5IP, B1EA, B1EP, B1IA, and B1IP respectively with respect to the reference specimen B0. While the beam without steel fiber and full internally strengthening B0IA had an increase percent of 50% with respect to the reference specimen B0.

Table 4-10: Deflections at mid-span of specimens at service and ultimate loads

Specimens	Deflection at Service Load (mm)	% Decrease in Deflection at Service Load	Deflection at Ultimate Load of Ref. (55.11kN) Specimen=55.11kN	% Decrease in Deflection at The Ultimate Load of Ref. Specimen	Deflection at Ultimate load (mm)	% Increase in Deflection at Ultimate Load
B0	7.5	Ref.	12	Ref.	12	Ref.
B0EA	4.1	45	6.2	48	17	42
B0EP	5.2	31	9	25	21.5	79
B0IA	7.2	4	18	-50 (increase)	46.9	290
B0IP	7.6	-1.3	11	8	41	242
B0.5EA	4	47	5.2	57	17.1	43
B0.5EP	5	33	8	33	19.95	66
B0.5IA	6.7	11	10.9	9	43.9	266
B0.5IP	7	6.7	10.3	14	39.7	231
B1EA	3.9	48	4.4	63	17.3	44
B1EP	4.8	36	6.8	43	19.99	67
B1IA	6.6	12	10.5	13	44	267
B1IP	6.8	9.3	6.3	48	38.9	224

Chapter five
Conclusions and recommendations

5.1 General

The main objective of this thesis is to investigate the performance of reinforced sustainable concrete beams externally and internally strengthened with carbon fiber reinforced polymer sheet (CFRP) attached to their flexural sides. The main variables of the experimental work are the location of CFRP sheet (internal or external), length of CFRP, and volume fraction of steel fiber. In the present study tested beams are divided into three groups according to the added steel fiber percent (0, 0.5, 1) %, each group has four samples with different lengths and locations of CFRP, as well as reference beam without strengthening or fiber. Also, the laboratory tests of hardened Pozzolime concrete were done.

5.2 Conclusions of test results of control specimens

1. The percent of steel fibers had a minor influence on the fresh density for pozzolime concrete. Adding 0.5 and 1% steel fibers to the reference specimen enhanced the fresh density by 0.2% and 0.4%, respectively. Also, the percent of steel fibers had a slight influence on the dry density. Adding 0.5 and 1% steel fibers to the reference specimen raised the dry density by 0.9% and 1.6%, respectively. While the percent of steel fibers has a significant impact on compressive strength (f_{cu}). Adding 0.5 and 1% steel fibers increased compressive strength by 2.4% and 16.3%, respectively, compared to the reference specimen at 7 days. Adding 0.5 and 1% steel fibers increased compressive strength by 4.1% and 37.6% compared

97

to the reference specimen at 14 days. The addition of steel fibers enhanced compressive strength by 4.9% and 12.8% compared to the reference specimen at 28 days.

2. The percent of steel fibers has a substantial influence on splitting tensile strength (fsp) at 28 days. Adding 0.5 and 1% steel fibers enhanced splitting tensile strength by 11.8% and 23.2% respectively, compared to the reference specimen.

3. The percent of steel fibers affected the modulus of elasticity (Ec) at 28 days. Adding 0.5 and 1% steel fibers increased Ec by 1.7% and 5%, respectively, compared to the reference specimen.

5.3 Conclusions of strengthened beams tests

1. The first flexural crack was occurred at a different first crack load (**Pcr**) / ultimate load (**P u**) percent of about (21.2 to 33.9 %). Increase the added external CFRP sheets length has a significant effect on the **Pcr** / **P u** percent, while increase the added internal CFRP sheets length has a small effect on the **Pcr** / **P u** percent, also, increase the added steel fibers percent has a significant effect on the **Pcr** / **Pu** percent.

2. Two kinds of failure modes observed in the strengthened beams in this experiment. The first is the intermediate flexure crack-induced debonding failure which occurred in the externally strengthened beams. The second is the intermediate flexure crack-induced debonding along with the internal CFRP sheets that began from the mid-span with a horizontal crack with concrete cover separation and delamination.

3. That adding steel fibers has a significant effect on stiffness of beams which leads to decrease the ultimate crack width.

4. From load-deflection curves, it was cleared that the beams have the same stiffness in the elastic region while after yielding of tension reinforcement the increase of

steel fibers percent was directly proportional with beam stiffness or in other words, the deflection decrease at the same load level. And the externally CFRP sheets strengthening was better than the internally strengthening.

5. The deflections at mid-span for all specimens at the ultimate load of reference beam (55.11kN) where the precents of decrease in deflection were 8, and 63 % for specimens beam with internal partial CFRP and 0 percent of steel fibers, and beam with external full CFRP and 1 percent of steel fibers) respectively with respect to the reference specimen B0. While the beam without steel fiber and full internally strengthening had an increased percent of 50% with respect to the reference specimen.

6. The percent of added steel fibers has a small effect on the ductility factor. And externally strengthening gives ductility factor less than internally, where range of the ductility factor values of externally strengthened beam where (2.1 to 2.24), while for internally where (2.93 to 3.36).

7. The percent of increase in ultimate load was 46.1, and 14.9 % for specimens beam with external full CFRP and 1 percent of steel fibers, and beam with internal full CFRP and 0 percent of steel fibers respectively, with respect to the reference specimen.

8. For Full externally strengthening, the effect of increase steel fibers percent on ultimate load was 3.3, and 5.7% for specimens with percent of steel fibers of 0.5 and 1% compare with the reference specimen with percent of steel fibers of 0% respectively. While the percentage of the increase in ultimate load was 3, and 5.6% for specimens with percent of steel fibers of 0.5 and 1% respectively with respect to the reference specimen with percent of steel fibers of 0% , regarding the group of externally partial strengthening.

9. For Full externally strengthening, the percentage of the increase in ultimate load was 4.4, and 7.7% for specimens with percent of steel fibers of 0.5 and 1%

respectively with respect to the reference specimen with percent of steel fibers of 0%. The percentage of the increase in ultimate load was 2.9, and 6% for specimens with percent of steel fibers of 0.5 and 1% respectively with respect to the reference specimen with percent of steel fibers of 0%, regarding the group of internally partial strengthening.

10. The toughness of internal strengthened beams have the large values, while the reference un-strengthened one has the small value.

11. Increasing the external adding CFRP sheets length increases the stiffness, as shown in figure 4.11. Also, increasing the percent of added steel fibers increases the stiffness, and the external CFRP sheets was better than the internal CFRP sheets.

12. The best strengthening case based on all properties was the beam with external full CFRP and 1 percent of steel fibers, where the percent of increase in ultimate load was 46.1% for this specimen with respect to the reference specimen.

5.4 Recommendations for future research work

Based on the results of this work, for further research the following fields are suggested:

1- Studying the performance of reinforced Pozzolime concrete beams with CFRP under dynamic and impact loads.

2- Studying the performance of reinforced Pozzolime concrete beams (with another precents) with CFRP under high-temperature effect.

3- Studying the performance of reinforced Pozzolime concrete beams with partially prestressed.

4- Studying the performance of beam reinforced Pozzolime concrete (with another Pozzolime materials types) strengthened with CFRP sheet internally and externally under monotonic and repeated loads.

5- Studying the performance of reinforced Pozzolime concrete beams repaired with NSM CFRP bars.

References

Abdul-Rahman, M. B., Alya'a, A. A., & Younus, A. M. 2018. Effecting of steel fibers and fly ash on the properties of concrete. Tikrit Journal of Engineering Sciences, v. 25(4), p. 30-36.

A. J. Alsaad, T. S. Al-Attar, and B. S. Al-Shathr. 2020. Utilization of Mineral Sequestration for CO2 Capturing in Car Parks and Tunnels. Eng. Technol. J., v. 38, p. 25-35.

Ali, A. M., Falah, M. W., Hafedh, A. A., Al-Khafaji, Z. S., & Radhi, S. 2022. Evaluation the influence of steel-fiber on the concrete characteristics. Periodicals of Engineering and Natural Sciences, v. 10(3), p. 368-379.

A. Moropoulou, A. Cakmak, K. C. Labropoulos, R. Van Grieken, and K. Torfs. 2004. Accelerated microstructural evolution of a calcium-silicate-hydrate (C-S-H) phase in pozzolanic pastes using fine siliceous sources: Comparison with historic pozzolanic mortars. Cem. Concr. Res. v. 34, p. 1-6.

ACI Committee 318. 2019. Building code requirements for structural concrete, (ACI 318M-19) and commentary (318R-19). American Concrete Institute, Farmington Hills, Michigan, USA.

ACI Committee 440-2R. 2017. "Guide for the Design and Construction of Externally Bonded FRP Systems for Strengthening of Concrete Structures", American Concrete Institute, Michigan, USA.

al-Attar, T. S., Abdulqader, S. S., & Rashid, R. M. 2020. Experimental evaluation of stress-strain relations in compression for Pozzolime concrete. IOP Conference Series: Materials Science and Engineering v. 737, No. 1, p. 40-50.

Al-Attar, T. S., Al-Zuheriy, A. S. J., & Hamza, S. M. 2021. Optimum Steel Fiber Content of High Strength Pozzolime Concrete. Engineering and Technology Journal v. 39(12), p. 1869-1874.

Arezoumandi, M., & Volz, J. S. 2013. Effect of fly ash replacement level on the shear strength of high-volume fly ash concrete beams. Journal of Cleaner Production, v. 59, p.120-130.

ASTM A496. 2007. Standard specification for steel wire, deformed, for concrete reinforcement. Annual book of ASTM standard, v. 01.05, p. 425-429.

ASTM C 138-06. 2006. "Standard Test Method for Density (Unit Weight), Yield , and Air Content (Gravimetric)," Annu. B. ASTM Stand. Am. Soc. Test. Mater., v. 04.02, no. C, p. 4–7.

ASTM C143. 2003. Standard test method for slump of hydraulic- cement concrete.

West Conshohocken, Pennsylvania.

ASTM C143-06. 2006. "Standard Test Method for Slump of Hydraulic-Cement Concrete," Annu. B. ASTM Stand. Am. Soc. Test. Mater., v. 04.02, no. C, p. 3–6.

ASTM C192. 2007. Standard practice of making and curing concrete test specimens in the laboratory. West Conshohocken, Pennsylvania, p. 1-8.

ASTM C469. 2002. Standard test method for static modulus of elasticity and Poisson's ratio of concrete in compression. *Annual book of ASTM Standards*, Vol.04.02 concrete and aggregates, West Conshohocken, PA, United State.

ASTM C496/ C496M. 2011. Standard test for splitting tensile strength of cylindrical concrete specimens. *Annual book of ASTM Standards*, v. 04.02 concrete and aggregates, West Conshohocken, PA, United State.

ASTM-C1240-15, 2015. "Standard Specification for Silica Fume Used in Cementitious Mixtures," Annu. B. ASTM Stand. Am. Soc. Test. Mater. Vol. 04.02.

ASTM-C1240-15, 2015. "Standard Specification for Silica Fume Used in Cementitious Mixtures," Annu. B. ASTM Stand. Am. Soc. Test. Mater. Vol. 04.02.

ASTM-C494-13. 2015. "Standard Specification for Chemical Admixtures for Concrete," Annu. B. ASTM Stand. Am. Soc. Test. Mater. Vol. 04.02.

ASTM-C494-13. 2015. "Standard Specification for Chemical Admixtures for Concrete," Annu. B. ASTM Stand. Am. Soc. Test. Mater. Vol. 04.02.

Barris, C., Sala, P., Gómez, J., & Torres, L. 2020. Flexural behavior of FRP reinforced concrete beams strengthened with NSM CFRP strips. Composite Structures, v. 241, 112059.

Bashandy, A. A. 2013. Flexural strengthening of reinforced concrete beams using valid strengthening techniques. Archives of Civil Engineering, v. 59(3), p.275-293.

Berg, A. C., Bank, L. C., Oliva, M. G. and Russel, J. S. 2006. "Construction and Cost Analysis of an FRP Reinforced Concrete Bridge Deck", J. of Construction and Building Materials, v. 20, p. 515-526.

Berndt, M. L. 2009. Properties of sustainable concrete containing fly ash, slag and recycled concrete aggregate. Construction and building materials, v. 23(7), p. 2606-2613.

BS EN12390-3. 2009. "Testing hardening concrete, compressive strength of test specimens," vol. 3.

C. Al-Mahmoud, F. Castel, A. François, and R. Tourneur. 2009. "Strengthening of RC members with near-surface mounted CFRP rods," Compos. Struct., v. 91, p. 138–147.

Concrete – the responsible choice, Cement Concrete & Aggregates Australia, 2010.

concrete. In MATEC Web of Conferences.2009. (Vol. 120, p. 02009). EDP Sciences.

Daouadji, T. H., Rabahi, A., Abbes, B., & Adim, B. 2016. Theoretical and finite element studies of interfacial stresses in reinforced concrete beams strengthened by externally FRP laminates plate. Journal of adhesion science and Technology, v.30(12), p.1253-1280.

Dong, J., Wang, Q., He, D., & Guan, Z. 2011, July. CFRP sheets for flexural strengthening of RC beams. In 2011 International Conference on Multimedia Technology (pp. 1000-1003).

Duthinh, D. and Starnes, M., 2001, "Strength and Ductility of Concrete Beams Reinforced with FRP and Steel", National Institute of Standards and Technology, NISTIR 6830, 16 P.

El-Hacha, R., Rizkalla, S., & Kotynia, R. 2005. Modelling of reinforced concrete flexural members strengthened with near-surface mounted FRP reinforcement. ACI Special Publication, 230(95), 1681-1700.

Ferreira, A. J. M., Camanho, P. P., Marques, A. T., and Fernandes, A. A. 2001."Modeling of Concrete Beams Reinforced with FRP Re-bars", Composite Structures, V. 53, pp. 107-116.

G Karayannis, C., K Kosmidou, P. M., & E Chalioris, C. 2018. Reinforced concrete beams with carbon-fiber-reinforced polymer bars—Experimental study. Fibers, 6(4), 99.

G. K. Mohammed, K. F. Sarsam, and I. N. Gorgis. 2020. Flexural Performance of Reinforced Concrete Built-up Beams with SIFCON, Eng. Technol. J., v.38. p.669–680.

Gemi, L., Madenci, E., & Özkılıç, Y. O. 2021. Experimental, analytical and numerical investigation of pultruded GFRP composite beams infilled with hybrid FRP reinforced concrete. Engineering Structures, 244, 112790.

Hashmi, A. F., Shariq, M., & Baqi, A. 2020, June. Flexural performance of high-volume fly ash reinforced concrete beams and slabs. In Structures (Vol. 25, pp. 868-880).

Hawileh, R. A., Rasheed, H. A., Abdalla, J. A., & Al-Tamimi, A. K. 2014. Behavior of reinforced concrete beams strengthened with externally bonded hybrid fiber reinforced polymer systems. Materials & Design, 53, 972-982.

Hoque, M. M. 2006."3D Nonlinear Mixed Finite Element Analysis of RC Beams and Plates with and without FRP reinforcement", M.Sc. Thesis, University of Manitoba, Canada, 106 P.

Iraqi Specification Standard. 1984. "Natural Aggregate Resource That Used in Building and Concrete," vol. No 45.

Iraqi specification stander. 2019. "Portland cement," vol. No. 5.

Iraqi specification.2004 "Lime That Used in Building," vol. NO. 807.

J. A. Siegel, J. A. Mirakovits, and B. Hudson. 2013. Concrete mix design, quality control and specification. CRC Press.

J. Lee, D. Cheng, L. Hui. 2012. "Bond characteristics of various NSM FRP reinforcements in concrete," J. Compos. Constr., v. 17, p. 117–129.

K Al-Chaar, G., Alkadi, M., & Asteris, P. G. 2013. Natural pozzolan as a partial substitute for cement in concrete. The Open Construction & Building Technology Journal, 7(1).

Kara, I. F., Ashour, A. F., & Köroğlu, M. A. 2015. Flexural behavior of hybrid FRP/steel reinforced concrete beams. Composite Structures, v.129, p.111-121.

Khan, A. R. 2002. "Repair and Strengthening of Reinforced Concrete Structures using CFRP Plates", FEST Hamadard University, India.

Kim, S., & Kim, S. 2019. Flexural behavior of concrete beams with steel bar and FRP reinforcement. Journal of asian architecture and building engineering, 18(2), 89-97.

Klaiber, F.W., Wipf, J.J. and Kempers, B.J. 2003. "Repair of Damaged Prestressed Concrete Bridges using CFRP", Proceedings of the 2003 Mid Transportation Research Symposium, Ames, Iowa, by Iowa State University, www.ctre.iastate.edu.

Lamanna, A., Bank, L. C. and Scott, D. W. 2004. "Flexural Strengthening of Reinforced Concrete Beams by Mechanically Attaching FiberReinforced Polymer Strips", Journal of Composites for Construction, Vol. 8, No. 3, June 1, p. 203-210.

Lau, D., & Pam, H. J. 2010. Experimental study of hybrid FRP reinforced concrete beams. Engineering Structures, 32(12), 3857-3865.

Lin, X., & Zhang, Y. X. 2013. Bond–slip behaviour of FRP-reinforced concrete beams. Construction and Building Materials, 44, 110-117.

M. A. Mansur, L. M. Huang, K. H. Tan, S. L. Lee. 1992. 'Deflections of Reinforced Concrete Beams with Web Openings', ACI Structural Journal, V. 89, No. 4.

Meier, U. 1987. "Bridge Repair with High Performance Composite Materials", Mnferiril iiiitl Teclznik, Vol. 15, p. 125- 128.

Mouli, M., & Khelafi, H. 2008. Performance characteristics of lightweight aggregate concrete containing natural pozzolan. Building and environment,v. 43(1), p.31-36.

N. Kadum, T. al-Attar, and Z. Al-Azzawi. 2017. "Evaluation of pozzolime mixtures as a sustainable binder to replace portland cement in structural concrete," MATEC Web Conf., vol. 120, p. 02009.

N. Saikia and J. de Brito. 2012. Use of industrial waste and municipality solid waste as aggregate, filler or fiber in cement mortar and concrete, in Municipal Solid Waste.

Nitereka, C., and Neale, K. W.1999. "Analysis of Reinforced Concrete Beams Strengthened in Flexure with Composite Laminates", Canadian Journal of Civil Engineering, V. 26, pp. 646-654.

Oh, B. H. 1992. Flexural analysis of reinforced concrete beams containing steel fibers. Journal of structural engineering, 118(10), 2821-2835.

P. K. Mehta and P. J. M. Monteiro. 2006. "Concrete: microstructure, properties, and materials," Concrete. p. 684.

P. K. Mehta and P. J. M. Monteiro. 2006. "Concrete: microstructure, properties, and materials," Concrete. p. 684.

P. Valerio. 2009. "Realistic Shear Assessment and Novel Strengthening of Existing Concrete Bridges," PhD Thesis, Dep. Archit. Civ. Eng., BATH University, p. 240, November.

Panahi, M., Zareei, S. A., & Izadi, A. 2021. Flexural strengthening of reinforced concrete beams through externally bonded FRP sheets and near surface mounted FRP bars. Case Studies in Construction Materials, 15, e00601.

S. P. Shah and B. V. Rangan. 1971. Fiber Reinforced Concrete Properties, J. Proc., 68. 126–137.

Shahawy, M. A., Arockiasamy, M., Beitelman, T., and Sowrirajan. 1996. "Reinforced Concrete Rectangular Beams Strengthened with CFRP Laminates", Composites: Part B, V. 27B, pp. 225-233.

Sharifianjazi, F., Zeydi, P., Bazli, M., Esmaeilkhanian, A., Rahmani, R., Bazli, L., & Khaksar, S. 2022. Fibre-Reinforced Polymer Reinforced Concrete Members under Elevated Temperatures: A Review on Structural Performance. Polymers, 14(3), 472.

Shen, K., Wan, S., Mo, Y. L., & Jiang, Z. 2018. Theoretical analysis on full torsional behavior of RC beams strengthened with FRP materials. Composite Structures, 183, 347-357.

Sika, "Sika ViscoCrete-PC 20. 2018. [Online]. Available: www.sika.com.tr.

Sika, "Sika ViscoCrete-PC 20. 2018. [Online]. Available: www.sika.com.tr.

Sun, Z., Fu, L., Feng, D. C., Vatuloka, A. R., Wei, Y., & Wu, G. 2019. Experimental study on the flexural behavior of concrete beams reinforced with bundled hybrid steel/FRP bars. Engineering Structures, 197, 109443.

Sunayana, S., & Barai, S. V. 2018. Flexural performance and tension-stiffening evaluation of reinforced concrete beam incorporating recycled aggregate and fly ash. Construction and Building Materials, v.174, p.210-223.

Van Nguyen, C., Lambert, P., & Bui, V. N. 2020. Effect of locally sourced pozzolan on corrosion resistance of steel in reinforced concrete beams. International Journal of Civil Engineering, v.18(6), p.619-630.

Yang, J., Haghani, R., Blanksvärd, T., & Lundgren, K. 2021. Experimental study of FRP-strengthened concrete beams with corroded reinforcement. Construction and Building Materials, v.301, p.124-134.

Yoo, S. W., Ryu, G. S., & Choo, J. F. 2015. Evaluation of the effects of high-volume fly ash on the flexural behavior of reinforced concrete beams. Construction and Building Materials, v.93, p.1132-1144.

Yue-lin, H., Jong-hwei, W., Tsong, Y., Chien-hsing, H. and Yiching, L. 2005. "Strengthening Reinforced Concrete Beams using Prestressed Glass Fiber-Reinforced Polymer-Part I: Experimental Study", J. of Zhejiang University Science, http://www.zju.edu.cn/jzus. v.6A (3), p. 166-174.

APPENDIX A

BEAM SPECIMEN DESIGN CALCULATION ACCORDING TO THE ACI 318

A.1 Calculation of flexural capacity for beam without strengthening

Beam clear span (L)	1300mm
Compressive strength (f_c')	25 MPa
Yield strength (Fy)	420 MPa
Height of beam section (h)	200 mm
Width of beam section (w)	120 mm
Cover (c)	20 mm
Effective depth d=	167 mm
Diameter of long. reinforcement	10 mm
Diameter of shear reinforcement	8 mm
Steel modulus of elasticity (E_s) , assumed	200000 MPa
Concrete modulus of elasticity	23500 MPa

Use bar 2 Ø10

$$\rho = \frac{A_S}{b \times d} = 0.008$$

$$\rho_{min} = \frac{0.25\sqrt{f_c'}}{f_Y} = 0.003 \qquad OR \qquad \rho_{min} = \frac{1.4}{f_Y} = 0.003$$

$$\therefore \rho_{min} = 0.003 \quad \dots\dots\dots\dots\dots\dots\dots\dots\dots\dots\dots \quad \text{ACI318 -14 (9.6.1.2)}$$

$$\beta_1 = 0.85 \quad \dots\dots\dots\dots \quad \text{ACI318 -14 (Table 22.2.2.4.3)}$$

$$\rho_b = 0.85 \times \beta_1 \times \frac{f_c'}{f_Y} \times \frac{600}{600+fy} = 0.025$$

$$\rho_t = 0.85 \times \beta_1 \times \frac{f_c'}{f_Y} \times \frac{0.004}{0.004+\varepsilon} = 0.016$$

$$\rho_{max} = 0.85 \times \beta_1 \times \frac{f_c'}{f_Y} \times \frac{0.003}{0.003+\varepsilon} = 0.018$$

$$\therefore \rho_{min} < \rho < \rho_{max}$$

Mn = 0.124+0.45P

$$M_n = \rho \, b \, d^2 \, F_Y \left(1 - 0.59\rho \frac{fy}{fc\prime}\right) = 10.35 \; KN.m \quad ,$$

10.35=0.124+0.45P

P= 22.724 kN

2P= 45.448 kN

A.2 Calculation of shear capacity for beam without strengthening

V_C = nominal shear strength provided by concrete, KN

V_S = nominal shear strength provided by shear reinforcement, KN

V_n = nominal shear strength, KN

V_u = 22.724+(24.5*0.12*0.2*1.3)/2 = 23.106 kN

V_{ud} = 23.204 kN

$V_C = \frac{1}{6} \sqrt{f_c'} \; bd = 17.034 \; KN$

Vc/2 = 8.517 kN

$V_s = V_{ud} - V_c = 14.687$ kN

$V_s < 2V_c =$

    1- d/2 = 83.5 mm

    2- 600mm

    3- 3Av fy /b = 1055 mm

    4- 16 Av fy / b$\sqrt{fc'}$ = 1125 mm

So S max = 83.5 mm , use Smax =60mm

$S = \frac{Av\,fy\,d}{Vs} = 480.5 > 60$

For more safety, assume that first stirrups start at the distance 20 mm rather than half of the depth as mention in code.

n = 2($\frac{450-20}{60}$ +1) =16.33 , use n= 18

A.3 Development length

C_b is equal to the lesser of the following

    1- (clear spacing + dp)/2 = 27 mm

    2- Clear cover + dp/2 = 25 mm

    3- clear spacing = 44 mm
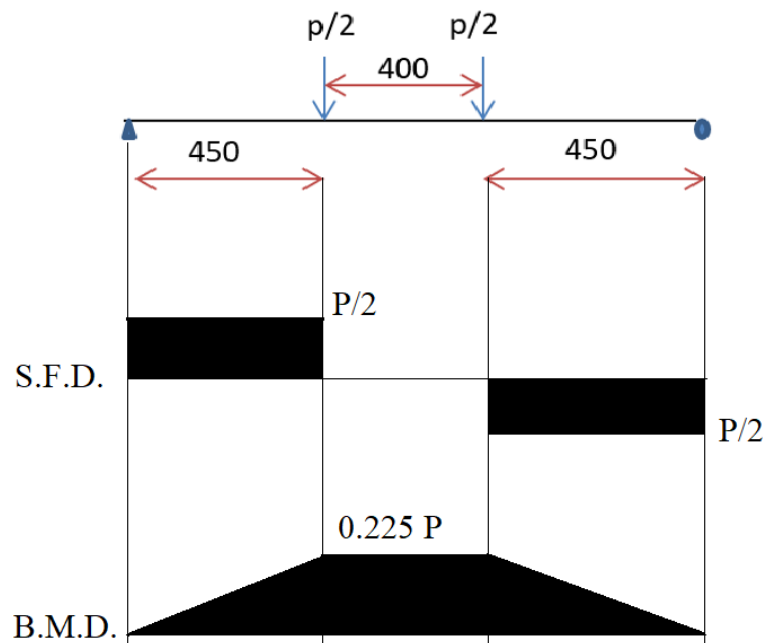
    So C_b = 25 mm

$$K_{tr} = \frac{Atr*fyt}{10\ S\ n} = 25.12$$

$\frac{c_b+k_{tr}}{dp} = 5.012 > 2.5$, so use 2.5

From table (ACI318 -25.4.2.4)

$\Psi_t = 1$, $\psi_e = 1$, $\psi_s = 0.8$

$$L_{d,\ required} = (\frac{fy}{1.1\ \eta\sqrt{fc\prime}} * \frac{\psi t + \psi e + \psi s}{\frac{c_b+k_{tr}}{dp}}) = 244.4 \text{ mm}$$

$L_{d,\ provided}$ =1400/2 -20 = 680mm > 244.4 mm → ok.

S.F.D.

B.M.D.

الخلاصة

كانت صناعة الخرسانة موجودة منذ 120 عامًا فقط ، لكنها تركت بالفعل علامة مهمة على شكل المناظر الطبيعية. تتمثل الأهداف الرئيسية لهذه الرسالة في دراسة سلوك خواص خرسانة البوزولانية ودراسة استجابة عتبات الخرسانة المسلحة بالبوزولانه لاختبار الانحناء بأربع نقاط. تم استخدام التقوية بصفائح CFRP للاختبار ، والذي ركز على تحديد كيفية تأثير النسبة المئوية لألياف الحديد وطول صفائح ومكان تثبيتها CFRP على النتائج. المتغيرات الرئيسية للعمل التجريبي هي موقع لوح CFRP (داخلي أو خارجي) ، وطول CFRP ، ونسبة الألياف الحديد المضافة.

يتكون البرنامج التجريبي من اختبار ثلاثة عشر عتبة خرسانية مسلحة مصممة على شكل عتبات بسيطة الاسناد وباستخدام خرسانة البوزولانة ، حيث يعتبر أحد العتبات بمثابة العتبة المرجعية والتي تم اختبارها حتى الفشل من أجل مقارنة النتائج مع العتبات الأخرى. جميع العتبات لها نفس الأبعاد والتسليح. يبلغ طولها الإجمالي 1400 ملم ، وطولها الفعال 1300 ملم ، وعرضها 120 ملم ، وارتفاعها 200 ملم. تم اختبار جميع العينات تحت حمولة من نقطتين. يتم تقسيم العينات إلى ثلاث مجموعات بالإضافة إلى عينة مرجعية وفقًا لتقنيات التقوية والنسبة المئوية للألياف الفولاذية المستخدمة في كل مجموعة.

تظهر نتائج البرنامج التجريبي أن نسبة ألياف الحديد لها تأثير كبير على مقاومة الانضغاط. حيث تؤدي إضافة 0.5 و 1٪ ألياف الحديد إلى زيادة مقاومة الانضغاط بنسبة 2.4٪ و 16.3٪ على التوالي ، مقارنة بالعينة المرجعية في 7 أيام. وان إضافة 0.5 و 1٪ ألياف الحديد تزيد من مقاومة الانضغاط بنسبة 4.1٪ و 37.6٪. أدت إضافة ألياف الحديد إلى تعزيز مقاومة الانضغاط بنسبة 4.9٪ و 12.8٪ مقارنة بالعينة المرجعية في 28 يومًا. هناك نوعان من أوضاع الفشل التي حدثت على العوارض المقواة بألياف الكربون المقوى في هذه التجربة. الأول هو فشل إزالة الترابط الناجم عن الانثناء الوسيط والذي حدث في العوارض المقواة خارجيًا. والثاني هو نزع الطبقة المتوسطة الناجم عن الانثناء مع صفائح البلاستيك المقوى بألياف الكربون (CFRP) التي بدأت من منتصف الامتداد مع صدع أفقي مع فصل الغطاء الخرساني وتفكيكه. تتمتع العتبات بنفس الصلابة في المنطقة المرنة بينما بعد بدا التشقق ، فإن زيادة نسبة الألياف الفولاذية المضافة تتناسب طرديًا مع صلابة العارضه ، بمعنى آخر ، ينخفض الهطول عند نفس مستوى الحمل.. وكانت النسبة المئوية للزيادة في الحمل النهائي 3 ، و 5.6٪ للعينات ذات التقوية الخارجية الحاوية على نسبة الياف حديد تساوي 0.5 و 1% على التوالي فيما يتعلق بالعينة المرجعية

ذات التقوية الخارجية والخالية من الياف الحديد ، اما فيما يتعلق بمجموعة التقوية الجزئية الخارجية وتقوية CFRP خارجيًا أفضل من التقوية الداخلية. حيث كانت النسبة المئوية للزيادة في الحمل النهائي 4.4 ، و 7.7٪ للعينات ذات التقوية الداخلية الحاوية على نسبة الياف حديد تساوي 0.5 و 1% على التوالي فيما يتعلق بالعينة المرجعية ذات التقوية الداخلية غير الحاوية على نسبة الياف حديد .

جمهورية العراق

وزارة التعليم العالي و البحث العلمي

جامعة كربلاء

كلية الهندسة

قسم الهندسة المدنية

سلوك الأنحناء للعتبات الخرسانية المسلحة ذات الخرسانة المستدامة والمقواة باستخدام البوليمر المقوى بألياف الكربون والياف الحديد

رسالة مقدمة الى مجلس كلية الهندسة / جامعة كربلاء وهي جزء من متطلبات نيل درجة الماجستير في علوم الهندسة المدنية

كتبت بواسطة:

علي ناصر حسين

(بكالوريوس في الهندسة المدنية – 2017)

باشراف :

أ.م.د. زينب محمد رضا عبد الرسول

أ.م.د .أيمن جميل كاظم

كانون الاول - 2022   جمادي الاول - 1444